VISIBLE AND INFRARED STUDIES OF CATACLYSMIC VARIABLE STARS

Thesis by

Graham Berriman

In Partial Fulfillment of the Requirements

for the Degree of

Doctor of Philosophy

California Institute of Technology

Pasadena, California

1983

(Submitted February 7, 1983)

To Melinda.

Lot of poor men got the Cumberland Blues.

ACKNOWLEDGEMENTS.

It is my pleasure to thank Eric Persson for his expert supervision and sane advice over the past three years. I am especially grateful to him for obtaining the observations of OY Car in Chile, the analysis of which forms a substantial fraction of this Thesis. I must also extend especial thanks to Stefan Mochnacki, for teaching me all I know about tidally distorted stars and for his unfailing support and generosity, and to Ian and Cathy Gatley for their friendship and fluid encouragement.

I have been financially supported by Caltech over the past 5 years, and have had the pleasure of attending a three week conference in Santa Cruz and of observing in Hawaii. For making this possible, my thanks go to Wal Sargent, Marshall Cohen, Peter Wannier and Fred Lo.

The pundits of the infrared group guided my first efforts at research: Gerry Neugebauer, Tom Soifer, Mike Werner and Keith Matthews. Without these people, infrared astronomy would not be quite what it is.

The Directors of the former Hale Observatories and the present Mount Wilson and Las Campanas Observatory, Maarten Schmidt and George Preston, provided a generous allowance of observing time at Mount Wilson. The night assistants -- Howard Lanning, Jim Frazer and Mike Deak -- gave unflagging support at the telescope and around the television (not the

kind used for guiding).

I thank my collaborators and fellow Cataclysmic Variable pundits for sharpening my knowledge of Mother Nature's subtleties: Richard Wade, Keith Horne, Paula Szkody, Don Schneider, the late Peter Young, Jeremy Mould and Bev Oke.

In addition to those mentioned above, I also thank the following for their companionship, support and friendship when most needed: Georg, Fred, Helen and George, Todd, Larry B., Richard the Biologist and Maureen, Jeff, Beth and Richard the Scouse, Kris, Young Ennis, Brad and Pauline, Crazy Roger, Abi, Alex, Dave the Braves Fan (may they finish second next year). My apologies to anyone omitted.

Finally, my greatest thanks of all go to Melinda, whose love and support finally saw me through.

SUMMARY.

The purpose of this Thesis is to investigate the infrared properties of Cataclysmic Variable Stars, in particular, to develop the techniques needed to study the contributions to the infrared light of the red dwarf and the accretion disc around its white dwarf companion. A particular requirement of these techniques is that they do not rely on a model of the poorly understood discs. They can be applied not only to Cataclysmic Variable Stars, but also to other interacting systems containing a red star, such as symbiotic stars.

Analysis of the visible to infrared colours of fourteen largely uneclipsing systems, based on flux ratio diagrams, shows that the red dwarfs and the opaque gas in the disc supply most of the infrared light, but the contributions of each vary widely from system to system, with more light coming from the red dwarfs in the longer period systems than in the shorter period ones. For nearly all the systems studied, upper limits can be found to the fluxes of the red dwarfs that are approximately independent of spectral type and of the conditions in the accretion discs.

In highly inclined systems, measurements of the amplitudes of the tidally induced ellipsoidal variations of the red dwarfs provide a more precise measure of the proportion of light coming from the red dwarf. A technique to simulate the light curves of tidally distorted red dwarfs successfully acounts for the infrared light curves of U

Geminorum, a system in which the red dwarf supplies nearly all the infrared light.

Completing the Thesis is a visible and infrared study of the eclipsing dwarf nova OY Carina in quiescence. This system has been studied because in the visible, the red dwarf is seen to eclipse the white dwarf. Analysis of these eclipses, based on the assumption that the red dwarf fills its Roche Lobe, allows the determination of several fundamental properties of the system: the inclination of the system is 73.5^{o} to 81^{o}, the mass of the white dwarf lies in the broad range 0.4-1.4 $M_{\odot}$ and the red dwarf lies either on or slightly below the Main Sequence mass radius relation. The principal source of uncertainty in the analysis is that the semi-amplitude of the radial velocity variations of the white dwarf is poorly known. The infrared light curves show an eclipse of the disc and, half a cycle later, a secondary minimum produced by the ellipsoidal variations of the red dwarf and its eclipse by the disc. The depth of this minimum and the colours of the system imply that the red dwarf supplies approximately one-half of the uneclipsed light of the system and that it eclipses more than three-fifths of the light of the disc. The latter result requires that the K magnitude of the red dwarf lies in the range 14.2 to 14.7. The distance to the system, as deduced from these limits and an estimate of the surface brightness of the red dwarf lies in the range 100 to 300pc. The infrared light of the disc comes largely from optically thin emission; the opaque gas occupying most of the disc does not supply much of

the infrared light because the disc is atypically small and more highly inclined compared with other systems.

TABLE OF CONTENTS

PREFACE.

The visible spectra of most Cataclysmic Variable Stars (hereafter, CVs) shortward of 6000Å show a flat continuum and strong Balmer emission lines. Both these features originate in an accretion disc, surrounding a white dwarf, made of matter transferred from a red dwarf companion through the process of Roche Lobe overflow. The continuum comes from hot (T>10,000K) opaque gas thought to occupy most of the disc; this gas is hot because it liberates potential energy as it falls into the deep gravitational well of the white dwarf. The presence of the emission lines shows that some of the gas is optically thin in the continuum; it most probably lies in the outer disc or in a chromosphere above the disc.

The red dwarfs can be seen directly in the visible in only a few systems, usually long period ones (>5h), which can accommodate larger and more luminous stars. Though made difficult by the emission of the disc, the study of the red dwarfs is necessary in finding the distances to these systems. The distances give the luminosities of the accretion discs, required in the construction of realistic disc models, and the space density of the systems, required in understanding the evolution of these systems. The question of evolution is particularly intriguing: being short period systems (<9h) and containing a white dwarf, CVs must have lost nearly all their angular momentum during their lifetimes, but how this happens is unknown.

The study of the red dwarfs is best carried out in the near infrared (1-2 μm), where they emit most of their light. The emission from the disc may still be significant at these wavelengths, as it is in the red in many systems. Furthermore, its character is likely to be different from that at shorter wavelengths, where most of the light comes from the hot, opaque gas. In the infrared, more of the light will come from the optically thin gas that produces the Balmer emission lines, and from cool, opaque gas in the outer disc, both of which have a red spectrum. Given that the observed infrared light of a CV comes from both the red dwarf and the disc, the principal purposes of this thesis are (1) to study the nature of the infrared light of CVs, and (2) to develop the analytic techniques needed to decompose the light into the contributions of each component. A specific requirement of these techniques is that they do not depend on a model of the poorly understood accretion discs. Such methods can be applied not only to CVs but also to other interacting systems containing a cool star, such as symbiotic stars.

The most sensitive probe of the red dwarfs in CVs would be measurements of their infrared absorption bands, but sensitivity limitations prevent such observations. The most readily obtained infrared data are broad band measurements at 1.25 μm (J), 1.65 μm (H) and 2.2 μm (K). These data are most useful when combined with broad band visible photometry (V), because the visible to infrared colours of red dwarfs measure the slopes of their continua. This Thesis presents four

separate investigations of visible and infrared photometry of CVs.

Chapter 1 discusses the infrared properties of a sample of fourteen CVs, and deduces a very useful result, that the maximum contributions of the red dwarfs to the infrared light are roughly independent of the properties of the disc and the spectral type of the red dwarf.

It would be preferable to devise a method of obtaining a more precise estimate of the fluxes of the red dwarfs than an an upper limit. The infrared light curves of highly inclined CVs provide such a method. They show a "secondary minimum", half a cycle later than the eclipse of the disc, which arises from the ellipsoidal variations of the tidally distorted red dwarf and its eclipse by the disc, the latter being always shallow because the disc is heavily foreshortened at high inclinations. The ellipsoidal variations of a star filling its Roche Lobe vary with the inclination of the system and the fraction of the light supplied by the red dwarf. For a system whose inclination is known, the amplitude of the secondary minimum measures directly the contribution of the red dwarf to the infrared light at the wavelength under study.

Chapter 2 describes a technique to simulate the light curves of tidally distorted stars. The simulations account for the observed infrared ellipsoidal light curves in U Geminorum, a highly inclined system whose infrared light comes entirely from the red dwarf.

Chapters 3 and 4 present a study of simultaneously measured visible and infrared light curves of OY Carinae, a highly inclined dwarf nova whose infrared light curves show both an eclipse of the disc and a secondary minimum. It was selected for study because it is one of only three known CVs where the eclipse of the white dwarf by the red dwarf is seen in the visible light curves. Based on the assumption that the red dwarf fills its Roche Lobe, Chapter 3 presents an analysis of these eclipses to find the following properties of the system: the inclination, the masses of the components and the radius of the red dwarf. Chapter 4 discusses the infrared light curves at J, H and K. The analysis addresses the questions of the contributions to the infrared light of the red dwarf and disc, deduced from the colours and the depth of the secondary minima, the distance to the system, and the nature of the infrared light of the disc and the region of the disc producing it.

Each chapter described above is a self-contained paper, intended for publication in the Monthly Notices of the Royal Astronomical Society. For this reason, British spellings are used throughout. Co-authors in these papers are as follows: Chapter 1, P. Szkody; Chapter 2, Ian Gatley, T. J. Lee, D. H. Beattie, P. Szkody and S. Mochnacki; Chapter 3, none, and Chapter 4, S. E. Persson.

Chapter 1.

INFRARED PROPERTIES OF CATACLYSMIC VARIABLE STARS.

SUMMARY

We present broad-band visible and infrared photometry (V, J, H, K) of fourteen Cataclysmic Variable Stars, and red photometry for seven of them. Analysis of the data based on flux ratio diagrams shows that the infrared light of these systems comes largely from the red dwarfs and from the opaque gas that occupies most of the accretion disc that surrounds the white dwarf companion, but the proportions of each vary widely from system to system. In systems having periods longer than 5h, such as SS Cyg, the red dwarfs supply nearly all the light at H, whilst in shorter period systems, such as UX U Ma, they supply less, no more than 50 to 80 per cent.

The diagrams also give upper limits to the fluxes of the red dwarfs at H that are insensitive to the physical conditions in the accretion disc and to the spectral types of the red dwarfs. Lower limits that are also independent of spectral types can be found in a number of systems only if it can be established that the opaque gas in the disc is hotter than 5000K.

Finally, we show that conditions around accretion discs are unfavourable to the formation of dust grains, whose thermal emission thus does not contribute significantly to the observed light of these systems. This result disagrees with previous work.

1. INTRODUCTION

The observational study of the red dwarfs in Cataclysmic Variable Stars (hereafter, CVs) is a difficult task because of the presence around the white dwarf companion of an accretion disc, made of matter transferred from the red dwarf through the process of Roche Lobe overflow (Warner 1976; Robinson 1976). This disc produces much of the visible and infrared light of these systems, and has thwarted previous searches for the red dwarfs (Wade 1982, Young and Schneider 1981). Observations in the near infrared (1-2μm), where a red dwarf chiefly radiates, hold much promise for the study of the red dwarfs in CVs. However, the emission from the disc may still be significant, and will complicate the analysis of infrared data because its character is likely to differ from that of the visible light. The latter comes largely from the hot, opaque gas occupying most of the disc (see, e.g., Williams 1980; Mayo et al 1981), but the infrared light will have a much larger contribution from the optically thin gas producing the Balmer emission lines and from cool opaque gas in the outer disc (Frank and King 1981) , both of which have a red energy distribution.

Because CVs have not been widely studied in the infrared and because the study of the red dwarfs is necessary in finding the distances to the systems, we examine in this paper the nature of the infrared light of fourteen CVs. We pay particular attention to the question of how much of the infrared light the red dwarf and the disc each supply.

2. OBSERVATIONS.

Table 1 presents the observational data. The objects consist largely of dwarf novae in quiescence, and span a wide range of orbital periods (90min to 9h). The JHK measurements of 1978 to 1980 were obtained at the 1.5m telescope at Mount Wilson Observatory and at the 1.3m telescope at Kitt Peak National Observatory. The data, obtained with cold InSb detectors and cold filters, were calibrated by frequent measurements of Johnson and CIT standard stars (Neugebauer, 1978; private communication), and have been placed in the CIT photometric system through the transformation of Frogel et al (1978). The 1σ uncertainties in these data are typically ± 0.04 mag, unless otherwise stated.

The American Association of Variable Star Observers (AAVSO) provided the corresponding visual magnitudes, where available (Mattei, 1981; private communication). In addition, the Variable Star Section of the Royal Astronomical Society of New Zealand (RASNZ) provided visual photometry of EX Hya (Bateson, 1981; private communication). These data are averages of the visual observations of an object made on the night of the infrared observations, and have typical uncertainties of ± 0.1 - 0.2 mag.

The fact that some of these systems are highly variable on short time scales and others are eclipsing does not introduce significant errors into the AAVSO and RASNZ data. For the eclipsing system EM Cyg, the uncertainty of ± 0.2 mag

at V is approximately the depth of its primary eclipse (Jameson et al 1981). The light curves of U Gem show not only an eclipse of the disc, but also a broad shoulder as the hot spot rotates into the line of sight (Warner and Nather 1971). However, the mean AAVSO magnitude is consistent with the mean magnitude of the visible light curve of Paczynski (1965), which is in turn consistent with the brightness of the uneclipsed disc. For the highly variable object YZ Cnc (Moffett and Barnes 1974), Table 1 quotes the ranges of its visual brightness during the nights of the infrared observations. The visible brightness of EX Hya was approximately constant during the infrared observations, but it too is usually highly variable (Warner 1972).

The VrJHK data of 1975 and 1976 are taken from Szkody (1977). The r filter is that of Sandage and Smith (1963), but it is adequate for our purposes to assume that its effective wavelength is identical to that of the Johnson (1966) R filter. Szkody's data are the averages of many observations on a given night. The data have not all been obtained simultaneously, but are generally reproduceable at all wavelengths from night to night and are consistent with the data of the objects in common observed in 1978 to 1980 (excepting TT Ari). Errors introduced into the data by flickering and cycle-to-cycle variability are thus small, especially so longward of r, where such variability is much less than in the visible (Szkody 1976).

Corrections for interstellar reddening, as deduced from the the 2200Å absorption band and from the colours of stars nearby on the sky, are generally small, having typical values of $E(B-V) < 0.05-0.10$ mag. There are occasional disagreements over the reddenings; in HR Del for example, values of E(B-V) from 0.06 to 0.29 mag have been found (see, e.g., Szkody 1981 and Krautter et al 1981, and references therein). Such reddenings do not, however, alter the essential results of this paper.

3. ANALYSIS.

(a) Properties of the red dwarfs and the accretion discs.

The red dwarfs in CVs most probably have the colours of Main Sequence stars, and their spectral types most probably lie in the range K0 to M6. Such red dwarfs have been found in the few systems where they have been studied (see, e.g., Tanzi et al 1981, Jameson et al 1981, Wade 1979, Berriman et al 1983).

The observed light comes from the red dwarf and from the disc, and must be decomposed into the relative contributions of each. This decomposition is difficult to perform because the disc consists of both optically thick and optically thin gas, both of which could have have a wide range of temperatures. Theoretical and observational studies, discussed in Appendix 1, show that the temperatures of the optically thin gas lie between 5,000K and 50,000K, and those of the opaque gas, between 3,000K or 5,000K and 50,000K. The uncertainty in the lowest temperature of the opaque gas comes about because the physical conditions in the outer disc, where this gas is found, are very poorly understood. Given the uncertainties in our knowledge of the structure of accretion discs, our analysis supposes that the light of the disc may consist of any combination of emission from opaque and transparent gas having the above range of temperatures.

This analysis improves upon that of previous infrared studies of CVs in two ways (see, e.g., Sherrington et al 1980, Jameson, King and Sherrington 1981, Frank et al 1981a): it takes account of the optically thin gas, which has a red energy distribution, but has hitherto been ignored; and, it does not assume that the disc has a spectrum of the form $F \propto \nu^{1/3}$, that of a steady state disc composed of black bodies. Appendix 1 discusses why such a model is unrealistic in the case of CVs.

Thermal emission from dust grains would, if significant, severely complicate the analysis of the infrared data. Dust grains form in many astrophysical environments (Cassinelli 1979), but a detailed analysis of the physical conditions in CVs, presented in Appendix 2, shows that they are unfavourable to the formation of dust grains. This conclusion disagrees with that of Frank et al (1981b), who proposed that a dust shell produces an upturn in the 2-3.5 μm spectrum of EX Hya; their data are, however, of low statistical accuracy.

(b) The flux ratio diagram.

The actual decomposition is best done with a flux ratio diagram, which is similar to a colour-colour diagram, but is based on the monochromatic fluxes at the wavelengths under consideration (Rabin 1980, 1982; Wade 1980). Figure 1a shows such a diagram based on the ratios $F_\nu(K)/F_\nu(H)$ and $F_\nu(V)/F_\nu(H)$. On it are shown the loci of the Lower Main Sequence, of the Upper Main Sequence (for temperatures

5000K<T<12000K), and of optically thin and optically thick emission. Black bodies have been used to represent the spectra of optically thick emission because theoretical colours have not been calculated over the wide range of temperatures considered here. This does not introduce significant errors into the analysis because the locus of black body spectra coincides with that of Upper Main Sequence dwarfs, whose gravities are similar to those of accretion discs (Mayo et al 1981).

The value of the diagram is that the contributions to the infrared light made by the red dwarf and the accretion disc can be found directly from it. This can be done because the observed ratios of a composite object lie on a straight line joining the ratios of its components, a consequence of the linearity of the axes. A generalisation of this rule is that the flux ratios of a disc consisting of arbitrary combinations of optically thin and optically thick emission of temperatures 5,000K - 50,000K must lie within the boundary ABC (shown on the figure). If the lowest temperature of the optically thick gas is 3000K, then the ratios of the disc must lie in the area AA'BC. Furthermore, the flux ratio of a CV lies along the line joining the ratios of its red dwarf to that of any point in area ABC (AA'BC).

As an example of the use of the diagram, consider that SS Cyg, whose flux ratio is shown as point S in Figure 1a, contains a K7 dwarf, and that the disc is everywhere hotter than 5,000K. The flux ratios of the disc then lie along the

line XY. The position of the line shows that SS Cyg contains a red disc (should the red dwarf be a K7 star), which implies that both optically thick and optically thin matter contribute to its infrared light. The proportions of the light at H supplied by the red dwarf and the disc are simply found from the diagram: if the flux ratio of the disc actually lay at W, then the distance SW represents the fractional contribution of the red dwarf, and the distance K7-S, that of the disc.

(c) The infrared light of the CVs.

We shall make use of two diagrams: the one described above, and a second one based on r rather than V, and shown in Figure 2. Both diagrams make use of the ratio $F_\nu(V)/F_\nu(H)$, the best available discriminator between red dwarfs and optically thin gas : the H-K colours of optically thin gas are always redder than those of red dwarfs, which is not true of the J-H and J-K colours (Frogel et al 1978; Ferland 1980).

Figures 1b and 2 show the positions of the CVs on the flux ratio diagrams. Where several measurements of a system have been made, the flux ratios of the most accurate data are shown. TT Ari is the only system to have varied significantly from measurement to measurement, but its flux ratios stayed approximately constant. Because the flux ratios of every system lies within the allowed area of the diagram, our prescription for the structure of a CV in the infrared is essentially correct. Of the three possible contributing sources, the red dwarf and opaque gas supply most of the infrared light, as no system is redder than $F_\nu(K)/F_\nu(H) = 0.9$ (H-K = 0.4). However, the large range of $F_\nu(V)/E_\nu(H)$, from 0.2 to 4 (V-H = 3.4 to 0.0), demands that the contributions of each vary widely from system.

(i) Systems having periods longer than 5h.

The longer period systems (P>5h) can accommodate larger, more luminous red dwarfs because their orbital dimensions are larger. In SS Cyg, EM Cyg and AE Aqr (all having periods of 6-9h), early K dwarfs supply roughly half the visible light (Stover et al 1980; Stover, Robinson and Nather 1981; Chincarini and Walker 1981). That these systems lie close to the Main Sequence in Figures 1b and 2 shows that the red dwarfs supply nearly all the infrared light (roughly 90 per cent). RX And, AH Her and SY Cnc are also long period systems. Because their flux ratios are close to those of SS Cyg, EM Cyg and AE Aqr, it is likely that most of the infrared light comes from the red dwarfs and not from cool, opaque gas (T~5,000K), whose flux ratios are similar to those observed.

Even though the red dwarfs supply most of the infrared light, their spectral classes nevertheless cannot be found accurately from the present data. Should a red dwarf of a given type be present in a CV, the extension of the line joining the ratios of the dwarf and the CV must intersect area ABC (or AA'BC), otherwise no combination of light from the disc and the red dwarf can account for the observed colours. The classifications in the long period CVs, deduced from an application of this rule to the data, are subject to two difficulties:

(1) Because the disc has a wide range of allowed colours, the observations can be reproduced by two kinds of combinations of a red dwarf and a disc: by either a K dwarf and a red disc or a late M dwarf and a blue disc;

and (2) Because the CVs lie close to the bluest allowed $F_\nu(K)/F_\nu(H)$ ratios and because in red dwarfs this ratio does not change quickly with spectral type, the range of spectral types permitted by the observed flux ratios are sensitive to their uncertainties. For the flux ratio of SS Cyg plotted on Figure 1a, this range is K3 to M2, but for a ratio 1σ redder than that plotted, the range becomes K0 to M6.

Visible spectroscopy thus provides the best classifications of the red dwarfs in the long period CVs. Until such observations of RX And, SY Cnc and AH Her are published, the best available classifications are those found from the present data: in RX And and AH Her, the red dwarf is later than K5 (from Figure 2), and in SY Cnc, later than K0 (from Figure 1b). Of the two diagrams, Figure 2 gives the better clasifications because the fact that the dwarfs supply more of the red light overcomes the slightly weaker dependence of their r-K colours on temperature.

By analogy with AE Aqr, SS Cyg and EM Cyg, it is likely that these three systems do contain K dwarfs. If this is so, the flux ratio diagrams show that their discs are redder than those of the short period systems (discussed below), presumably because the transparent gas supplies more of the

infrared light. Should any long period CV actually contain an M dwarf, it must be somewhat larger than a Main Sequence star of the same spectral type, presumably because of the effects of mass transfer.

(ii) Systems having periods shorter than 5h.

The remaining sytems have periods shorter than 5h, with the possible exception of TZ Per, whose period is unknown. These systems contain smaller, less luminous red dwarfs than the long period systems. Moreover, in the nova-like systems TT Ari and UX U Ma and in the dwarf nova Z Cam at standstill, the discs are thought to resemble those of dwarf novae in outburst, when the disc becomes hotter and much more luminous (see, e.g., Warner 1976, and Kiplinger 1980). For these two reasons, the short period systems are bluer than the long period ones, and thus lie inside boundary ABC. The red dwarfs supply as much as 50 to 80 per cent of the light at H, depending on the system.

U Gem is the exception to this rule, as nearly all the infrared light comes from the red dwarf (Wade 1979, Berriman et al 1983). To date, it is the only system having a period less than 5h of which this is true, and comes about because the disc is atypically underluminous and more highly inclined compared with other systems (Wade 1979).

The positions of TT Ari and Z Cam, close to the boundary AC, is consistent with the view that their discs are largely hot and optically thick. Visible observations suggest that neither system contains much optically thin material: TT Ari has weak emission lines superposed on wide absorption troughs (Cowley et al 1975), and Z Cam at standstill has absorption lines (Kiplinger 1980).

The redder $F_\nu(K)/F_\nu(H)$ ratios of the other short period systems most probably relect the fact that the optically thin gas supplies more infrared light than in TT Ari and Z Cam, as they all show emission lines, except UX U Ma. This system is unusual, in that its spectrum changes irregularly from emission to absorption (Holm, Panek and Schiffer 1982). Its infrared light may thus have a contribution from either optically thin gas or cool, optically thick gas (T~3000K).

The similarity of the ratios of UX U Ma and EX Hya to those of a disc having a spectrum $F_\nu \propto \nu^{1/3}$ led Sherrington et al (1980) and Frank et al (1981a) to conclude that such a disc is present in these systems. However, Figure 1b shows that there is not a unique interpretation of these observations: appropriate combinations of the light of a red dwarf, optically thin and optically thick gas also resemble the above energy distribution.

4. CONTRIBUTION OF THE RED DWARFS TO THE INFRARED LIGHT.

a) Maximum contributions of the red dwarfs.

Consider first the bluest systems in the sample, which have largely hot optically thick discs, and which lie in area ABC. The red dwarf makes its maximum contribution to the infrared light if opaque gas at the highest allowed temperature gives rise to the light of the disc, which then has its bluest colours. In the present case, where we take this temperature to be 50,000K, the maximum contribution to the light at H of a red dwarf of a specified type is given by the distance from the observed ratios to the boundary line BC, along the line joining the red dwarf to the CV (as discussed in Section 3a, above).

Because the slope of the locus of the Main Sequence is similar to that of the line BC, these contributions do not depend strongly on the spectral type of the red dwarf present in the CVs, an important result because the spectral types are unknown in most cases.

An exception to this rule is TT Ari. Should it contain a dwarf earlier than K7, its contribution is independent of the spectral type. However, since it is a short period system (P = 3h 50m), it most probably contains an M dwarf, as do other short period systems whose red dwarfs have been studied (e.g. DQ Her, AM Her, MV Lyr and U Gem; Young and Schneider 1981, 1980; Schneider et al 1981; Wade 1979). For such a

dwarf to be present in TT Ari, the $F_\nu(K)/F_\nu(H)$ ratio must lie inside ABC, which is allowed by the uncertainties in the data. Figure 1 shows that the actual contribution of the M dwarf depends on how far inside the boundary the ratio actually lies. Z Cam also lies close to the lower boundary of the flux ratio diagram, but does not suffer from the same problem because it is known that the red star is a K5-K7 star (Wade 1982).

A second important result is that the maximum contributions are roughly independent of the assumed maximum temperature present in the disc. This is because the energy distributions of hot, opaque gas in the visible and infrared approximate a Rayleigh Jeans spectrum at all temperatures. If, for example, the opaque material were no hotter than 20,000K, rather than 50,000K, then the red dwarf would be able to supply ~10 per cent less of the light for all the blue systems, excepting HR Del and TT Ari (should its spectral type be earlier than K7; see above), where they supply ~25 per cent less. They are somewhat bluer than the other systems, and the contributions of their red dwarfs are thus more sensitive to the limiting temperature.

These maximum contributions and the observed H magnitudes together give bright limits to the H magnitudes of the red dwarfs, to be used in a future paper to estimate the distances to the CVs (Berriman 1983). The uncertainties discussed above do not introduce serious errors into these distances, since to derive them the magnitudes of the red dwarfs are divided by

five.

In the long period systems, similar maximum contributions of the red dwarfs can be found, but for a different reason: because most of the infrared light comes from the red dwarfs, the proportions they contribute are insensitive to the limiting temperatures. This is particularly important if, as seems likely, the discs in these systems are redder than those in the short period systems, as the actual proportion depends more on the lowest temperature of the transparent gas than that of the opaque gas. The $F_\nu(K)/F_\nu(H)$ ratios of cool plasmas are very sensitive to temperature: they effectively measure the slope of the Pfund continuum, which becomes redder at lower temperatures because the amount of free-free emission declines rapidly.

Consider, for the sake of example, that the transparent gas is as cool as 2,500K. The flux ratios of its recombination emission are $F_\nu(K)/F_\nu(H) = 1.8$ (H-K = 1.2) and $F_\nu(V)/F_\nu(H) = 0.2$ (V=H = 3.2) (Ferland 1980; the actual ratios would be bluer, because the H^- ion would give rise to most of the opacity ; see Mihalas 1978). The colours are much redder than those of a plasma at 5,000K, yet the red dwarfs in the CVs would be able to supply ~5 per cent more of the light.

Table 1, discussed below, presents the bright limits to the H magnitudes of the red dwarfs deduced from the flux ratio diagrams.

(b) Minimum contributions of the red dwarfs.

Just as the red dwarfs contribute most to the infrared light when the disc is bluest, so they contribute least when the discs are reddest. Such lower limits can only be found for the longer period systems, where the reddest disc colours can still be bluer than those observed. However, should the disc contain any opaque gas cooler than ~5,000K, then such minimum contributions cannot be found, because the gas is indistinguishable from the red dwarfs.

The faint limits presented in Table 1 have been deduced for a disc that is everywhere hotter than 5,000K. As in the case of the bright limits, they are roughly independent of spectral type because boundary line AB has a slope similar to that of the Main Sequence. In view of the uncertainties in the lowest temperatures in the disc, these faint limits should not be regarded as definitive, but rather as illustrative of the weak dependence on spectral type.

(c) Results.

Table 2 presents the variation with spectral type of the H magnitudes of the red dwarfs. The restrictions on the spectral types in AE Aqr, EM Cyg, SS Cyg, Z Cam and U Gem are based on visible spectra (as discussed in Section 3). For the other systems, the broad limits given are those deduced from the flux ratio diagrams.

For the short period systems, the table gives the bright limits to the H magnitudes of the red dwarfs. For the long period systems, it gives both the bright and faint limits.

YZ Cnc has been excluded from the table because the uncertainties in its flux ratios are too large to allow accurate determinations of the conribution of the red dwarf. For TT Ari, only the bright limits for red dwarfs earlier than K7 are given, because the contributions of later type stars depend critically on the uncertainties in the data (as discussed above).

The H magnitudes for the long period systems have uncertainties of <0.2 mag. They come largely from the statistical errors in the infrared photometry, and reflect the fact that the difference between the infrared colours of red dwarfs and of optically thin emission is small. Uncertainties of ± 0.06 and ± 0.09 in the ratio $F_\nu(K)/F_\nu(H)$ introduce errors of ± 0.1 and ± 0.2 mag into each H magnitude. The spectral baselines of the $F_\nu(V)/F_\nu(H)$ and $F_\nu(r)/F_\nu(H)$ ratios are much

longer than that of the above ratio, and uncertainties in V and r produce correspondingly smaller errors in the H magnitudes. Typically, uncertainties of ±0.1 and ± 0.2 mag in V give errors of ±0.05- 0.10 mag in H. Two other sources of uncertainty produce errors of <0.05 mag in H:

1. The data of Veeder (1974) show that there is a dispersion in the V-H and H-K colours of M dwarfs (in the system of Boeshaar) of ±0.05 mag.

2. The Hα and Bγ lines contaminate the r and K filters, respectively. For the objects studied here, the Hα lines (Oke and Wade 1982) produce <2% of the flux transmitted by the r filter. The Bγ line strengths in CVs have not been measured, but for the temperatures and densities believed to be found in accretion discs (T~ 5,000K-50,000K; N~10(12)-10(15) cm-3), their strengths are <0.1 of those of Hα (Drake and Ulrich 1980). Typically, Bγ should contribute no more than 3 per cent of the light transmitted by the K filter.

5. CONCLUSIONS.

We have presented broad-band photometry of fourteen CVs. The data show that:

1. The red dwarfs and the opaque gas supply most of the infrared light, but the proportions of each vary widely from system to system. In the longer period systems, the red dwarfs can supply nearly all of the light at H, and in the shorter period systems, up to 50-80 per cent, depending on the system.

2. The data give bright limits to the infrared brightness of the red dwarfs. In most systems, these limits are insensitive to the assumed physical conditions in the accretion discs and to the spectral types of the red dwarfs.

3. Faint limits to the brightness of the red dwarfs are difficult to obtain because the lowest temperature of the opaque gas is not well known. Such limits can be obtained for a number of systems, if it can be established that the outer disc is hotter than 5,000K. Again, these limits are roughly independent of the spectral types of the red dwarfs.

APPENDIX 1.

PHYSICAL CONDITIONS IN ACCRETION DISCS.

The detailed structure of the discs has been vigorously studied in the past decade, but remains poorly understood (Pringle 1981). It is thought that the bulk of the gas is optically thick and that its temperature increases radially inwards. This increase comes about because viscous drag makes the gas move slowly inwards, whereupon its temperature increases as it falls deeper into the gravitational well of the white dwarf.

Most models of accretion discs predict that this opaque gas attains a temperature of ~50,000K in the inner disc, which is generally consistent with the temperatures deduced from ultra-violet observations (see, e.g., Krautter et al 1981).

The lowest temperature, found in the outer disc, depends largely on the viscosity of the gas, a poorly known parameter (see Pringle, op cit). At progressively higher viscosities, the material moves inwards more rapidly, causing the density of the outer disc to decrease; consequently, the optical depth and the radiative efficiency of the gas also decrease, and the temperature increases. For the viscosities thought to be found in CVs, the lowest temperature may lie between 5000K (Williams 1980) and 3000K (Frank and King 1981). These temperatures correspond, respectively, to the viscosities produced by supersonic turbulence, a very efficient mechanism in removing the angular momentum of the gas, and subsonic

turbulence, which is much less efficient.

The transparent gas provides more of the infrared than of the visible light because it has a red spectrum at all temperatures. In this regard, Berriman and Persson (1983) argue that most of the infrared light of the disc in OY Car comes from optically thin gas. Its emission in the visible may also be significant,however, as Kiplinger (1979) found that some of the Balmer continuum emission of SS Cyg must be optically thin, to reproduce the observed spectrum and luminosity.

The available spectroscopic observations do not unambiguously determine the location or temperature of the optically thin gas (Young and Schneider 1980; Stover 1981; Williams and Ferguson 1982). It most probably lies in the outer disc, at a temperature of ~5000K (Williams 1980) or in a chromosphere at T= 10(4)K-10(5)K produced by X-ray photo-ionization of the outer skin of the disc (Jameson, King and Sherrington 1980). Again, the lowest temperature of this gas is somewhat uncertain, but is unlikely to be much lower than 5000K because transparent gas cannot radiate efficiently and because X-ray photoionization and mass transfer will maintain its internal energy.

In this paper, we do not suppose, as has been done in the past, that the disc has a spectrum of the form $F_\nu \propto \nu^{1/3}$. This is the spectrum of a steady state disc that radiates everywhere as a black body, a model that is unrealistic

because it ignores the modification of the spectrum by line blanketing, which is severe in the hotter regions, and by electron scattering, which will flatten the spectrum. Furthermore, this model cannot reproduce the observed spectra and luminosities of the discs in U Gem and SS Cyg in quiescence, two systems whose distances are known (Wu and Panek 1982; Kiplinger 1979).

APPENDIX 2.

DUST IN CATACLYSMIC VARIABLE STARS.

We explore both an observational and a theoretical approach to this problem. Section a) derives the maximum infrared luminosity of a dust shell, considered to produce all the observed reddening in the line of sight to a CV. Section b) examines whether conditions in CVs are favourable to the formation of CVs.

a) Infrared emission from dust.

We estimate the maximum infrared luminosity of a spherical dust shell and show that it is a small fraction of the integrated light of the red star and disc.

As discussed in Section 2, the observed reddenings are no more than E(B-V)= 0.3 mag. From this value can be estimated the number of grains in the shell, which is presumed to have a diameter, d, no larger than the dimensions of the system, ~10(11)cm. The column density of hydrogen (HI + H2) in the shell is roughly proportional to its colour excess (Bohlin et al 1978); the column density corresponding to a colour excess of 0.3 mag is 2 x 10(21) cm-2. For a gas-to-dust ratio of ~100 by mass (Wynn-Williams et al 1972), the corresponding mass of dust in the shell, Mg, is given by

$$M_g = 2 \times 10^{16} \left(\frac{d}{10^{11}\,cm} \right) M_\odot$$

A shell of this mass contains N_d graphite grains of radius a ,

and density, ρ, of 3 g cm-3 where

$$N_g = 2 \times 10^{32} \left(\frac{a}{0.05\mu m}\right)^{-3} \left(\frac{d}{10^{11} cm}\right)^{2}$$

Each grain, at a temperature Tg, radiates a power Lg, given by (Dwek et al 1980):

$$L_g = 1.2 \times 10^{-9} \left(\frac{a}{0.05\mu m}\right)^{3} \left(\frac{T_g}{1500K}\right)^{5} \text{ Watts}$$

for $a > 0.05\mu m$, and

$$L_g = 1.8 \times 10^{-10} \left(\frac{a}{0.05\mu m}\right)^{4} \left(\frac{T_g}{1500K}\right)^{6} \text{ Watts}$$

for $a < 0.05\mu m$. The total infrared luminosity of the shell, P, is

$$P = L_g N_g$$

$$= 2.7 \times 10^{23} \left(\frac{T_g}{1500K}\right)^{5} \left(\frac{d}{10^{11} cm}\right)^{2} \text{ Watts}$$

for $a > 0.05\mu m$, and

$$P = 4 \times 10^{22} \left(\frac{T_g}{1500K}\right)^{6} \left(\frac{a}{0.05\mu m}\right) \left(\frac{d}{10^{11} cm}\right)^{2} -$$

$$- \text{Watts}$$

for $a < 0.05\mu m$.

Grains around accretion discs will be no hotter than 1500K (see next Section). Such grains radiate chiefly at 2-3μm, and will supply the maximum contribution of dust grains to the infrared light of a CV. The expressions immediately above show that this contribution is <10% of the 2μm power of a CV having, e.g., K=14 and lying at 250pc.

b)The formation of dust in CVs.

There are two places in CVs where dust can condense: in a shell surrounding the system (where the X and UV radiation of the inner disc irradiate the grains) and in or near the outer disc (where the main body of the disc shields the grains from the light of the inner disc). For these two regions, we discuss separately the formation of dust grains and their subsequent rate of growth. These discussions are based on the theory of the formation of graphite grains in nova shells (Clayton and Wickramasinghe 1976), which has successfully explained the properties of dust in novae shells (see, e.g. , Gehrz et al 1980).

i) The formation of dust grains.

Dust grains condense through collisions between carbon atoms and "condensation nuclei", groups of diatomic molecules (CH, CH+ etc) (Wickramasinghe 1972). The condensing grains radiate inefficiently, and can only form far from the disc, whose light must become sufficiently dilute that it is in thermal equilibrium with the grains. From this condition, the minimum distance from the disc, r_o, where grains can condense is:

$$\pi a_o^2 \left(\frac{L}{4\pi r_o^2}\right) \bar{Q}(T_*, a_o) = 4\pi a_o^2 \sigma T_g^4 \times \bar{Q}(T_g, a_o) \quad -(1)$$

Here, a_o is the radius of a condensation nucleus at a temperature Tg . L is the luminosity of the disc, and T* is its temperature, considered here to be uniform. $\bar{Q}(T,a)$ is the absorption efficiency of a grain averaged over a Planck distribution. For small (a<0.1μm) graphite grains at T<1500K, it is given approximately by (Clayton and Wickramasinghe 1976):

$$\bar{Q} = 3.22 \left(\frac{T}{10K}\right)^{1.65}$$

At temperatures hotter than 10,000K, characteristic of the temperatures in accretion discs, the absorption efficiency, $\bar{Q}$, is approximately unity, independent of grain size.

Equation (1) may thus be re-written

$$\frac{L}{4\pi r_o^2} = 4\sigma T_g^4 \times 3.22\, a_o \left(\frac{T_g}{10K}\right)^{1.65}$$

and r_o is thus given by

$$r_o = 0.92 (\pi\sigma)^{-1/2} L^{1/2} a_o^{-1/2} T_g^{-2.82} \quad -(2)$$

Circumsystem dust shell

The presence of P Cygni absorption profiles in the UV emission lines of some CVs (Krautter et al 1981; Cordova and Mason 1982) shows that winds carry away significant quantities of matter from the disc. The winds have velocities <5000 km s-1, the approximate velocity of escape from the white dwarf.

Dust grains condensing out of this wind would form a shell around the system. The condensing grains will have temperatures of at most 1500K (Wickramasinghe 1967) for the densities of condensable carbon atoms to be considered here (<1000 cm-3). The X and UV luminosities of accretion discs are typically $1L_{\odot}$ (Fabbiano et al 1981; Cordova et al 1981; Krautter et al 1981). In this case, r_o is given by

$$r_o = 120\left(\frac{L}{1L_{\odot}}\right)^{1/2}\left(\frac{T_g}{1500K}\right)^{-2.82} R_{\odot}$$

where a_o=3 x 10(-7)cm.

Dust grains in the plane of the disc

Some of the matter transferred from the red dwarf carries angular momentum away from the disc by flowing out of the system through the outer Langrangian point (see Novikov and Thorne 1973). The outer wall of the disc irradiates dust grains condensing out of this escaping matter.

The luminosity of the wall is

$$L = 2\pi r_d z \sigma T_*^4$$

where r_d and z are the radius and thickness of the disc, respectively, and T* is the temperature of the outermost regions of the disc. Typically, $r_d = 5 \times 10(10)$cm (Sulkanen et al 1981); z = 10(10)cm (Mayo et al 1981) and $T^* \gg 3000K$; hence, we find $L = 0.004 L_\odot$. Equation (2) then gives r_o:

$$r_o = 7.6 \left(\frac{L}{0.004 L_\odot}\right)^{1/2} \left(\frac{T_g}{1500K}\right)^{-2.82} R_\odot$$

ii) Rate of growth of dust grains

As the matter matter leaving the disc expands beyond r_o, the rate of growth of grains is given by (Wickramasinghe 1972):

$$\frac{da}{dt} = \left(\frac{\alpha}{\rho_g}\right)(n_c)_o \left(\frac{t}{t_o}\right)^{-3} \left(\frac{k m_c}{2\pi}\right)^{1/2} \left\{T(t)\right\}^{1/2}$$

$(n_c)_o$ is the density of condensable carbon atoms at $r=r_o$ and t_o is the time for the matter to travel there. ρ_g is the density of graphite, α is the probability that an atom of carbon sticks to a condensation nucleus in a collision; $\frac{\alpha}{\rho_g}$ =0.1 cm3 g-1 for graphite. k is Boltzmann's constant and m_c is the mass of a carbon atom. T(t) is the gas temperature. The final results of the analysis do not depend strongly on its value (Clayton and Wickramasinghe discuss this point in detail). Here, we consider it to equal the temperature of a black body which would produce the same flux as the disc at a distance r_o from it:

$$\frac{L}{4\pi r_o^2} = 4\sigma T^4$$

If the dust shell expands uniformly outwards, then

$$T^4 = \left(\frac{L}{16\pi\sigma r_o^3}\right)$$

The rate of growth of the grains may thus be expressed as

$$\frac{da}{dt} = 4.4\times10^{-21}(n_c)_o L^{1/8} r_o^{-1/4} (t/t_o)^{-3.25} \mu m\, s^{-1}$$

$$= K(n_c)_o \left(\frac{t}{t_o}\right)^{-3.25}$$

The solution to this equation gives the radius of the grain at time t:

$$a = a_o + 0.44\, K (n_c)_o\, t_o \left\{ 1 - \left(\frac{t}{t_o} \right)^{-2.25} \right\}$$

As t becomes very large, the grain grows by an amount a_∞, where

$$a_\infty = 0.44\, K (n_c)_o\, t_o$$

Circumsystem dust shell

For a dust shell condensing at $r_o = 120 R_\odot$ from a wind of solar metal abundance moving at 5000 km s-1 and carrying away mass at a rate 5 x 10(-11)$M_\odot$ yr-1 (inferred from the P Cygni profiles), we find: $(n_c)_o = 1.5$ cm-3, t =16800s; as before, $L = 1 L_\odot$. Thus, $a_\infty = 5 \times 10(-12) \mu$m.

Dust grains cannot condense out of the wind because the density of condensable atoms is very low. Densities of nine or more orders of magnitude higher will permit the formation of grains; such densities are found in the dust shells of novae (Gehrz et al 1980)

Dust grains in the plane of the disc

The properties of the matter flowing from the outer Lagrangian point are highly uncertain. Prendergast and Taam (1974) suggested a density of ~10(9)cm-3 and and a velocity ~300km s-1. The largest grains which can grow from this stream will be those condensing from matter escaping as a jet, so that the density does not significantly decrease. For the conditions specified above and for $r_o = 1.8 R_\odot$, $(n_c)_o = 3.5 \times 10(5)$cm-3 and t =17700s. Then, a =10(-6)μm. Again, the density of condensable atoms is too low to allow dust grains to condense.

iii) Formation of grains in the outer disc.

If the outer disc has a temperature as low as ~2000K, the density of condensable atoms is sufficiently high (n_c ~10 (10)cm-3) that grains may grow there. The thermal emission from these grains is negligible because the grains radiate much less efficiently than the material in the disc, as the following argument shows.

Consider a disc of radius 5x10(10)cm having a thickness 10(10)cm and a cool outer region of the same width (Mayo et al 1981). For a gas-to- dust ratio of ~100 by mass (Wynn Williams et al 1972), the mass of dust in the outer disc is

$$M_g = 4 \times 10^{-12} M_\odot$$

The total number of graphite grains is

$$N_g = 3 M_g / 4\pi a^3 \rho_g = 7 \times 10^{22}$$

The total power radiated by these grains in the near infrared is ~6x10(15) watts . If, as seems probable, the hot, optically thick regions of the disc is hotter than 10,000K and has a radius 10(10)cm, its near infrared luminosity of >10(23) Watts is much higher than that of the grains.

Table 1: Compilation of the VrJHK photometry of the Cataclysmic Variable Stars.

Object	Class	Period (days)	Date (UT) (yr/m/d)	Phase	V	r	J	H	K
(1)	(2)	(3)	(4)	(5)	(6)	(7)	(8)	(9)	(10)
RX And	DN	0.23	75/7/27	min	13.39	13.83	11.83	11.43	11.21
AE Aqr	NL	0.41	75/8/1,2,3	-	11.39	10.58	9.43	8.80	8.71
			79/5/26	-	11.3 ± 0.1	-	9.43	8.83	8.76
			79/6/9	-	11.3 ± 0.1	-	9.46	8.82	8.74
TT Ari	DN	0.14	76/7/13	max	10.69	-	10.66	10.68	10.68
			78/7/3	max	10.3 ± 0.1	-	10.14	10.22	10.21
			78/7/5	max	10.5†	-	10.19	10.26	10.20
			79/11/11	max	10.5†	-	10.20	10.21	10.22
			79/1/2	max	10.5†	-	10.15	10.17	10.15
Z Cam	DN	0.29	75/11/14,15,16	s	11.47	11.30	10.78	10.46	10.40
			78/1/2	s	11.5 ± 0.1	-	10.8 ± 0.1	10.5 ± 0.1	10.4 ± 0.1
			79/1/13	s	11.6 ± 0.1	-	10.9 ± 0.1	-	10.3 ± 0.1
SY Cnc	DN	0.49	80/1/5	min	13.3 ± 0.1	-	11.51	11.48	11.21
YZ Cnc	DN	-	79/12/8	min	13.7 - 14.3	-	12.9 ± 0.1	12.5 ± 0.1	12.4 ± 0.1
EM Cyg	DN	0.29	78/7/1	min	13.9 ± 0.2	-	11.76	11.33	11.08
SS Cyg	DN	0.27	76/8/11	min	12.01	11.28	9.98	9.53	9.40
			79/6/1	min	12.2 ± 0.1	-	10.02	9.54	9.40
			79/6/8	min	12.2 ± 0.1	-	10.00	9.57	9.41
HR Del	N	0.17	78/7/2	-	12.0 ± 0.2	-	11.95	11.88	11.73
U Gem	DN	0.18	79/2/26	min	14.7	-	11.95††	11.32††	11.05††
AH Her	DN	0.26*	75/8/2	min	14.17	13.55	12.41	12.03	11.63
			79/4/16	min	14†	-	12.3 ± 0.1	12.0 ± 0.1	11.5 ± 0.1
EX Hya	DN	0.07	78/7/2	min	12.0 ± 0.1	-	12.1 ± 0.1	12.08 ± 0.06	11.78 ± 0.06
TZ Per	DN	-	75/8/23	s	13.25	12.98	12.11	11.96	11.81
UX U Ma	NL	0.20	78/7/2	-	12.79	12.70	12.03	11.96	11.68
			79/5/20	-	13†	-	12.1 ± 0.1	11.0 ± 0.1	11.8 ± 0.1

Notes:

Column (2): DN= dwarf nova; NL= nova-like; N= nova.

Column (3): Orbital period, taken from the literature, except *Horne, 1982 (private communication).

Column (4): Outburst phase of dwarf novae: min= minimum; max= maximum; s= standstill

†No AAVSO data available; eye estimate of V.

††Mean magnitudes of system through orbit; see text.

Table 2: Apparent H magnitudes of the red dwarfs in Cataclysmic Variable Stars.

Red Dwarf	K0	K2	K5	K7	M0	M2	M4	M6
Object (1)	(2)	(3)	(4)	(5)	(6)	(7)	(8)	(9)
RX And	-	-	11.7 - 13.6	11.6 - 13.8	11.6 - 14.1	11.6 - 14.2	11.5 - 14.2	12.3 - 14.2
AE Aqr	-	-	8.8	-	-	-	-	-
TT Ari	>11.3	>11.3	>11.3	-	-	-	-	-
Z Cam	>10.2	>10.7	>10.7	>11.5	-	-	-	-
SY Cnc	>11.8	>11.8	>11.7	>11.7	>11.7	>11.7	>11.6	>11.5
EM Cyg	-	-	11.5 - 11.9	11.5 - 12.1	-	-	-	-
SS Cyg	-	-	9.7 - 9.9	9.6 - 10.2	-	-	-	-
HR Del	>12.6	>12.7	>12.7	>12.6	>12.5	>12.5	>12.5	>12.7
AH Her	-	-	12.5 - 13.4	12.5 - 13.7	12.5 - 13.8	12.4 - 13.8	12.3 - 13.9	12.3 - 14.0
EX Hya	>12.7	>12.7	>12.7	>12.7	>12.6	>12.6	>12.6	>12.7
TZ Per	>12.2	>12.2	>12.2	>12.2	>12.2	>12.3	>12.7	>13.4
UX U Ma	>12.5	>12.5	>12.5	>12.5	>12.4	>12.4	>12.3	>12.3

Columns (2) to (9) give the apparent H magnitudes that red dwarfs of types K0 to M6 may have if present in the systems listed in Column (1).

REFERENCES

Berriman G. 1983, In preparation.

Berriman G and Persson SE. 1983, In preparation.

Berriman G, Beattie DH, Gatley I, Lee TJ, Mochnacki SW and Szkody P. 1983, Mon Not Roy ast Soc, In press.

Boeshaar P. 1976, Ph.D Thesis, Ohio State University.

Bohlin RC, Savage BD and Drake JF. 1978, Astrophys J, 224,132.

Bohm-Vitense E. 1981, Ann Rev Astron Astrophys,19,295.

Cassinelli, J.P. 1979, Ann Rev Astron Astrophys, 17, 275.

Chincarini G and Walker MF. 1981, Astron Astrophys, 104, 24.

Clayton DD and Wickramasinghe NC. 1976, Astrophys Spa Sci, 42, 463.

Cordova FA, Jensen KA and Nugent JJ. 1981, Mon Not Roy ast Soc,196,1.

Cordova FA and Mason KO. 1982, Astrophys J, submitted.

Cowley, AP, Crampton, D, Hutchings, JB, and Marlborough, JM . 1975, Astrophys J, 195, 413.

Drake SA and Ulrich RF,1980. Astrophys J Suppl Ser,42,351.

Dwek E, Sellgren K, Soifer BT and Werner MW. 1980, Astrophys J, 238,140.

Fabbiano G, Hartmann L, Raymond J, Steiner J, Branduardi-Raymont G and Matilsky T. 1981, Astrophys J,243,911.

Ferland GJ. 1980, Pub Ast Soc Pac,92,596.

Frank J and King AR. 1981, Mon Not Roy ast Soc,196,507.

Frank J, King AR, Sherrington MR, Jameson RF and Axon DJ. 1981a, Mon Not Roy ast Soc,195,505.

Frank J, King AR, Sherrington MR, Giles AB and Jameson RF.1981b, Mon Not Roy ast Soc,196,921.

Frogel JA, Persson SE, Aaronson M and Matthews K. 1978, Astrophys J, 220,75.

Gehrz RD, Hackwell JA, Grasdalen GL, Ney EP, Neugebauer G, Sellgren K. 1980, Astrophys J, 239,576.

Holm, AV, Panek, RJ, and Schiffer, FH III. 1982, Astrophys J, 252, 135.

Jameson RF, King AR and Sherrington MR. 1981, Mon Not Roy ast Soc,195, 235.

----------1980, Mon Not Roy ast Soc,191, 559.

Johnson HL. 1966, Ann Rev Astron Astrophys,4,193.

Kiplinger AL. 1980, Astrophys J, 236, 840.

------ 1979, Astrophys J, 234, 997.

Krautter J, Klare G, Duerbeck HW, Rahe J, Vogt N and Wargau W. 1981, ESO Preprint 152.

Mayo SK, Wickramasinghe DT and Whelan JAJ.1981, Mon Not Roy ast Soc, 193,793.

Mihalas D. 1978, " Stellar Atmospheres" (WH Freeman and Co, San Francisco), p102.

Moffett TJ and Barnes TG III. 1974, Astrophys J,194,141.

Oke JB and Wade RA. 1982, Astron J, 87,670.

Paczynski, B. 1965, Acta Astron, 15, 89.

Prendergast KH and Taam RE.1974, Astrophys J,189,125.

Pringle, JE. 1981, Ann Rev Astron Astrophys, 19, 37.

Rabin DM.1982,Preprint.

---------1980, Ph.D Thesis, Calif. Inst. Tech.

Robinson EL.1976, Ann Rev Astron Astrophys, 14,119.

Robinson EL, Nather RE and Patterson J. 1978, Astrophys J, 219, 168.

Sandage AR and Smith LL. 1963, Astrophys J, 137,1057.

Schneider DP, Young PJ and Schectman SA.1981, Astrophys J,245,644.

Sherrington MR, Lawson PA, King AR, Jameson RF. 1980 Mon Not Roy ast Soc,191,185.

Stover RJ, Robinson EL and Nather RE.1981, Astrophys J,248,696.

Stover RJ, Robinson EL, Nather RE and Montemayor TJ. 1980, Astrophys J, 240,597.

Szkody, P. 1981, Astrophys J, 247,577.

----------1977, Astrophys J, 217,140.

----------1976, Astrophys J, 207, 824.

Sulkanen ME, Brasure LW and Patterson J.1981, Astrophys J,244,579.

Tanzi EG, Chincarini G and Tarenghi M. 1981, Pub Ast Soc Pac,93,68.

Veeder GJ. 1974, Astron J, 79,1056.

Wade, RA. 1982, Astron J, 87, 1558.

----------1979, Astron J, 84, 562.

Warner B.1976, Proc IAU Symp 73, PP Eggleton et al,eds. (Reidel, Dordrecht).

---------1972, Mon Not Roy ast Soc,158,425.

Warner B and Nather RE. 1971, Mon Not Roy ast Soc, 152,219.

Wickramasinghe NC.1972, "2nd Advanced Course in Astrophysics, Saas-Fe", Wickramasinghe NC et al,eds (Geneva Observatory).

----------1967, "Interstellar Grains" (Chapman and Hall).

Williams RE. 1980, Astrophys J,235,939.

Williams RE and Ferguson DF.1982, Astrophys J submitted.

Wynn-Williams G, Becklin EE and Neugebauer G.1972, Mon Not Roy ast Soc 160,1.

Wu, CC, and Panek RJ. 1982, Astrophys J, 244, 252.

Young PJ and Schneider DP.1981, Astrophys J,247,960.

---------- 1980, Astrophys J,238,955.

FIGURE CAPTIONS.

Figure 1

(a) A flux ratio diagram based on the ratios $F_\nu(V)/F_\nu(H)$ and $F_\nu(K)/F_\nu(H)$. It shows the loci of monochromatic black body spectra, of filter-averaged optically thin spectra, of the Lower Main Sequence and of the Upper Main Sequence (for 5000K<T<12000K). The black bodies describe optically thick emission from the accretion disc. The optically thin spectra are from Ferland (1980). The effective temperatures of the Upper Main Sequence are from Bohm- Vitense (1981), and the flux ratios derived from Johnson (1966) and Neugebauer (1978; private communication). The flux ratios of the Lower Main Sequence are from Frogel et el (1978), Young and Schneider (1981) and Johnson (1966). The spectral types of M dwarfs refer to the classification scheme of Boeshaar (1976).

The flux ratios of a physically plausible disc lie within the area ABC if the lowest temperature of the optically thick gas is 5000K, and within area AA'BC, if it is 3000K. Point S represents the flux ratio of SS Cyg,used in the text to illustrate the use of the diagram. The text explains the points X,Y and W.

(b) Positions of the observed flux ratios ofthe CVs are shown on the diagram.

Figure 2.

A flux ratio diagram for discs hotter than 5000K ,based on the ratio $F_\nu(r)/F_\nu(H)$, rather than $F_\nu(V)/F_\nu(H)$. The features of this diagram are similar to those of Figure 1.

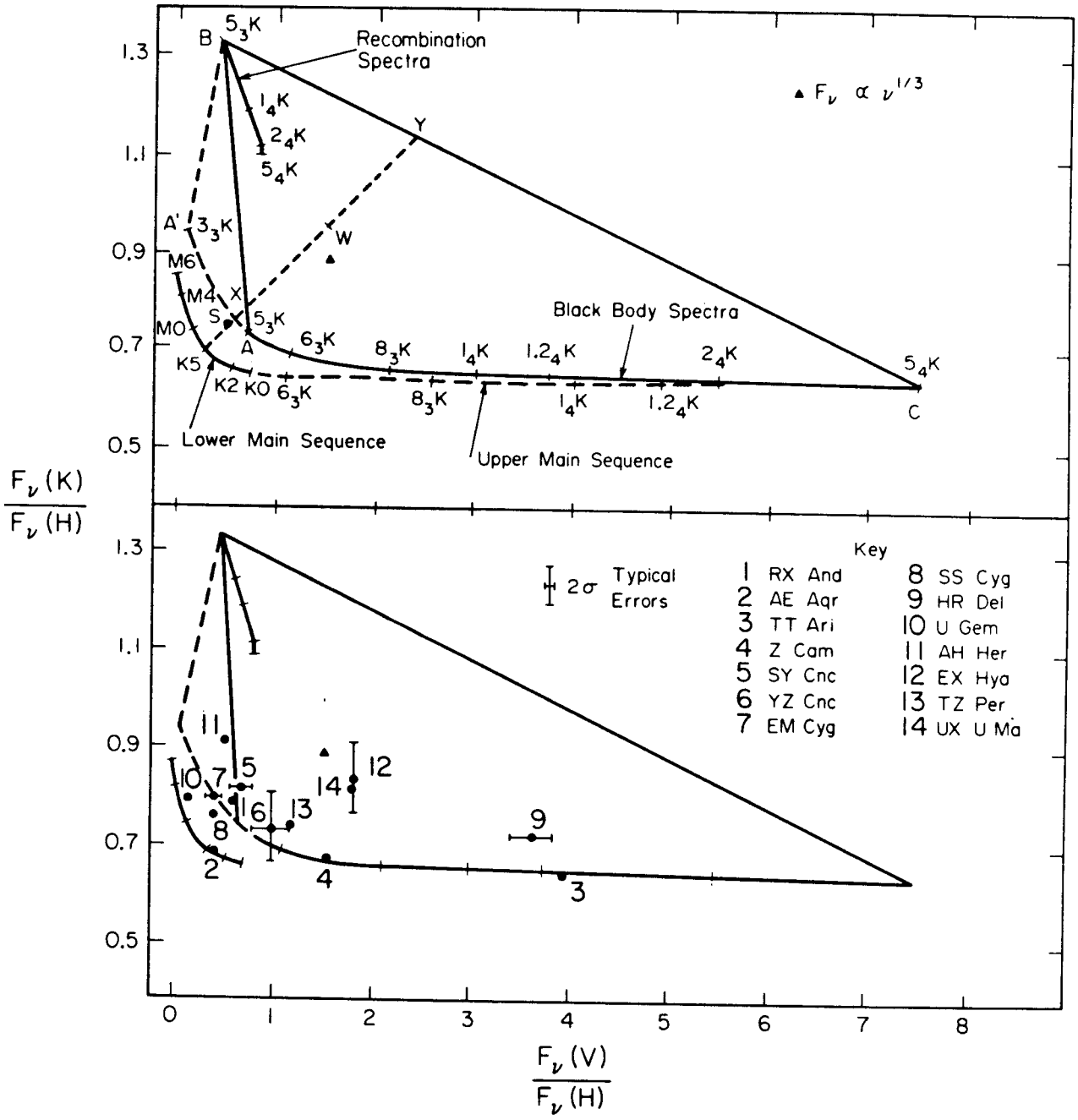
B
5_3K
Recombination Spectra
1_4K
2_4K
5_4K
Y
W
A'
3_3K
M6
M4
X
S
MO
5_3K
A
6_3K
8_3K
1_4K
1.2_4K
2_4K
5_4K
C
K5
K2
KO
6_3K
8_3K
1_4K
1.2_4K
Black Body Spectra
Lower Main Sequence
Upper Main Sequence
▲ $F_\nu \propto \nu^{1/3}$
$\frac{F_\nu(K)}{F_\nu(H)}$
1.3
1.1
0.9
0.7
0.5
2σ Typical Errors
Key
1 RX And
2 AE Aqr
3 TT Ari
4 Z Cam
5 SY Cnc
6 YZ Cnc
7 EM Cyg
8 SS Cyg
9 HR Del
10 U Gem
11 AH Her
12 EX Hya
13 TZ Per
14 UX U Ma
0
1
2
3
4
5
6
7
8
$\frac{F_\nu(V)}{F_\nu(H)}$

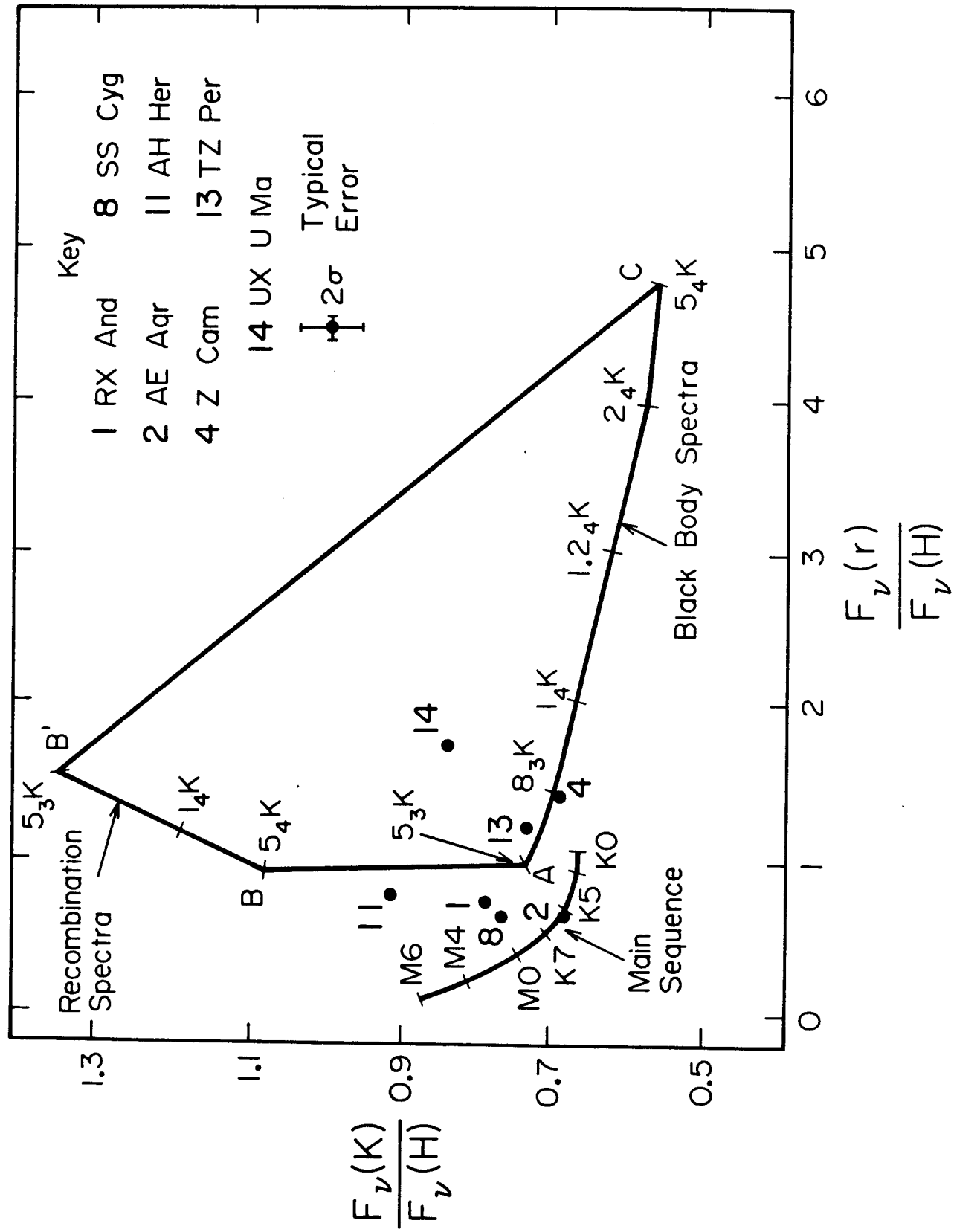
Key
1 RX And
2 AE Aqr
4 Z Cam
8 SS Cyg
11 AH Her
13 TZ Per
14 UX U Ma
Typical Error
2σ
Recombination Spectra
Black Body Spectra
Main Sequence
A
B
B'
C
5_3K
1_4K
5_4K
2_4K
1.2_4K
8_3K
M6
M4
M0
K7
K5
K0
1.3
1.1
0.9
0.7
0.5
0
1
2
3
4
5
6
$\frac{F_\nu(K)}{F_\nu(H)}$
$\frac{F_\nu(r)}{F_\nu(H)}$

Chapter 2.

AN INFRARED STUDY OF THE ECLIPSING DWARF NOVA U GEMINORUM.

SUMMARY

We present broadband infrared photometry (J, H, K) of the cataclysmic binary system U Geminorum throughout two orbital cycles; one series of data was obtained several days before an outburst, and a second series when the system had returned almost to quiescence from the same outburst. In quiescence, the red star, an M4 - M5.5 dwarf, supplies most of the infrared luminosity of the system. The quiescent light curves, which are doubly sinusoidal with a peak-to-peak amplitude of 0.22 magnitudes, are the tidally induced ellipsoidal variations of the red dwarf. The amplitude of the light curves is such that the red dwarf must fill, or nearly fill, its Roche Lobe, and shows directly that Roche Lobe overflow is important in cataclysmic variable stars.

The disc is brighter after outburst. Its infrared colours can lie in the range J-H = 0.3 to 0.8 and H-K = 0.3 to 0.7. These colours suggest that cool, optically thick gas ($T \leq 2500 - 3000K$) and optically thin gas supply most of the infrared light of the disc.

1. INTRODUCTION

Studies of the eclipsing dwarf nova U Geminorum have been fundamental to our understanding of the properties of cataclysmic variable stars. An analysis of its visual light curves in quiescence independently led Smak (1971) and Warner and Nather (1971) to propose the now accepted model of the structure of these stars. A late type dwarf (conventionally, the secondary star) fills its Roche Lobe and transfers matter to a white dwarf (the primary star). The large angular momentum of this material causes it to form a thin disc around the white dwarf. The recently transferred matter strikes the outer disc and forms a "hot spot", whose size is small compared with that of the disc. The broad shoulder seen in the light curve between phases 0.6 and 0.9 (see Figure 2 of Warner and Nather 1971) arises because the hot spot rotates into the line of sight; between phases 0.1 and 0.6 the disc (presumed to be optically thick in the visual) obscures it. At phase 0.0 the red dwarf totally eclipses the hot spot and partially eclipses the accretion disc.

The red dwarf (hereafter, U Gem B) must be studied in the red and infrared because the visual luminosity of the system comes chiefly from the accretion disc and the hot spot. Wade (1979) determined that U Gem B, a M4-M5 dwarf,[1] contributes 80-90 per cent of the luminosity of the system at 1μm. Given the large tidal distortion of the secondary star in close binary systems containing a degenerate primary star, the ellipsoidal variations will be the principal source of orbital variability in the infrared. The amplitude of these variations measures the degree to which the star fills its Roche Lobe.

---

[1] In this paper, all spectral types of M dwarfs are in the system of Boeshaar (1976).

Infrared observations are also useful in the study of optically thin and cool, optically thick gas in the accretion disc, because the hot (T > 10,000K) optically thick material comprising the bulk of the disc supplies most of the visible light (Warner and Nather 1971; Mayo et al 1981). The presence of Balmer emission lines in the visible spectrum of U Gem shows that there is optically thin gas in the disc. Cool, optically thick gas is found in the outer disc; Frank and King (1981) have argued that it can be as cool as 2500-3000K.

2. OBSERVATIONS

U Gem underwent an outburst on 1979 December 31 (the previous outburst had occurred on UT 1979 September 27). It remained at maximum for two days, attaining a visual magnitude of V $\sim$ 9.8, and declined to quiescence by January 8th, 1980 (Mattei, 1980; private communication). The eruption was somewhat atypical in that the duration of the maximum and of the decline to quiescence were shorter than usual, and the peak visual brightness of the system was one magnitude fainter than usual. We have obtained two broadband infrared light curves at J, H and K, both in quiescence and following the outburst. The light curves were acquired in quiescence on UT 1979 December 27 (when V = 14.7) and in decline on 1980 January 7 (when V = 13.9).

a) Measurements During Quiescence

The measurements were made with an InSb photovoltaic detector system, mounted at the Cassegrain focus of the United Kingdom Infrared Telescope at Mauna Kea Observatory, Hawaii. Broadband photometry was performed successively at J (1.25μm), H (1.65μm) and K (2.2μm). At each wavelength data were taken in 20 second integrations for a total of several minutes; in this time the orbital phase changed typically by 0.015. This method of observation permitted measurements of short time

scale variations (flickering) and of the orbital variations. The magnitudes of U Gem were established by hourly observations of standard stars, on a system which does not differ significantly from those on the CIT system. The typical 1σ error of a datum, ± 0.03 magnitudes at each wavelength, arises principally from absolute calibration uncertainties; the relative errors in the photometry are ± 0.01 mag.

b) Measurements After Outburst

The data were acquired with a cold InSb detector (the detector package "Otto") at the Cassegrain focus of the 1.3 metre telescope at Kitt Peak National Observatory. Measurements were made successively at J, H and K; no high time resolution measurements were made. The orbital phase typically changed by 0.01 during the course of the measurements. These measurements have been transformed to the CIT system, according to the discussion of Frogel et al (1978).

c) Orbital Phases

The adopted times of the measurements in all cases are the time of the mid-point of the integration. Times were converted to heliocentric orbital phases through the quadratic ephemeris of Arnold et al. (1976). The timing of all data is accurate to better than 0.1% of an orbital period.

3. U GEMINORUM IN QUIESCENCE

a) Origin of the Visual and Infrared Continuum Spectrum

Figure 1 displays the composite spectrum of U Gem in quiescence at phase 0.09, when the red dwarf obscures the hot spot. From an analysis of the visual and red data Wade (1979) found that U Gem B produces the steepening of the spectrum longward of 6000 A. The small discontinuity between the red and infrared measurements in Figure 1 arises because the disc was fainter at the time of our measurements; the luminosity of the

disc declines slowly with the time after outburst (Paczynski, 1965), and the two sets of measurements were made 30 and 92 days after an outburst, respectively. Wade (1979) found a value of ∿5mJy at 1μm for the flux density from the disc, whilst our measurements indicate a value of ~3mJy.

The contribution of the disc to the infrared luminosity of U Gem is sufficiently small (see Figure 1) that it does not significantly affect the observed infrared colors of the system. This being so, the data will allow equally well any spectral shape for the disc between the Rayleigh-Jeans law and a flat spectrum.

The effective temperature of a red dwarf determines the slope of its red continuum. A comparison of the red and infrared spectrum of the system with the colours of several late type stars (Figure 1) confirms Wade's classification of M4 to M5.5. The present classification is also consistent with that of Stauffer et al. (1979), based on TiO and CaH bands in the red spectrum of the system. Frank et al's (1981) mean J-K colour of U Gem of 1.1 is 0.3 mag redder than ours, and is consistent with that of a late M giant (Frogel et al., 1978). Their data are, however, of lower accuracy than ours and they measured different cycles at J and K.

b) The Nature of the Infrared Variability

Figure 2 shows that the orbital light curves at J, H and K are doubly sinusoidal with an amplitude of 0.22 magnitudes at all wavelengths and that the J-H and H-K colours are constant. Because U Gem B supplies nearly all the infrared light (§3a), the ellipsoidal variations of this tidally distorted star produce most of the observed variability. Light curves of the present accuracy would not reveal the structure of an eclipse of the disc by U Gem B, but such an eclipse

would slightly increase the amplitude of the infrared light curves beyond that of the ellipsoidal variations. Smak (1971) found that U Gem B eclipses 40 per cent of the visual light from the disc. If it obscures a similar fraction of the infrared light of the disc, then the predicted depth of the eclipse of a flat spectrum disc in the infrared (F_ν = 3.0 mJy) is 0.04 magnitudes. The amplitude of the ellipsoidal variations is therefore in the range (0.18-0.22) magnitudes.

c) Analysis of the Light Curves

A tidally distorted star is roughly "tear drop" shaped. It gives rise to a doubly sinusoidal light curve because its surface area projected on to the sky changes continuously throughout the orbital cycle. The degree to which the star fills its Roche Lobe determines the amplitude of the sinusoid: the amplitudes of the ellipsoidal variations of a star decrease as it lies further inside its Roche Lobe because it becomes more spherical. To ascertain this degree of filling in the case of U Gem B, the observed amplitudes have been compared with those of a simple model of the light curves, described in the Appendix. Figures 3a and 3b present the dependences of the modelled amplitudes on mass ratio and inclination; the "fill-out factor", F, specifies the degree to which the star fills its Roche Lobe; F=1 when the star just fills its lobe.

i) Dependence on Mass Ratio (Figure 3a)

The amplitudes of the light curves do not depend strongly on the mass ratio. The size of the Roche Lobe increases slightly with increasing mass ratio, as do the amplitudes of ellipsoidal variation. There is disagreement over the mass ratio of U Gem: Wade (1981) and Stover (1981) determined values of 2.8 and 2.0, respectively. The disagreement centres on the measurement of the correct value of the

amplitude of the radial velocity of the white dwarf. However, the amplitudes of the computed light curves change by only 0.01 magnitudes within the above range of mass ratios.

ii) Dependence on Inclination (Figure 3b)

Warner and Nather (1971) have shown that the inclination of U Gem lies in the range: $59° < i < 75°$. The calculated amplitudes increase with increasing inclination because the secondary star presents a larger variation of surface area at larger inclination. For the allowable range of inclinations the models show that the "filling factor", F, is $\leq$ 0.97; that is, U Gem B fills or nearly fills its Roche Lobe. This result shows directly that Roche Lobe overflow is important in cataclysmic binaries.

iii) Dependence on Irradiating Luminosity (Figure 3c)

That the infrared light curves of U Gem B are doubly sinusoidal shows that the light of the disc does not significantly heat it. Such heating would produce a light curve in which the minimum at phase 0.5 would be brighter than that at phase 0.0 because only the inner hemisphere of the red dwarf is irradiated. Light curves have been computed for irradiating luminosities, P_x, in the range 0.1 - $1L_\odot$; X-ray and ultra-violet observations of dwarf novae in quiescence have shown that the luminosities of quiescent discs lie in this range (Cordova et al. 1981; Fabbiano et al. 1981). The models show that when F is less than unity, the reflection effect is important, and becomes more pronounced as P increases. For given value of P_x, the ellipsoidal variations become the dominant source of variability as F approaches and exceeds unity.

A comparison of the observations with the model calculations demands that U Gem B is irradiated by a source whose luminosity is less

than $0.1L_{\odot}$. This result is interesting, as Fabbiano et al. (1981) have observed in U Gem an ultra-violet source having a Rayleigh-Jeans spectrum for which they suggest a luminosity $\sim 1L_{\odot}$. Such a source directly irradiating U Gem B would produce a pronounced reflection effect in the infrared light curve. Fabbiano et al., proposed that the UV source originates in nuclear burning in a small area of the surface of the white dwarf. If such a luminous spot is present the absence of a reflection effect can be explained provided that the nuclear burning takes place near the equator of the white dwarf (where the material in the disc is accreted), and the inner disc (presumed to be optically thick to the UV and x-rays) shields U Gem B from the source.

d) The Absence of the Hot Spot in the Infrared

The hot spot, which has a mean temperature of 50,000K and a mean density of 10^{15} cm^{-3} (Warner, 1976), is optically thick in the visual and infrared continua. The fact that the hot spot does not make a significant contribution to the infrared luminosity of the system is shown by the absence of asymmetry in the infrared light curves between phases 0.6 and 0.9. This is also consistent with the optically thick hypothesis: a hot spot having a Rayleigh-Jeans spectrum between 0.5μm and 2μm and whose flux at V is 45 mJy (Oke, 1981, private communication; Paczynski, 1965) contributes less 3 per cent of the observed fluxes at J, H and K.

The origin of the pronounced flickering seen in the visual light curves of U Gem is thought to be rapid variations in the density and velocity of the infalling material which produce rapid fluctuations in the temperature of the hot spot (Warner and Nather, 1971). Szkody (1976) found that fluctuations of 30-40 per cent in the temperature of the hot spot from a mean of T ~ 50,000K adequately explain both the

amplitude of the visual flickering in quiescent dwarf novae and the marked decrease in the flickering to the red. The present high time resolution data are qualitatively consistent with Szkody's conclusions. At each wavelength, the data did not reveal the presence of infrared flickering having an amplitude greater than the 2σ error of a datum, on time scales of between 10 and 40 seconds.

e) Implications of the Absence of a Secondary Eclipse

The light curves do not show evidence at phase 0.5 for the secondary eclipse of U Gem B by the accretion disc. Figure 4 illustrates the geometry of such an eclipse, which would be produced if the outer disc were to obscure U Gem B. From the absence of an eclipse, an upper limit of 5.5×10^{10}cm can be estimated to the radius of the region of the disc that is optically thick in the infrared. This value is deduced as follows: Figure 5 shows that an eclipse of U Gem B does not occur if the projected radius of the optically thick region of the disc normal to the line of sight, $R_d \cos i$, obeys the inequality:

$$R_d \cos i \leq a \cos i - R_1,$$

that is:

$$R_d \leq a - (R_1/\cos i)$$

The value of R_1, corresponding to an inclination of 65° is $0.37R_o$ (Mochnacki, 1972); we then find that:

$$R_d \leq 4.3 \times 10^{10}\text{cm} \ (\leq 0.6\ R_o)$$

Because the disc is foreshortened, it can be somewhat larger than this radius, and yet not produce a pronounced eclipse. Discs of radii 5×10^{10}cm and 5.5×10^{10}cm produce eclipses 0.04 and 0.08 mag deep, respectively. Because an eclipse is not seen in data having uncertainties of 0.03 mag., the former value is the best estimate of the upper limit to the radius. The region of the disc producing the visible

continuum has a radius 4 x 10^{10}cm (Smak, 1971), and is thus not significantly smaller than the region producing the optically thick infrared continuum.

f) The Phase of Spectroscopic Conjunction

Spectroscopic conjunction occurs at a phase of 0.975 in the infrared light curves, before the eclipse of the hot spot at phase 0.0. The displacement occurs because the spot forms at a point displaced in the direction of the orbital motion from the line joining the centers of mass of the two components. Our value of 0.975 is consistent with the values derived by Smak (1976) on the basis of an analysis of the profiles of the Balmer emission lines, and by Wade (1981) on the basis of the radial velocity variations of the sodium absorption lines. However, in the infrared light curves of Panek and Eaton, the conjunction occurs earlier (at phase 0.96), a result we do not confirm; further measurements of the phase of spectroscopic conjunction would thus be of interest.

4. U GEMINORUM DECLINING FROM OUTBURST

a) The Nature of the Variability

Figure 1 shows that in the post-outburst light curves the system is brighter out of eclipse than at the corresponding phases in quiescence. This is so because the disc is hotter, larger and more luminous in outburst and in the decline to quiescence than in quiescence (Smak, 1976).

The heating of U Gem B by the hotter disc is probably not significant; the depth of the secondary minimum is unchanged from quiescence. The luminosity, P, of the source irradiating U Gem B remains no greater than 0.1 $L_{\odot}$. (Compare §3d).

b) The Infrared Colours of the Disc

Here, we deduce the J-H and H-K colours of the disc and briefly discuss their nature. Since the measured fluxes in quiescence represent those of the red dwarf, the infrared colours of the disc can be evaluated from the difference of the measured fluxes between outburst and quiescence, at those phases at which the disc is not eclipsed. Figure 1 shows that out of eclipse, the system was brighter after the outburst by $\sim$0.2 mag. Small errors in the measured fluxes in both cycles can thus produce large errors in the deduced infrared colours of the disc. For data of the present accuracy, these colours can be uncertain by as much as $\pm$0.4 mag., an uncertainty reflected in the deduced colours: J-H lies in the range 0.3 to 0.8 mag., and H-K, 0.3 to 0.7.

Colours lying in the above ranges must arise largely from a superposition of the light of cool, opaque gas and transparent gas. The contributions of each type of emission cannot be determined explicitly from the present data, because the spectrum of the opaque gas is not well known and because the observed range of disc colours is large. Instead, simple arguments presented below derive estimates of their possible contributions. Briefly, we show that opaque gas most probably cannot supply all the infrared light of the disc, but that the transparent gas can. The calculations consider that U Gem lies at a distance of 76pc (Wade 1979).

If opaque gas supplies the infrared light of the disc, it must be cooler than 3000K because its H-K colour is redder than 0.3 (Frogel et al 1978). Frank and King (1981) have suggested that such temperatures are found in the outer disc. To supply all the infrared light, this cool gas must fill most of the disc. Were the gas to have a uniform

temperature of 3000K, it would fill ~40 per cent of a disc of radius 4 x 10^{10}cm (Smak 1971) to produce the 2μm disc flux of ~5mJy, and gas at 2000K would nearly fill the disc to produce this flux. Such extensive cool regions are most probably not present because hot gas (T>10,000K) usually fills more than half the disc (see, e.g., Krautter et al 1981; Williams 1980).

Suppose now that the optically thin gas produces the observed 2.2μm continuum power. The observed colours are consistent with those of an optically thin plasma, which has approximate colours of J-H~0.4 and H-K~0.7 (Ferland 1980). These colours are approximately independent of temperature over the range 5000K-100,000K, thought to be the range of temperatures of the optically thin gas in accretion discs (Williams 1980; Jameson et al 1980).

The emission measure of a plasma producing the 2.2μm continuum power is a few times 10^{54} cm^{-3} over the above temperature range (Ferland 1980). Such a plasma may be present in the disc because its emission integral is consistent with those deduced from the Balmer line strengths. The emission integral of the plasma producing the Hβ line, whose power is 1.76 x 10^{-16} W m^{-2} (Oke and Wade 1982), lies in the range 1 x 10^{54}-7 x 10^{55} cm^{-3}. This range reflects the fact that because the Balmer lines are optically thick, the integral deduced from the Hβ line strength may be underestimated by a factor of ∿70 (Drake and Ulrich 1980) for the densities and temperatures thought to prevail in accretion discs (N∿$10^{13}$$cm^{-3}$, T>3000K).

The study of the nature of the infrared emission of the disc in U Gem clearly requires the derivation of more accurate colours. To determine colours in the decline from an outburst to an accuracy of

several hundredths of a magnitude, the data must be of high accuracy (± 0.01-0.02 mag.) and the system should be 0.1-0.2 mag. brighter than in the cycle studied here.

5. CONCLUSIONS

We summarize our principal conclusions as follows:

1. U Gem B, a M4-M5.5 V star, fills or nearly fills its Roche Lobe.

2. Such X and UV radiation as arises from the surface of the white dwarf does not significantly heat the inner hemisphere of U Gem B.

3. The radius of the region of the disc that is optically thick in the infrared is not significantly larger than that of the region producing the visible light.

4. Two conclusions drawn from an analysis of the quiescent infrared light curve are consistent with deductions from observations in the visual and in the red:

   a) The hot spot is optically thick in the infrared continuum.

   b) Spectroscopic conjunction occurs at phase 0.975.

5. The bulk of the infrared light of the disc in the later stages of the decline to quiescence comes from optically thin and cool optically thick gas.

ACKNOWLEDGEMENTS

We wish to thank Drs. K.D. Horne, S.E. Persson and D.P. Schneider for reading the manuscript, the staff and night assistants of KPNO and the UKIRT for help at the telescope and Ms. J. Mattei for communicating the AAVSO data, Dr. R.A. Panek kindly allowed us to quote his work prior to publication. We also thank Miss A. Lucas and Mrs. Y. Boyce for their patient help with the manuscript. G.B. gratefully acknowledges financial support from NASA grants to infrared astronomy at Caltech.

APPENDIX

Model of the light curves in quiescence: Mochnacki and Doughty (1972) discussed in detail a technique to model the light curves of binary stars. It can be applied to contact and detached systems, and has successfully reproduced the visual light curves of W U Ma stars. Their technique has been used to synthesize the ellipsoidal variations of the red dwarfs in cataclysmic variable stars.

The shape of such a star becomes less spherical as the degree to which it fills its Roche Lobe increases. Consequently, the amplitude of its ellipsoidal variations also increases. Light curves have been computed to study the dependence of this amplitude on the degree to which the star fills its Roche Lobe.

In all the calculations, the photosphere of the red dwarf was represented by equipotentials given by the Roche approximation (viz. that the mass of the star is represented by a point mass at its centre of mass). The degree to which the star fills its Roche Lobe is most conveniently specified by its potential relative to those of the Roche surfaces. This "fill-out factor", F, is defined as follows:

i) if the star lies inside or is in contact with its Roche Lobe:

$$F = (C_1(q)/C_p) \quad (0 < F \leq 1)$$

where $C_1(q)$ is the potential of the first Roche surface, q is the mass ratio and C_p is the potential of the photosphere,

ii) if the star fills its Roche Lobe,

$$F = \frac{C_1(q) - C_p}{C_1(q) - C_2(q)} + 1 \quad (1 < F \leq 2),$$

where $C_2(q)$ is the potential of the second Roche surface.

Mochnacki and Doughty describe in detail the calculation of these potentials in cylindrical co-ordinates whose origin lies at the centre

of mass of the red dwarf. In this system, the co-ordinates of points on the equipotentials are symmetric about the line of centres of the components, an advantage over the more usually used Cartesian and spherical systems.

The calculations of the light curves of U Gem B include the effects of the heating of its inner hemisphere by the ultraviolet and X-radiation of the disc, hot spot and white dwarf and the effects of the gravity darkening of its surface.

The white dwarf, disc and hot spot are modelled as a point source, radiating isotropically at the location of the white dwarf. The use of this simple model is justified because most of the ultraviolet and X-radiation responsible for the heating arises in the inner disc (Fabbiano, et al., 1981). The incident radiation is considered to be re-radiated from the stellar surface with a bolometric albedo of 0.5, a value derived theoretically by Rucinski (1969) for stars having convective photospheres; this has not yet been verified by observations.

The gravity darkening of U Gem B is described by a law of the form:

$$T_e = T_o \left(g/g_o\right)^{\beta};$$

T_e is the effective temperature of the star at each element of the surface of the star. T_o is the flux-weighted mean temperature of the star, corresponding to a mean gravity given by:

$$g_o = \left(\frac{\int g^{4\beta}\, ds}{\int ds} \right)^{1/4\beta}$$

The constant β is the gravity darkening index, which for a convective envelope has a theoretical value of 0.08 (Lucy, 1967). This value is generally consistent with the observations of W U Ma stars of late spectral type (Rucinski, 1978). The effects of gravity darkening in the ellipsoidal light curves of convective dwarfs are small:

it decreases the amplitudes of the light curves of stars having a uniform surface temperature T_o by <0.03 mag.

The infrared limb darkening of U Gem B was excluded from the calculations because it is small in the infrared (Carbon and Gingerich, 1969). Its effect would be to produce in the light curves a minimum at phase 0.5 that is slightly deeper than that a phase 0.0, but this is not observed.

Each light curve (for a given mass ratio, inclination, irradiating luminosity and fill-out factor) is computed by integrating the flux emitted over the area of the photosphere visible in the line of sight of the observer, at phase intervals of 0.04 throughout the orbit. We have computed the dependence of the amplitudes of the light curves on the value of F. Figure 3 shows the dependence of the amplitudes on mass ratio, inclination, and irradiating luminosity. The figure also directly compares the observed amplitudes (derived in the text) with those of the models.

REFERENCES

Arnold, S., Berg, R. A. and Duthie, J. G., 1976. Astrophys. J., 206, 790.

Boeshaar, P., 1976, Ph.D. Thesis, Ohio State University.

Carbon, D. F., and Gingerich, O., 1969. In "Theory and Observations of Normal Stellar Atmospheres". Ed. Gingerich, O. MIT Press.

Cordova, F. A., Jensen, K. A., and Nugent, J. J., 1981 Mon. Not., R. Astr. Soc., 196:1.

Drake, S. A. and Ulrich, R. K., 1980, Astrophys. J., Suppl. Ser., 42:351.

Fabbiano, G., Hartmann, L., Raymond, J., Steiner, J., Branduardi-Raymont., G. and Mabilsky, T., 1981, Astrophys. J., 243:911.

Ferland, G. J., 1980, Pub. Ast. Soc. Pac., 92:602.

Frank, J. F. and King, A. R., 1981, Mon. Not., R. Ast. Soc., 196:507.

Frank, J. F., King, A. R., Sherrington, M. R., Jameson, R. F. and Axon, D. J., 1981, Mon. Not., R. Ast. Soc., 195:505.

Frogel, J. A., Persson, S. E., Aaronson, M. and Matthews, K., 1978, Astrophys. J., 220:75.

Jameson, R. F., King, A. R. and Sherrington, M. R. 1980. Mon. Not. Roy. Ast. Soc. 191, 559.

Krautter J., Klare G., Wolf, B. Duerbeck, H. W., Rahe J., Vogt, N., Wargau, W., 1981, ESO Preprint 152.

Lucy, L. B., 1967, Z fur Astrophys 65:89.

Mayo, S. K., Wickramasinghe, D. T. and Whelan, J. A. J., 1981, Mon. Not., R. Ast. Soc., 193:793.

Mochnacki, S. W., 1972, M. Sc. Thesis, University of Canterbury, New Zealand.

Mochnacki, S. W. and Doughty, N. A., 1972, Mon. Not., R. Ast. Soc., 156:51.

Oke, J. B. and Wade R. A., 1982, Astron. J., 87, 670.

Paczynski, B., 1965, Acta Astron., 15:89.

Panek, R. A. and Eaton, J. A., 1982, Ap. J., in press.

Persson, S. E., Aaronson, M. and Frogel, J. A., 1977, Astron. J., 82:729.

Rucinski, S. M., 1978 in "Non-Stationary Evolution of Close Binaries" (Polish Scientific Publishers, Warsaw 1978) p. 117.

Rucinski, S.M., 1969 Acta Astron., 19:245.

Smak, J., 1976, Acta Astron., 76:277.
———— 1971, Acta Astron., 21:15.

Stauffer, J., Spinrad, H., and Thorstensen, J., 1979 Pub. Ast. Soc. Pac., 91:59.

Stover, R. J., 1981, Astrophys. J., 248:684.

Szkody, P., 1976, Astrophys. J., 207:824.

Veeder, G. J. 1974. Astron. J., 79, 1056.

Wade, R. A., 1981, Astrophys. J., 246:215.
———————— 1979, Astron. J., 84:562.

Warner, B., 1976, Proc. IAU Symp. 73, p85, eds., Eggleton, P. P., et al., Reidel, Dordrecht.

Warner, B. and Nather, E. L., 1971, Mon. Not., R. Ast. Soc., 152:219.

Williams, R. E., 1980, Astrophys. J., 235:939.

FIGURE CAPTIONS

Figure 1: The visual and infrared continuum spectrum of U Geminorum in quiescence at phase 0.09. The visual data are from Wade (1979); the emission lines have been excluded. The J, H, K data have been interpolated from the measurements reported in this paper. The figure also shows the continuum spectra of several late type dwarfs, taken from the RIJHK photometry of Veeder (1974) and Persson et al., (1977). The solid triangle shows the AAVSO datum on the night of the infrared measurements.

Figure 2: The infrared light curves of U Geminorum at K, and its J-H and H-K colours throughout the orbital cycles. $\pm 1\sigma$ error bars are shown in each panel. The dashed lines drawn through the data are to aid the eye. All magnitudes refer to the CIT system.

Figure 3: The variation of the amplitude of the primary (ΔK_p) and secondary (ΔK_s) minima of the simulated light curves at K, with fill-out factor F. The brightness of the curves has been arbitrarily set to 0.00 magnitudes at phases 0.25 and 0.75.

The horizontal lines in each set of panels represents the observed range of amplitudes of the ellipsoidal variations of U Gem B (as derived in the text).

(a) Variation with mass ratio, q at constant inclination, i, of 65°, and irradiating luminosity, P, of 0.1 $L_\odot$.

(b) Variation with inclination, at q = 2.8 and P = 0.1 $L_\odot$.

(c) Variation with irradiating luminosity, at q = 2.8 and i = 65°.

Figure 4: The idealised geometry of the secondary eclipse in U Gem; that is, the eclipse of U Gem B by the accretion disc, considered to have negligible thickness. The separation of components, a, has been derived by Kepler's law from the values of m_r, m_w, and P shown. The masses are from Wade (1981) and P is from Arnold et al. (1976) R_1 is the radius of U Gem B normal to tangent along the line of sight to the earth.

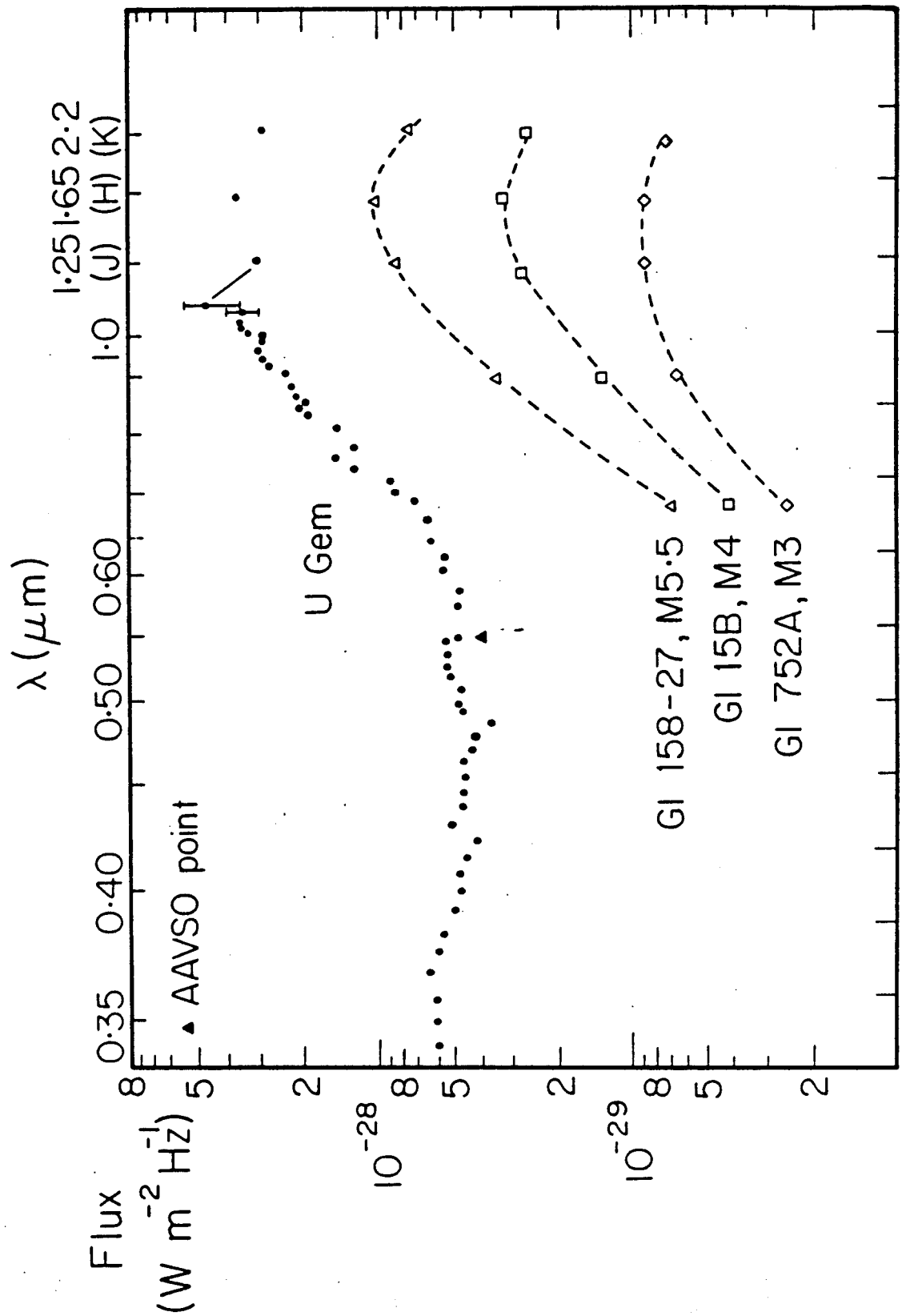
λ (μm)
0·35
0·40
0·50
0·60
1·0
1·25
1·65
2·2
(J)
(H)
(K)
AAVSO point
U Gem
GI 158-27, M5·5
GI 15B, M4
GI 752A, M3
Flux
(W m⁻² Hz⁻¹)
10⁻²⁸
10⁻²⁹
8
5
2
2·8
2·4
2·0
1·6
1·2
0·8
0·4
1/λ (μm⁻¹)

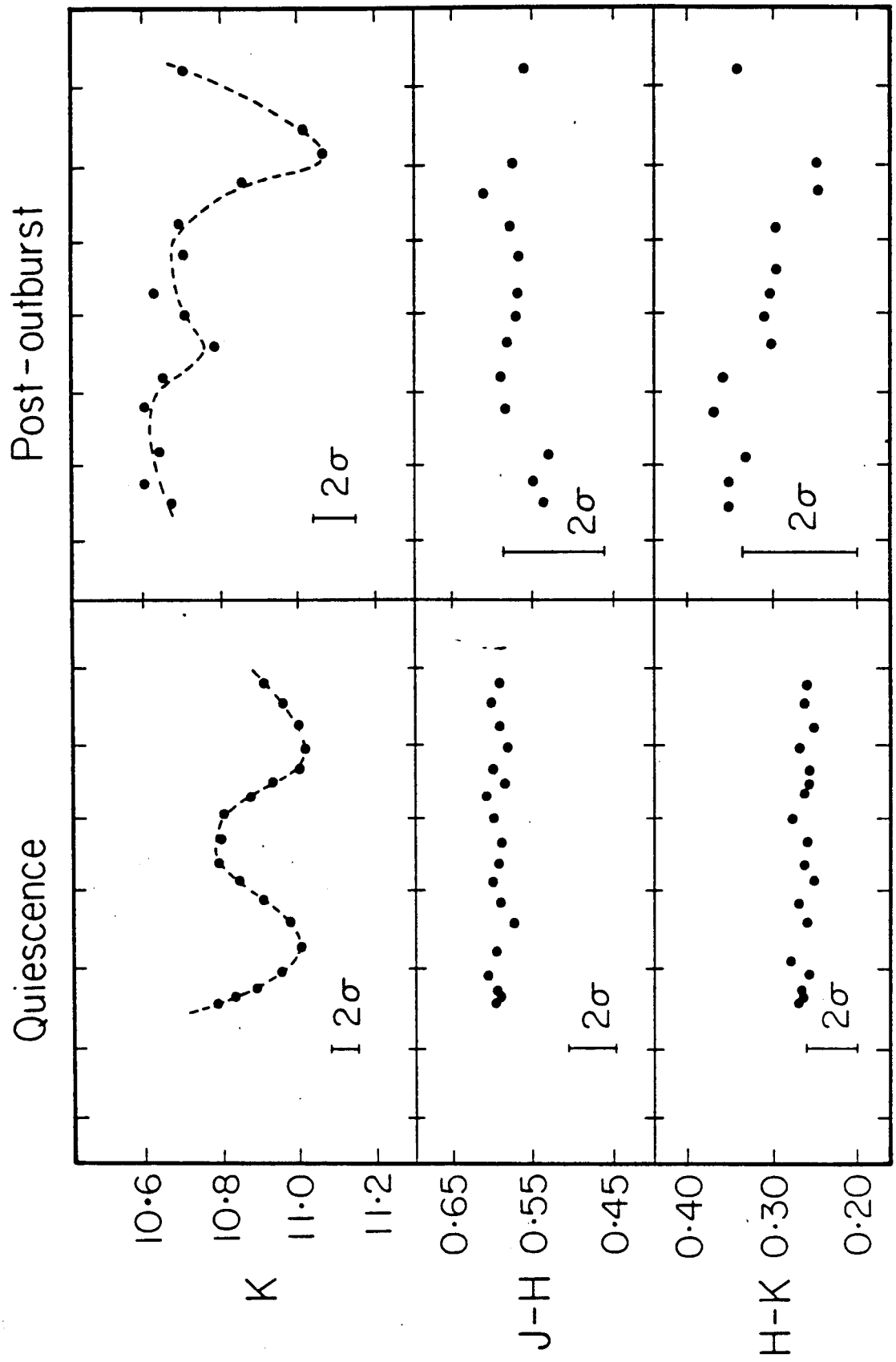
Quiescence
Post-outburst
K
J-H
H-K
2σ
10·6
10·8
11·0
11·2
0·65
0·55
0·45
0·40
0·30
0·20
0·0
0·4
0·8
1·2
Orbital Phase

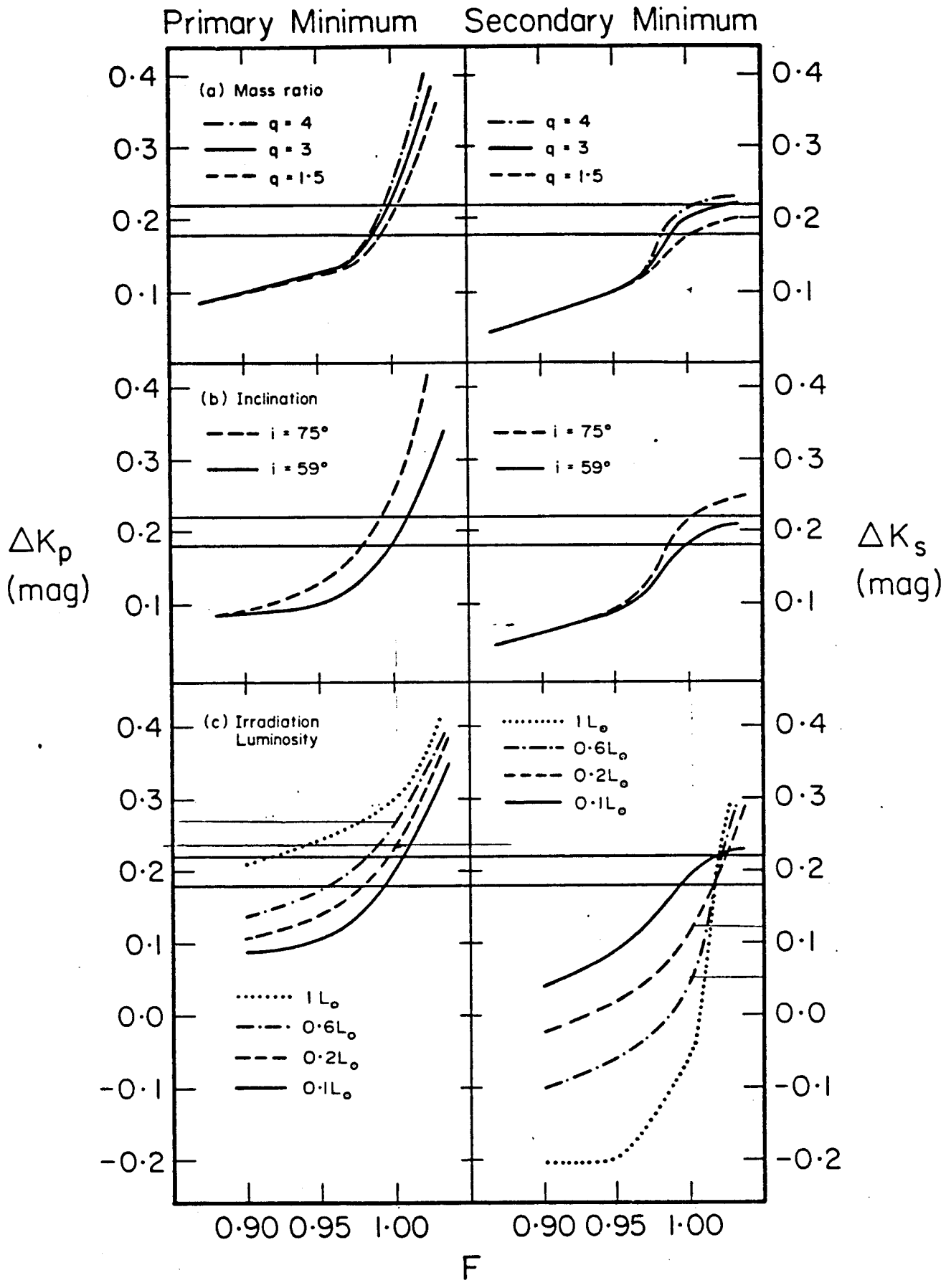
Primary Minimum
Secondary Minimum
(a) Mass ratio
q = 4
q = 3
q = 1·5
(b) Inclination
i = 75°
i = 59°
(c) Irradiation Luminosity
1 L⊙
0·6L⊙
0·2L⊙
0·1L⊙
ΔKp (mag)
ΔKs (mag)
0·4
0·3
0·2
0·1
0·0
-0·1
-0·2
0·90 0·95 1·00
F

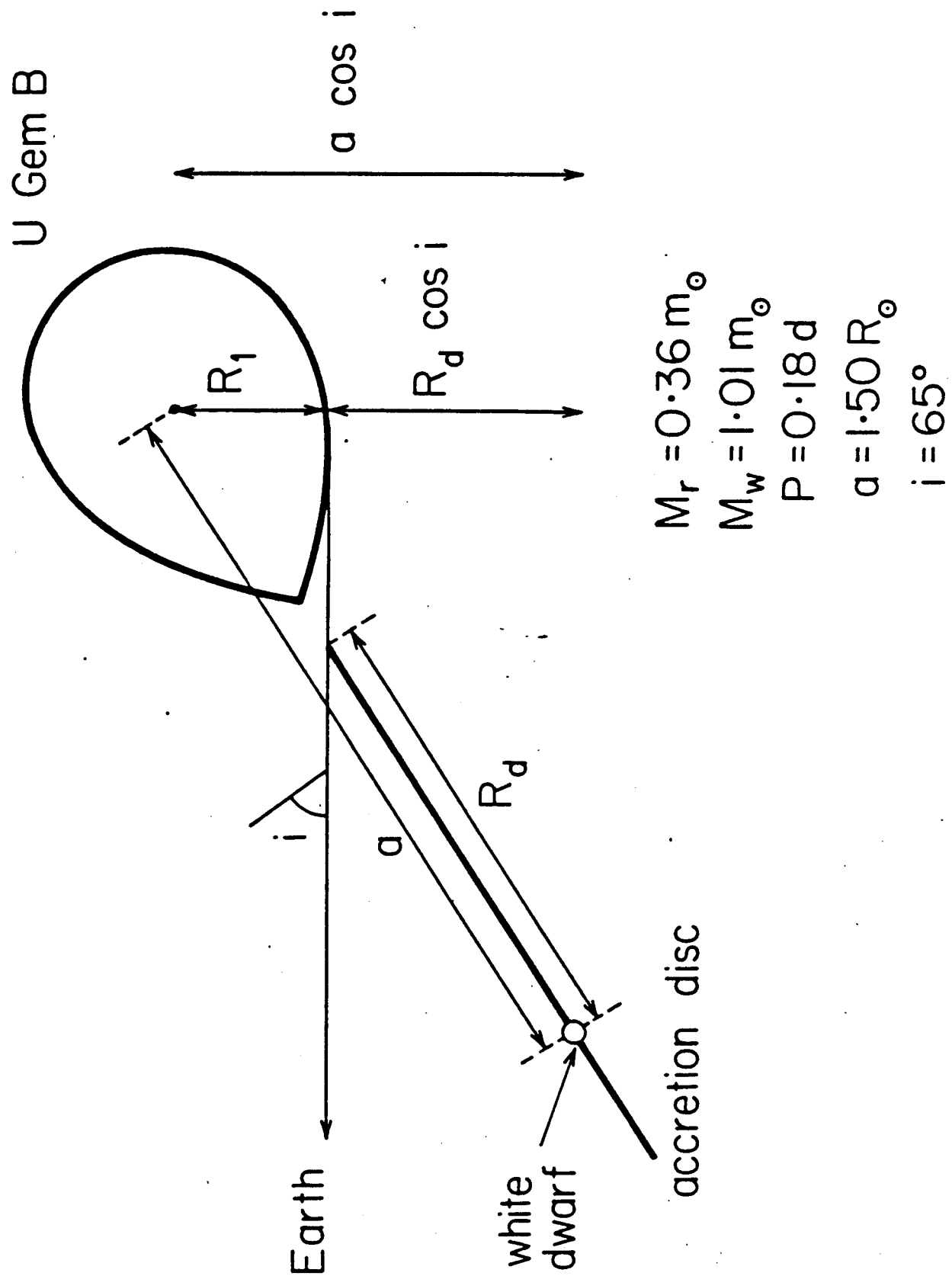
U Gem B
a cos i
R1
Rd cos i
Mr = 0·36 m⊙
Mw = 1·01 m⊙
P = 0·18 d
a = 1·50 R⊙
i = 65°
Rd
i
a
Earth
white dwarf
accretion disc

Chapter 3.

A VISIBLE AND INFRARED STUDY OF THE ECLIPSING DWARF NOVA OY CARINAE: I THE VISIBLE ECLIPSES OF THE CENTRAL OBJECT.

SUMMARY.

This paper presents four visible eclipses of the highly inclined Cataclysmic Variable Star, OY Carinae, in quiescence. These light curves show that the red dwarf eclipses both its white dwarf companion and the hot spot, which lies on the rim of the accretion disc surrounding the white dwarf. An analysis of the eclipses of the white dwarf, under the assumption that the red dwarf fills its Roche Lobe, gives the following properties of the system: the inclination lies between 73.5° and 81°, the mass of the white dwarf between $0.4M_{\odot}$ and $1.4M_{\odot}$, and the red dwarf lies either on or slightly below the Lower Main Sequence mass-radius relation. The principal source of uncertainty in the analysis is that the semi-amplitude of the radial velocity of the white dwarf is poorly known. The consequences of these findings are discussed in the light of current ideas about the evolution of Cataclysmic Variable stars.

1. INTRODUCTION

Of considerable importance in the study of the evolution of binary stars are the Cataclysmic Variable Stars (hereafter, CVs), a group of systems having short periods (P< 9h) and containing a white dwarf. As such, they have lost most of their angular momentum and mass during their evolution, but our knowledge of how this happens is rudimentary (Ritter 1982). The principal reason for this is that most of the visible light comes from an accretion disc around the white dwarf, thereby frustrating observations of the white dwarf and its red dwarf companion. The disc itself forms because the latter star fills its Roche Lobe, and transfers matter to the white dwarf. Both stars can be studied in the highly inclined system OY Car because the red dwarf is seen to eclipse the white dwarf (Vogt et al 1981). The properties of both components are of interest for different reasons.

The red dwarf in a CV may be unusual, in that its mass and radius may differ from those of Main Sequence stars, as is known to be the case in several systems; e.g U Gem (Wade 1981 and Stover 1981) and DQ Her (Young and Schneider 1981b). These differences come about because the processes thought to cause the red dwarf to fill its Roche Lobe -- gravitational decay of the orbit (Paczynski 1981) and magnetic wind braking in the red dwarf (Mochnacki 1981; Taam 1983)-- can act on sufficiently short timescales that the red dwarf comes out of thermal equilibrium. Whether the red dwarf in OY Car is a

Main Sequence star should thus provide a clue to the recent history of the system.

The white dwarf reveals much about the early history of the system, as it naturally formed prior to the present CV stage. However, published estimates of the mass of the white dwarf in OY Car, based on studies of these eclipses, differ widely. For example, from the same series of observations, Vogt et al (1981) find $M_w = 1M_\odot$, whereas Ritter (1980a) finds $M_w = 0.3M_\odot$.

Given that the red dwarf may be atypical of its kind and given the disagreement over the mass of the white dwarf, we present a rediscussion of the analysis of the eclipses of the white dwarf in OY Car, based on new visible light curves. We pay especial attention to the question of whether the discrepancies between the reported masses of the white dwarf arise largely from errors in the analysis. In a second paper, Berriman and Persson (1983) use infrared light curves, obtained simultaneously with the visible data, to study the contributions of the red dwarf and disc to the infrared light, the distance to the system, and the nature of the infrared light of the accretion disc.

2. OBSERVATIONS.

(a) The visible eclipses.

The data were obtained on 1981 March 1 with a two channel visible and infrared photometer, mounted at the Cassegrain focus of the 2.5m DuPont telescope at Las Campanas Observatory, Chile. The photometer is equipped with a dichroic beam splitter which reflects infrared light from an object and from a nearby sky reference field onto a cold InSb detector system, whilst the visible light passes through the dichroic to an S20 phototube. Since the dichroic absorbs much of the visible light, the statistical accuracy of the visible data obtained with this photometer is lower than would otherwise be obtained with a 2.5m telescope.

Four consecutive cycles of OY Car were observed simultaneously at V and in the infrared (J,H and K); the infrared data will be reported in Paper II (Berriman and Persson 1983). Figure 1 presents the four visible eclipses, obtained at a time resolution of 10 seconds. The cycle numbers in the Figure have been derived from the Epoch of Vogt et al (1981):

$$JD = 2443993.553241 + 0.0631209247\ E.$$

The V magnitudes of OY Car, given on the right hand sides of the panels of Figure 1, have been calibrated by measurements, made between cycles, of the nearby star used as a spectrophotometric standard by Bailey and Ward (1982). Its

V magnitude is 14.72± 0.02, which has been established by measurements of Landolt's (1973) standards. To avoid contamination from nearby field stars, all the measurements were made through a focal plane aperture 10arcsec in diameter, and with the object and reference fields separated by 33arcsec.

The four eclipse light curves are similar to those measured by Vogt et al (1981), as well as to those of HT Cas (Patterson 1981) and Z Cha (Bailey 1979). They show that two bodies are eclipsed, the rapid eclipse of the smaller body being followed by the slower eclipse of the larger. Furthermore, the rapid flickering seen before the eclipse disappears during the eclipse. These features are readily explained by the widely accepted model for the structure of a CV. In this model (Warner and Nather 1971; Smak 1971), the large angular momentum of the matter transferred from the red dwarf to the white dwarf causes it to form a thin disc around the latter. A "hot spot" forms where the recently transferred matter strikes the outer disc; it gives rise to the rapid flickering seen prior to the eclipses. The body eclipsed first is either the white dwarf or the boundary layer (where the material of the disc accretes on to the white dwarf), and that eclipsed second is the hot spot. The eclipse of the hot spot occurs second because it forms at a point displaced in the direction of the orbital motion from the line joining the centres of mass of the two components.

(b) The eclipse of the white dwarf.

Two quantities, shown on Figure 1, describe the eclipse of the white dwarf/boundary layer: the half width of the eclipse, $\Delta t_{1/2}$, and the duration of the ingress and egress, Δ_{wd}. They have been deduced from the four contact times t_1 to t_4 (also shown in Figure 1), and are given by:

$$\Delta t_{1/2} = \frac{1}{2}\left[(t_4 + t_3) - (t_2 + t_1)\right],$$

$$\Delta_{wd} = \frac{1}{2}\left[(t_4 - t_3) + (t_2 - t_1)\right].$$

The contact times have been found by two methods: by direct examination of the light curves; and by making linear fits to the data obtained in the eclipses, and subsequent estimation of the times corresponding to the observed counts at ingress and egress.

(i) Half-width of the eclipse.

The four eclipses give values of $\Delta t_{1/2}$ in the range 250 to 290 seconds, each value having a typical uncertainty of ± 20 seconds. The uncertainties comprise approximately equal contributions from the effects of the relatively low time resolution and the effects of the flickering (which would systematically decrease the half-width). The mean value of $\Delta t_{1/2}$, to be used in the subsequent analysis, is 270 ± 15 seconds. This value is consistent with that of Vogt et al (1981).

(ii) The duration of the eclipse.

The boundary layer produces the highly variable X-ray emission seen in CVs (Pringle and Savonije 1979). The emission of the layer, if significant in the visible, would be expected to give rise to variable eclipse durations and to corresponding changes in the visible brightness of the system.

The present data show no evidence for such variability. The observations lie in the range 42 to 63 seconds, each having an uncertainty of ±13 seconds. Again, the effects of flickering and the low time resolution contribute roughly equally to these uncertainties. The mean eclipse duration is 55 ± 8 seconds. Vogt et al (1981) do report large variations in the eclipse durations, finding values that lie between 21 and 55 seconds, but do not report whether this variability is correlated with changes in the visible brightness of the system. Consequently, we shall consider that in OY Car, Δ_{WD} lies between 21 and 55 seconds.

3. ANALYSIS OF THE LIGHT CURVES.

(a) The inclination of the system.

The inclination of the system must be found because the half-width of the eclipse then specifies uniquely the radius of the red dwarf and the mass of each component, if the red dwarf fills its Roche Lobe (as described below; Section b). The customary method of finding this quantity, from the curvature of the eclipses near ingress and egress, is inapplicable here: the curvature is small, because the red dwarf is much bigger than the white dwarf, and is hidden by the flickering. The inclination has therefore been found indirectly, by making use of the fact that the duration of the eclipse of the white dwarf specifies its radius at a given inclination; the radius so found is independent of the determination of its mass. The half-width and duration of the eclipses thus give the variation with inclination of the mass and radius of the white dwarf. The inclinations considered plausible are those at which the white dwarf obeys the Hamada-Salpeter mass-radius relation.

The above relation most probably holds for the white dwarfs in CVs, even though they are accreting material from the inner disc. Only at accretion rates sufficiently high to sustain thermonuclear burning (>10(-7)$M_\odot$ yr-1) does the relation become invalid, the white dwarf expanding to 1R or more (Paczynski and Rudak 1980). The accretion rates in CVs are, however, some 2-3 orders of magnitude lower than this

critical value (see, e.g., Rappaport, Joss and Webbink 1982). Moreover, if the white dwarf in OY Car were as large as $1R_{\odot}$, the components would have a separation of $\sim 70R_{\odot}$ in order to produce the observed eclipse duration of the white dwarf. In such a large system, the amplitudes of the radial velocities of the components would be ~19,000 km s-1, approximately two orders of magnitude higher than those observed in OY Car or any other CV.

(b) The component masses and the radius of the red dwarf.

We consider a simple model of a highly inclined system (i>70) in which a spherical red dwarf that fills its Roche Lobe eclipses a spherical white dwarf. For a given inclination, the observed half-width of the eclipse of the white dwarf gives uniquely the fractional radius of the red dwarf (i.e. its radius relative to the separation of the components), and the mass ratio of the components. The half-width determines the fractional radius of the red dwarf, rather than its absolute radius, because the length of time that the white dwarf is eclipsed depends not only on the radius of the eclipsing object, the red dwarf, but also on the velocities of the components, which are proportional to the orbital separation. The half width and fractional radius are related by the expression (Ritter 1980b):

$$\left(\frac{R_R}{a}\right)^2 = \left(\frac{\pi}{P}\right)^2 \Delta t_{1/2}^2 + \cos^2 i,$$

where P is the orbital period, R_R is the radius of the red dwarf and a is the separation of the components.

The observed half-width also gives the mass ratio of the system, because the fractional radius of a star filling its Roche Lobe depends on the mass ratio alone (Paczynski 1971). The mass ratio, q, taken to be the mass of the red dwarf relative to that of the white dwarf, is

$$q = \left(\frac{R_R}{a}\right)^3 \Big/ 0.0973 - \left(\frac{R_R}{a}\right)^3$$

The fractional radius in the above two expressions is that of a star whose volume equals the volume of its Roche Lobe. This value differs from that in the spherical approximation because a tidally distorted star is roughly tear-drop shaped, with the apex pointing towards its companion. The fractional radius and mass ratio deduced in the spherical approximation are thus underestimates of the true values. The uncertainties introduced into the deduced properties of the components of OY Car are, however, less than those introduced through the inaccuracies in the eclipse timings and the radial velocity measurements (as will be shown in Section 4).

To determine the radius of the red dwarf in absolute units, the separation of the components must be known. It is found from the observed semi-amplitude of the radial velocity variations of the white dwarf, K_w, and is given by

$$a = P K_w (1+q) / 2\pi \sin i \, q \,, \qquad -(1)$$

Whereas the fractional radius of the red dwarf decreases with inclination (as the white dwarf is eclipsed at a point nearer the centre of the red dwarf), its absolute radius increases because the orbital separation also increases. This comes about as follows. The semi-amplitude K_w reflects the motion of the red dwarf, not of the white dwarf, in the sense that if the red dwarf becomes progressively heavier, the centre of mass of the system will move towards it and cause the radial velocity amplitude of the white dwarf to increase. For an observed value of the semi-amplitude, the distance of the white dwarf from the centre of mass must remain constant. The red dwarf becomes less massive at higher inclinations (because it occupies a smaller fraction of the orbit). It must move further away from the centre of mass to keep the latter in the same position; the total separation then naturally increases with the inclination.

The mass of the red dwarf follows from the fact that the orbital period of the system specifies the mean density of the red dwarf, a further well known property of a star filling its Roche Lobe. The density, ρ, of a star in a CV of period P seconds is (Warner 1976):

$$\rho = 1.43 \times 10^9 / P^2 \quad \text{g cm}^{-3}$$

The mass of the red dwarf, M_R, is then

$$M_R = \frac{4}{3}\pi R_R^3 \rho = 34.54 \left(\frac{R_R}{R_\odot}\right)^3 M_\odot$$

From this mass and the already known mass ratio, the mass of the white dwarf follows simply.

(c) The radius of the white dwarf

Ritter (1980b) has shown that the radius of the white dwarf, R_w, is given by:

$$R_w = \left(\frac{\pi}{P}\right)^2 \Delta_{WD}\, \Delta t_{1/2} \left(\frac{a}{R_R}\right) a$$

which can be rewritten as:

$$R_w = \left(\frac{\pi}{P}\right)^2 \Delta_{WD}\, a \Big/ \sqrt{\left(\frac{\pi}{P}\right)^2 + \frac{\cos^2 i}{\Delta t_{1/2}^2}}$$

$$= k(P, i)\, a\, \Delta_{WD}. \quad -(2)$$

Figure 2 presents the relation between the radius of the white dwarf and the duration of its eclipse by the red dwarf, for inclinations from 70° to 90°. At each inclination, the orbital separations have been computed from equation (1), with K_w=115 kms-1 (Bailey and Ward 1982). These separations are constant at each inclination, as the mass ratio is specified uniquely. Because of this constancy and because the expression for the radius is independent of the radius itself, the gradient of each locus is the same at a given R_w, and depends only on R_w. The gradient is given by:

$$\left(\frac{\partial R_w}{\partial \log \Delta_{WD}}\right)\Bigg|_i = k \left(\frac{\partial \log R_w}{\partial \Delta_{WD}}\right)_i$$

For an observed eclipse duration, the variation of the radius of the white dwarf with inclination can be read from Figure 2, which shows that the radius increases with inclination. This simply reflects the fact that as the separation of the components increases with inclination, so does the tangential velocity of the red dwarf. The white dwarf must then become larger to reproduce the observed eclipse durations.

(d) The value of K_w.

One of the principal sources of uncertainty in the analysis is in the semi-amplitude of the radial velocity of the white dwarf, K_w, which is deduced from the radial velocity curves of the emission lines. Because these velocities more accurately reflect the motion of the disc than of the white dwarf, the value of K_w can suffer large systematic uncertainties that are difficult to quantify. An estimate of their probable size can be found from the observation that the zero-crossing of the radial velocity curves occurs later than photometric conjunction (Bailey and Ward 1982), a phenomenon seen in LX Ser (Young, Schneider and Shectman 1981a) and HT Cas (Young, Schneider and Schectman 1981b). It most probably arises from an asymmetric distibution of light in the disc, with more light coming from the side of the disc struck by the infalling matter. Wade (1981b) has shown that, if this is the case, the value of K_w can be uncertain by as much as a factor of 2.

Accordingly, the analysis has been carried out for three values of K_w: 115 km s-1 (Bailey and Ward; op cit), 75 km s-1 and 175 km s-1. For each have been calculated the radii of the white dwarf that correspond to eclipse durations of 21s and 55s. Figure 2 has been derived for K_w= 115 km s-1, but can be used to derive the radii of the white dwarf for the other two values of K_w. At a given inclination, the orbital separation decreases with K_w, and hence, so does R_w. Because R_w is proportional to both the separation and to Δ_{wd}, a decrease in the separation is equivalent to a decrease in K_w at constant separation. The radii appropriate to a value of K_w may thus be found by considering the separation to be constant and decreasing Δ_{wd} by $K_w/115$.

4. RESULTS.

(a) The inclination of the system and the mass of the white dwarf.

The mass of the white dwarf is found simply from $M_w = M_R/q$. The discussion of Section 3b shows that the mass ratio decreases rapidly with inclination, through its cubic dependence on the fractional radius of the red dwarf, as does the mass of the red dwarf, through its cubic dependence on its radius. Together, they make M_w increase rapidly with inclination, and make its uncertainty very sensitive to the uncertainties in M_R and q. Physically plausible inclinations are those for which the white dwarf obeys the mass-radius relation, shown as the solid line in Figure 3. Examination of the figure shows that the rapid increase with inclination of the mass of the white dwarf allows the inclination to be found to within a few degrees,but the large uncertainties in M_w prevent it from being found accurately.

For the allowed range of eclipse durations, Figure 3 shows that the inclination corresponding to K_w=115 kms-1 is between 76° and 78.5°. The ranges of the plausible inclinations at the other semi-amplitudes are nearly the same, but the values differ by a few degrees. Since the orbital separation is proportional to K_w (see equation 1),the estimates of the mass and radius of the red dwarf at a given inclination are larger at higher values of K_w. A simple

scaling of the data in Figure 3 shows that at K_w=175 kms-1, the inclinations are a little lower than those at K_w=115kms-1 - from 73.5° to 75.5°, in fact -- whereas those at K_w=75 kms-1 are higher -- from 78.5° to 81°. For the allowed range of K, then, the inclination of the system lies between 73.5° and 81°. Table 1 summarises the values of M_R, R_R and M_w appropriate to each K_w and inclination.

At each value of K_w, the mass of the white dwarf may equally well lie anywhere between $0.4M_\odot$ and $1.4M_\odot$. We suggest that the sensitivity of the mass to the inclination is the cause of the disagreement between previous workers over its value: Ritter (1980a) derived $M_w=0.3M_\odot$, and Vogt et al (1981), $M_w=1M_\odot$.

Being very large, the uncertainties in the mass are worthy of more detailed study. The mass itself has been found directly from M_R, which in turn has been found from R_R/a and a, or equivalently, from R_R/a, q and K_w. The uncertainties in q and K_w each contribute to the uncertainty in a according to the expression:

$$\frac{\sigma_a^2}{a^2} = \frac{\sigma_{Kw}^2}{K_w^2} + \frac{\sigma_q^2}{q^2(1+q)^2}$$

which is derived from equation 1. The fractional uncertainty in R_R is equal to that in a, the uncertainties in R_R/a being negligibly small here (see Column 3 of Table 1). Since the mass of a star is proportional to the cube of its radius, the fractional uncertainty in R_R is enlarged by a

factor of three in the corresponding uncertainty in M_R:

$$\frac{\sigma_{M_R}^2}{M_R^2} = 9\,\frac{\sigma_{R_R}^2}{R_R^2} = 9\left[\frac{\sigma_{K_W}^2}{K_W^2} + \frac{\sigma_q^2}{q^2(1+q)^2}\right] \quad -(3)$$

The total uncertainty in M_W is thus given by:

$$\frac{\sigma_{M_W}^2}{M_W^2} = 9\,\frac{\sigma_{K_W}^2}{K_W^2} + \frac{\sigma_q^2}{q^2}\left(\frac{q}{(1+q)^2} + 1\right)$$

The uncertainty in K_W, σ_{K_W}, is considered here to be 12 kms-1, that found by Bailey and Ward(1982). For this value and for the values of σ_q and q applicable to OY Car, given in Table 1, the uncertainty in K_W provides at least two-thirds of the total uncertainty in M_W. Improvements in the statistical accuracy of K_W are thus needed to improve the accuracy of the mass of the white dwarf, but are not likely to come about in the foreseeable future. This is because the principal source of uncertainty in the radial velocity determinations lies in the fact that the amplitude of the radial velocities is much smaller than the width of the emission lines, rather than in the fact that the objects are faint.

(b) The red dwarf.

Columns (6) and (7) of Table 1 present for each semi-amplitude, the masses and radii of the red dwarf appropriate to the upper and lower bounds to the inclination. When compared with the masses and radii of Lower Main Sequence dwarfs, as is done in Figure 4, the red dwarf in OY Car is seen to be either normal or undersized for its mass. The range of masses and radii corresponding to the allowed range of K_w is larger than the uncertainties in the individual values. An improvement in the mass and radius of the red dwarf therefore requires that the allowed range of values of K_w be narrowed. This will be a difficult task, as it is directly connected with the problem of understanding the complex motions and distribution of light in the disc (as noted in Section 4a). The uncertainties introduced here by K_w are different from those introduced into the mass of the white dwarf, which come from the statistical uncertainties in fitting a sinusoid to the radial velocity curves.

Column (7) shows that each mass of the red dwarf is uncertain by ~30-50 per cent. The origin of these uncertainties has been discussed above, the mass of the red dwarf being found as part of the calculation of the mass of the white dwarf. The total uncertainty in M_R is (equation 3 , above):

$$\frac{\sigma_{M_R}^2}{M_R^2} = q\left[\frac{\sigma_{K_w}^2}{K_w^2} + \frac{\sigma_q^2}{q^2(1+q)^2}\right]$$

For the values appropriate to OY Car, the uncertainty in K_w (12 kms-1) produces between half and three-quarters of the total uncertainty in the masses. Thus, an improvement in the accuracy of the masses of the red dwarf requires a roughly commensurate increase in the statistical accuracy of the semi-amplitude, rather than an increase in the accuracy of the eclipse half-widths.

Because the uncertainties in the radial velocity measurements produce most of the uncertainties in the mass of the red dwarf, the fact that the star is tear-drop shaped, rather than spherical, does not cause large errors in the masses and radii quoted in Table 1. An estimate of the size of such errors has been found from Kopal's (1978) tables of the sizes of the Roche Lobes in binary stars. His tables give, as a function of mass ratio, the radius of a spherical star having the same volume as the Roche Lobe of a star in a binary system. As given by these tables, the mass ratio corresponding to the fractional radius of the red dwarf presented in Table 1 is less than that deduced from Paczynski's formula (Section 3a), because the spherical approximation underestimates the radius of the red dwarf. The difference between the two values gives an estimate of the size of this underestimate. For the fractional radii and mass ratios presented in Table 1, the mass ratio is underestimated by 0.02, and the mass of the red dwarf is reduced by $0.07M_{\odot}$, less than its 1σ uncertainty.

5. DISCUSSION.

We have found that the mass of the white dwarf may lie between $0.4M_{\odot}$ and $1.4M_{\odot}$, and that the red dwarf lies either on or slightly below the Main Sequence mass-radius relation. We discuss these findings in the light of current theories of the evolution of CVs.

(a) The evolutionary state of the system.

The system most probably formed when a detached red dwarf-white dwarf binary (such as V471 Tau; Warner, Robinson and Nather 1971) lost orbital angular momentum through gravitational decay of the orbit (Paczynski 1981) and magnetic wind braking in the red dwarf (Taam 1983; Mochnacki 1981), thereby bringing the red dwarf into contact with its Roche Lobe. If these two processes act on a sufficiently short timescale, the red dwarf will come out of thermal equilibrium, and , having an adiabatic atmosphere, will subsequently expand. That the red dwarf in OY Car lies close to or slightly below the Main Sequence, as seen from Figure 4, indicates that it is still in thermal equilibrium. Its thermal timescale, for the masses and radii presented in Table 1, is (1 -4) x 10(9) years (this assumes that its temperature is similar to those of Main Sequence stars, which Berriman and Persson (1983) show is most probably the case). Because this timescale increases as the red dwarf loses mass, the system has been a CV for at most this long.

The red dwarf will remain on the Main Sequence for approximately this long again, since the above two processes are acting on timescales at least as short as the thermal equilibrium timescale of the red dwarf. Specifically, the timescale, τ_G, for angular momentum loss by gravitational radiation is (Paczynski 1981):

$$\tau_G = 1.5 \times 10^{10} \left(\frac{M_W}{M_\odot}\right)^{-2/3} \left(\frac{M_R}{M_\odot}\right)^{0.95} \text{ years}$$

For the properties of the components of OY Car specified in Table 1, τ_G is (1 -5) x 10(9) years.

The timescale appropriate to magnetic wind braking is much less securely known, largely because of our ignorance of the properties of the magnetic fields in cool dwarfs. Should this process be operating in addition to gravitational decay, it can, however, only decrease the timescale on which the red dwarf loses mass.

That OY Car contains a red dwarf either on or below the Main Sequence is inconsistent with the hypothesis of Paczynski and Sienkiewicz (1983) that the shortest period CVs are as old as the Galaxy. Being so old, the red dwarf would have lost lost so much mass that it came out of thermal equilibrium several billion years ago, and would have subsequently expanded. At present, it would have an approximate mass and radius of $\sim 0.02 M_\odot$ and $\sim 0.13 R_\odot$, clearly inconsistent with those deduced from the light curves.

(b) Previous evolution of the system.

(i) The white dwarf.

There are several CVs having periods between 80min and 2h (including OY Car) and between 3h and 4h, but there are none having periods between 2h and 3h. This "period gap" is thought to reflect a true absence of CVs of these periods (Rappaport, Joss and Webbink 1982). The relationship between the two adjacent groups is poorly known, but doubtless has much to reveal about the history of the systems.

Webbink (1976) proposed that the two groups formed independently. The short period CVs formed because the progenitors of the white dwarfs lost their envelopes during helium burning, and consequently contain low mass white dwarfs ($M \sim 0.45\ M_{\odot}$). In contrast, the progenitors of the white dwarfs in the long period systems lost their envelopes during carbon and oxygen burning, and thus contain more massive white dwarfs ($M > 0.55 M_{\odot}$). The hypothesis cannot be tested at present, because as we have shown, OY Car may equally well contain a low mass or a high mass white dwarf.

(ii) The red dwarf.

Because the white dwarf cannot be used as a probe of the previous evolution of the system, the red dwarf, whose properties are more securely known, must be used instead.

A Main Sequence dwarf.

In Webbink's hypothesis, discussed above, the progenitors of the white dwarfs in the shorter period CVs did not expand as much as the progenitors in the longer period systems, being of lower mass. They thus did not transfer a significant proportion of their mass to the red dwarfs, whose evolution they were unable to affect. That OY Car may contain a Main Sequence dwarf is therefore consistent with Webbink's hypothesis.

A different view is that the longer period systems evolve into the shorter period ones. If OY Car contains a Main Sequence dwarf, the system must have passed through the period gap without dramatic changes in the internal structure of the red dwarf. D'Antona and Mazzitelli (1982) have shown how this can take place. Mass loss alters the structure of the red dwarf slightly, through making the rate of thermonuclear reactions come out of equilibrium, and the red dwarf consequently contracts inside its Roche Lobe or expands outside it. If it contracts, systems in the period gap will be very faint (V>17) and difficult to find (Robinson et al 1981). If it expands, the mass transfer rate will increase dramatically, since it is very sensitive to the degree to which the star overflows its Roche Lobe (see e.g. Warner 1976, and references therein), and the system will evolve through the period gap so quickly that it cannot be observed (see e.g. Ritter 1982).

An undersized red dwarf.

It is plausible that OY Car contains a red dwarf that is atypically small for its mass. If we reject the idea that the star is a subdwarf, on the grounds that Population II binaries are rare, then it must be the product of mass loss from its ancestor. The history of such undersized stars in binary systems is poorly understood, but must be dramatically different from those of Main Sequence dwarfs. The most promising hypothesis of their origin is that of Webbink (1981), who proposed that the red dwarfs become more chemically homogenous than Main Sequence stars during phases of rapid mass transfer. The homogenisation arises because the star comes out of thermal equilibrium and develops a very deep convective zone, which is responsible for efficiently mixing the material in the star.

This phase of rapid mass transfer most probably occurs during an early stage of the evolution of a system, when the ancestor of the white dwarf was in its post-Main Sequence stage. As this star rapidly expanded, it transferred matter to a Main Sequence companion of $M \sim 0.8 M_{\odot}$ on a sufficiently short timescale that the latter is driven out of thermal equilibrium. The Main Sequence star, being in radiative equilibrium, subsequently expanded and filled its Roche Lobe; in this stage, it would be stripped of its outer envelope (see, e.g., Ritter 1982, for a review and references).

That the primary star was able to influence the evolution of its companion suggests that it was massive ($M \sim 4\text{-}5M_{\odot}$) and produced a massive white dwarf ($M > 0.6M_{\odot}$). The presence of an undersized red dwarf in OY Car would therefore suggest that the long and short period groups do not form independently, as this hypothesis requires that short period systems contain low mass white dwarfs (as explained in Section 5a).

It is improbable that an undersized dwarf would form as a consequence of the evolution of the system through the period gap (if it took place). For systems having periods of 3h, the time scale for mass loss by gravitational radiation and magnetic wind braking is similar to, or slightly shorter than, the thermal equilibrium timescale of the red dwarf. The latter thus cannot come out of equlibrium and expand sufficiently rapidly to induce the required dramatic increase in the mass transfer rate (Taam 1983).

6. CONCLUSIONS.

(1) The inclination of OY Car lies between 73.5° and 81°.

(2) Only broad limits to the mass of the white dwarf can be found: from $0.4M_{\odot}$ to $1.4M_{\odot}$.

(3) The radius of the red dwarf is either normal for its mass or slightly undersized. The presence of such a red dwarf requires that the system has been a CV for at most (1-4) x 10(9) years. The system cannot be as old as the Galaxy, as proposed by Paczynski and Sienkiewicz (1983), as it would necessarily contain a red dwarf that was oversized for its mass.

(4) The principal source of uncertainty in the analysis is that the semi-amplitude of the radial velocity of the white dwarf is poorly known, since it is found from the emission lines, which arise in the accretion disc.

(5) Normal and undersized red dwarfs are the products of very different evolutions. A normal dwarf would come from a low mass progenitor system, and an undersized dwarf from a high mass one.

Table 1: Solutions for the properties of the components of OY Car

Kw (km s^{-1}) (1)	i(°) (2)	Rr/a (3)	q (4)	a($R_\odot$) (5)	RR($R_\odot$) (6)	MR($M_\odot$) (7)	Mw($M_\odot$) (8)
75	78.5	0.250 ± 0.005	0.20 ± 0.02	0.57 ± 0.09	0.14 ± 0.02	0.09 ± 0.04	0.5 ± 0.2
	81	0.220 ± 0.005	0.12 ± 0.02	0.85 ± 0.14	0.19 ± 0.03	0.24 ± 0.12	2.0 ± 1.0
115	76	0.290 ± 0.005	0.32 ± 0.06	0.61 ± 0.09	0.17 ± 0.02	0.18 ± 0.05	0.6 ± 0.2
	78.5	0.250 ± 0.005	0.20 ± 0.03	0.87 ± 0.11	0.22 ± 0.08	0.37 ± 0.14	1.8 ± 0.7
175	73.5	0.320 ± 0.004	0.54 ± 0.03	0.65 ± 0.09	0.21 ± 0.03	0.32 ± 0.13	0.6 ± 0.2
	75.5	0.290 ± 0.005	0.36 ± 0.03	0.85 ± 0.08	0.25 ± 0.02	0.54 ± 0.16	1.5 ± 0.5

Column (2) gives the upper and lower bounds to the inclination of the system for the values of Kw in Column (1). The remaining columns give the following properties deduced at each inclination:

fractional radius of the red dwarf (3), the mass ratio (4), the orbital separation (5), the radius of the red dwarf (6), the mass of the red dwarf (7), and the mass of the white dwarf (8).

REFERENCES.

Bailey, J. 1979, Mon Not Roy ast Soc,187,645.

Bailey, J, and Ward, M. 1982, Mon Not Roy ast Soc,194,17p.

Berriman, G, and Persson, S.E. 1983, In Preparation.

D'Antona, F., and Mazzitelli, I. 1982, Astrophys J, 260, 722.

Grossman, A.S., Hays, D, and Graboske, H.C. 1974, Astron Astrophys,30,95.

Kopal, Z. 1978. "Dynamics of Close Binary Systems". (Reidel). p328.

Landolt, A.U. 1973, Astron J, 78, 959.

Mochnacki, S.W. 1981, Astrophys J,245,650.

Paczynski, B. 1981, Acta Astron,31,1.

———————— 1971, Ann Rev Astron Astrophys,9,183.

Paczynski, B., and Rudak, B. 1980, Astron Astrophys,82,349.

Paczynski, B., and Sienkiewicz, R. 1983, Astrophys J , submitted.

Patterson, J. 1981, Astrophys J Suppl Ser,45,517.

Pringle, J.E., and Savonije, G.J. 1979, Mon Not Roy ast Soc,187,777.

Pringle, J.E., and Webbink, R.E. 1975, Mon Not Roy ast Soc,172,493.

Rappaport, S., Joss, P.C., and Webbink, R.F. 1982, Astrophys J, 254,616.

Ritter, H. 1982, Proceedings of the Workshop on "High Energy Astrophysics" (Nanking).

———— 1980a, Astron Astrophys,85,362.

———— 1980b, Astron Astrophys,86,204.

Robinson, E.L. 1976,Ann Rev Astron Astrophys,14,119.

Robinson, E.L., Barker, G.S, Cochran, A.L., Cochran, W.D., and Nather R.E. 1981, Astrophys J, 251, 611.

Smak, J. 1971, Acta Astron,21,15.

Stover, R.J. 1981, Astrophys J,248,684.

Taam, R.E. 1983, Astrophys J, in press.

Vogt, N., Schoembs, R., Krzeminski, W., and Pederson, H. 1981, Astron Astrophys,94,L29.

Wade, R.A. 1981a, Astrophys J,246,215.

———————— 1981b, paper presented at the Santa Cruz Summer Workshop on "Cataclysmic Variables and Related Systems".

Warner, B. 1976, Proc IAU Sym 73. P.P. Eggleton et al,eds (Reidel).

Warner, B., and Nather, R.E. 1971, Mon Not Roy ast Soc,152,219.

Warner, B., Robinson, E.L., and Nather, R.E. 1971, Mon Not Roy ast Soc, 154, 455.

Webbink, R.F. 1981, Paper presented at the Santa Cruz Summer Workshop on "Cataclysmic Variables and Related Systems".

———————— 1976, Proc IAU Sym 73. P.P. Eggleton et al, eds (Reidel).

Young, P.J., and Schneider, D.P. 1981, Astrophys J,247,960.

———————————————————— 1979, Astrophys J,230,502.

Young, P.J., Schneider, D.P, and Schectman, S.A. 1981a, Astrophys J,244,259.

———————————————————————————————1981b,

Astrophys J,245,1035.

FIGURE CAPTIONS.

Figure 1.

The four eclipses of OY Car at V, measured on 1981 March 1. The cycle numbers (in parentheses) and phases refer to the Ephemeris of Vogt et al (1981). The counts on the left-hand axes have been corrected for the effects of atmospheric extinction. Typical 2σ uncertainties in each datum are shown on the light curves. The first body to be eclipsed in each cycle, shown by the dashed lines, is the white dwarf. Shown on panel a are the four contact times of its eclipse (t_1 to t_4), the half-width of the eclipse, $\Delta t_{1/2}$, and the duration of the eclipse of the white dwarf, Δ_{WD}.

Figure 2.

The variation of the radius of the white dwarf, R_w, and the duration of its eclipse by the red dwarf, Δ_{WD}, for inclinations between 70^0 and 90^6. The inclinations are labelled at the top of each locus. The gradient of each locus at a given R_w is the same at all inclinations, and is proportional to R_w; see the discussion in the text.

Figure 3.

The mass and radius of the white dwarf corresponding to K =115 kms-1, shown for the inclinations given at the top of each datum. The two curves shown correspond to the upper and

lower bounds on the duration of the eclipse of the white dwarf, Δ_{ω_D} , of 21s and 55. The dashed lines through each are hand drawn to aid the eye. Physically plausible inclinations are those at which the white dwarf obeys the mass-radius relation for white dwarfs, shown as a solid line, and computed from the formula of Pringle and Webbink (1975).

Figure 4

The masses and radii of the red dwarfs appropriate to the permitted bounds to the inclination, compared with the Lower Main Sequence mass-radius relation of Young and Schneider (1979), and the theoretical Zero Age Main Sequence of Grossman, Hays and Graboske (1974) (solid line) The three panels show the masses and radii for each value of K_w considered in this paper.

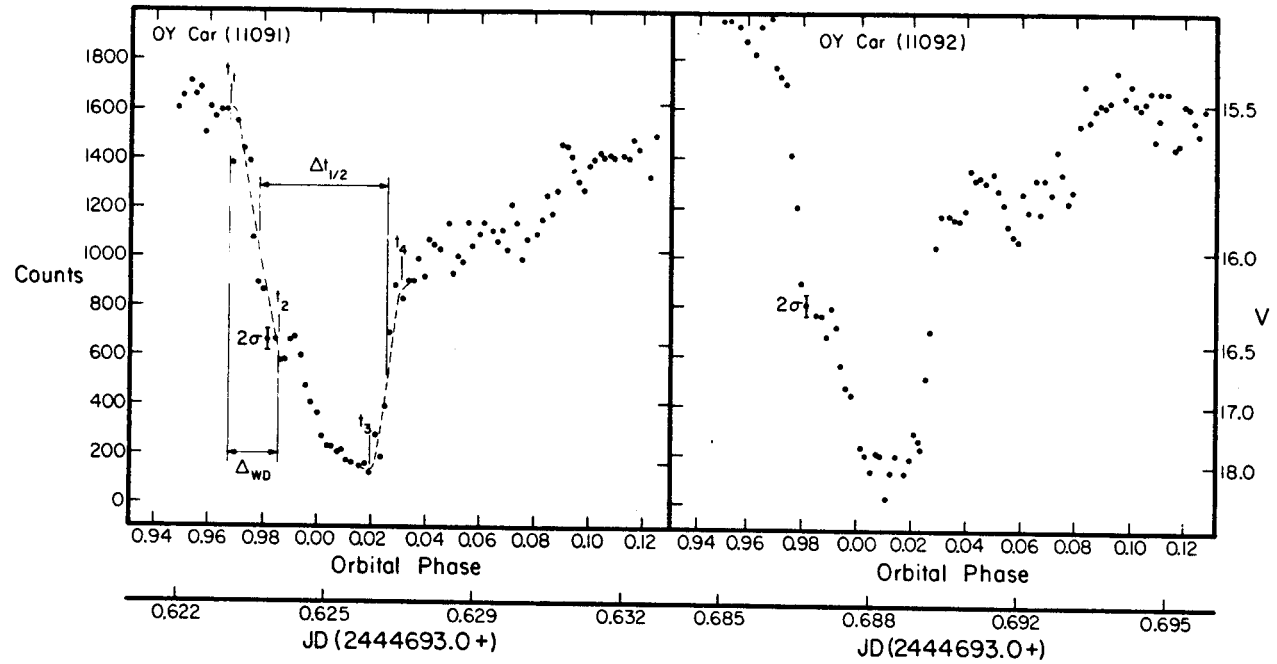
OY Car (11091)
OY Car (11092)
Counts
V
$\Delta t_{1/2}$
Δ_{WD}
2σ
t_1
t_2
t_3
t_4
Orbital Phase
JD (2444693.0+)

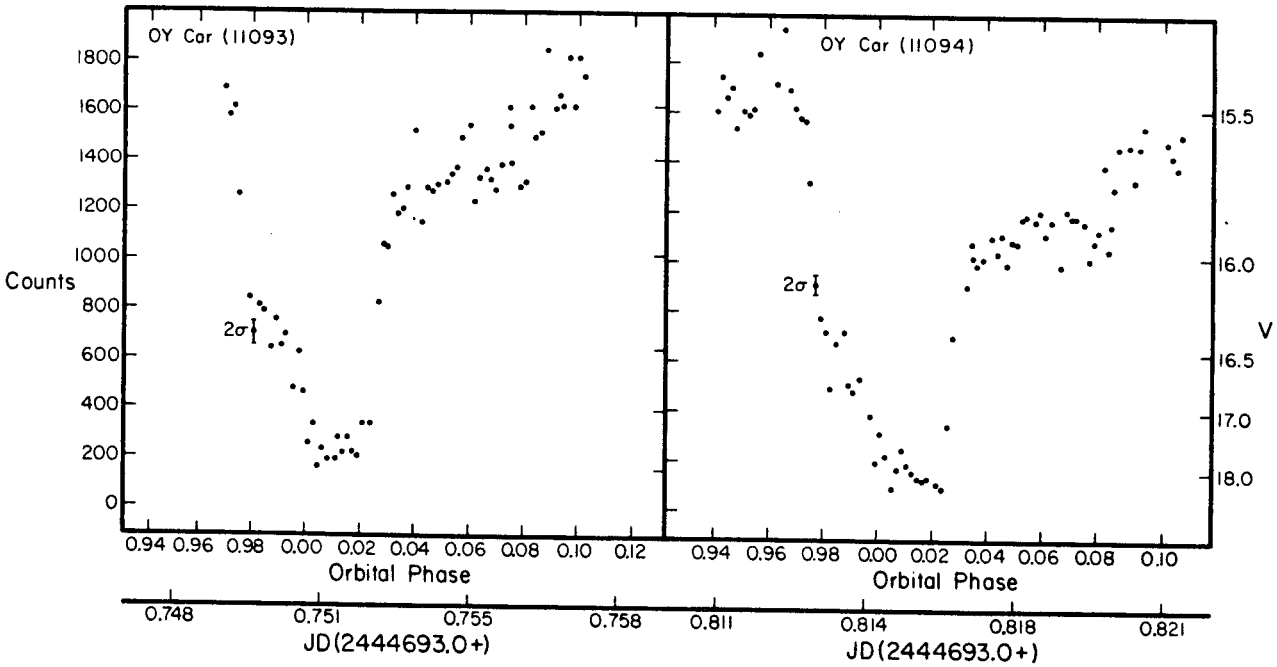
OY Car (11093)
OY Car (11094)
Counts
V
2σ
Orbital Phase
JD(2444693.0+)

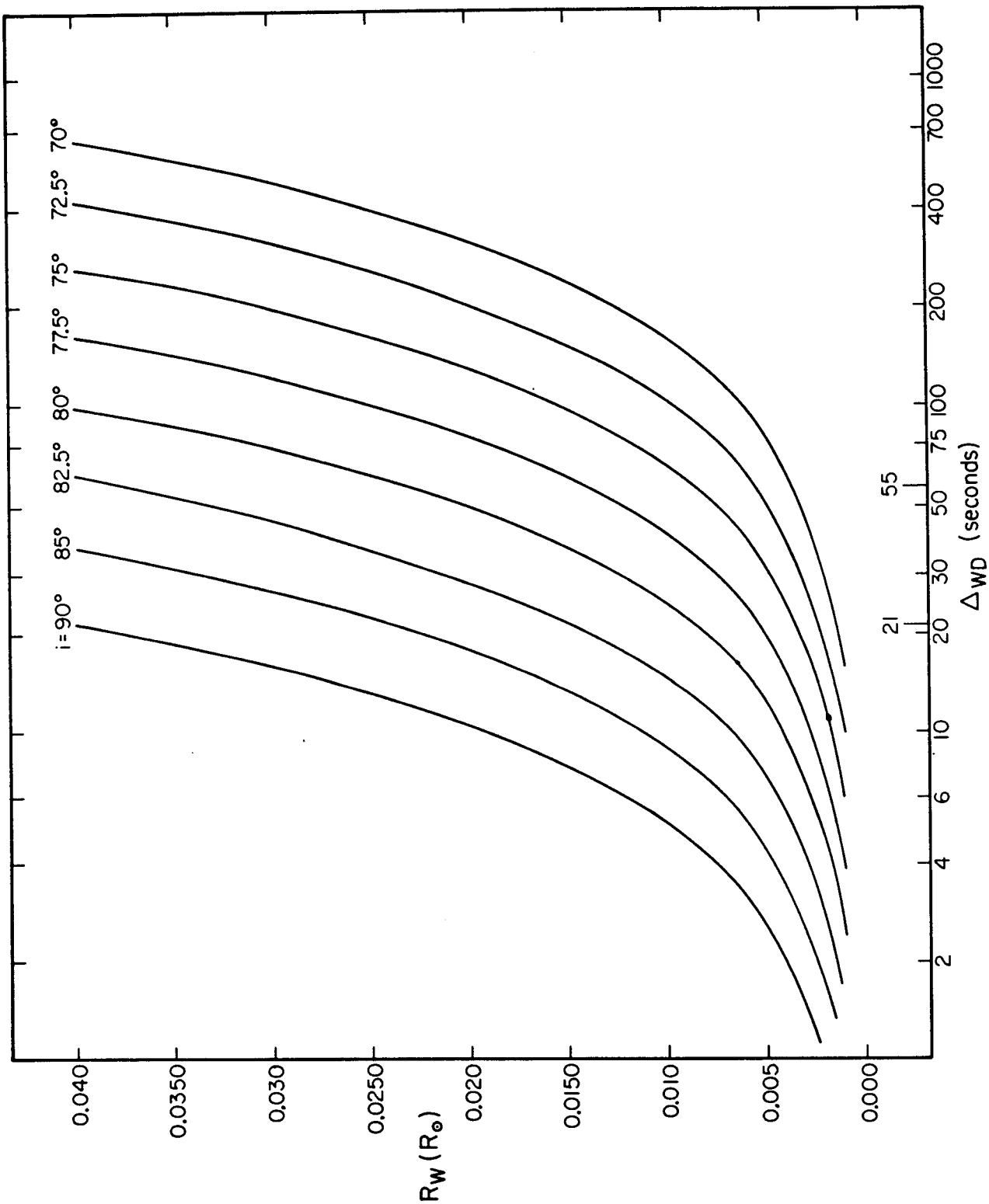
i=90°
85°
82.5°
80°
77.5°
75°
72.5°
70°
0.040
0.0350
0.030
0.0250
0.020
0.0150
0.010
0.005
0.000
R_W ($R_\odot$)
2
4
6
10
21
30
55
75
100
200
400
700
1000
Δ_{WD} (seconds)

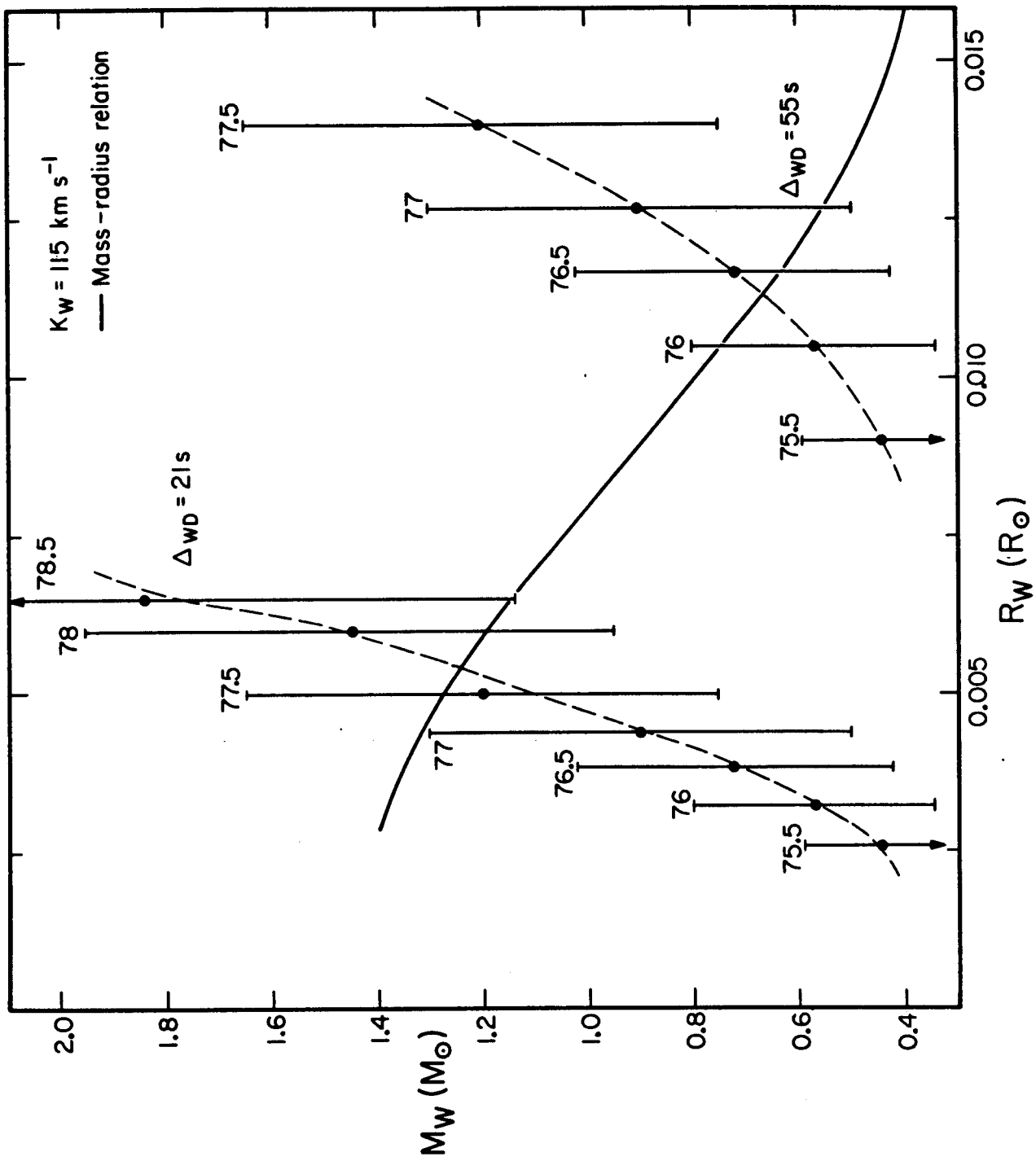
K_W = 115 km s^{-1}
Mass–radius relation
Δ_{WD} = 21s
Δ_{WD} = 55s
78.5
78
77.5
77
76.5
76
75.5
M_W ($M_\odot$)
R_W ($R_\odot$)
2.0
1.8
1.6
1.4
1.2
1.0
0.8
0.6
0.4
0.005
0.010
0.015

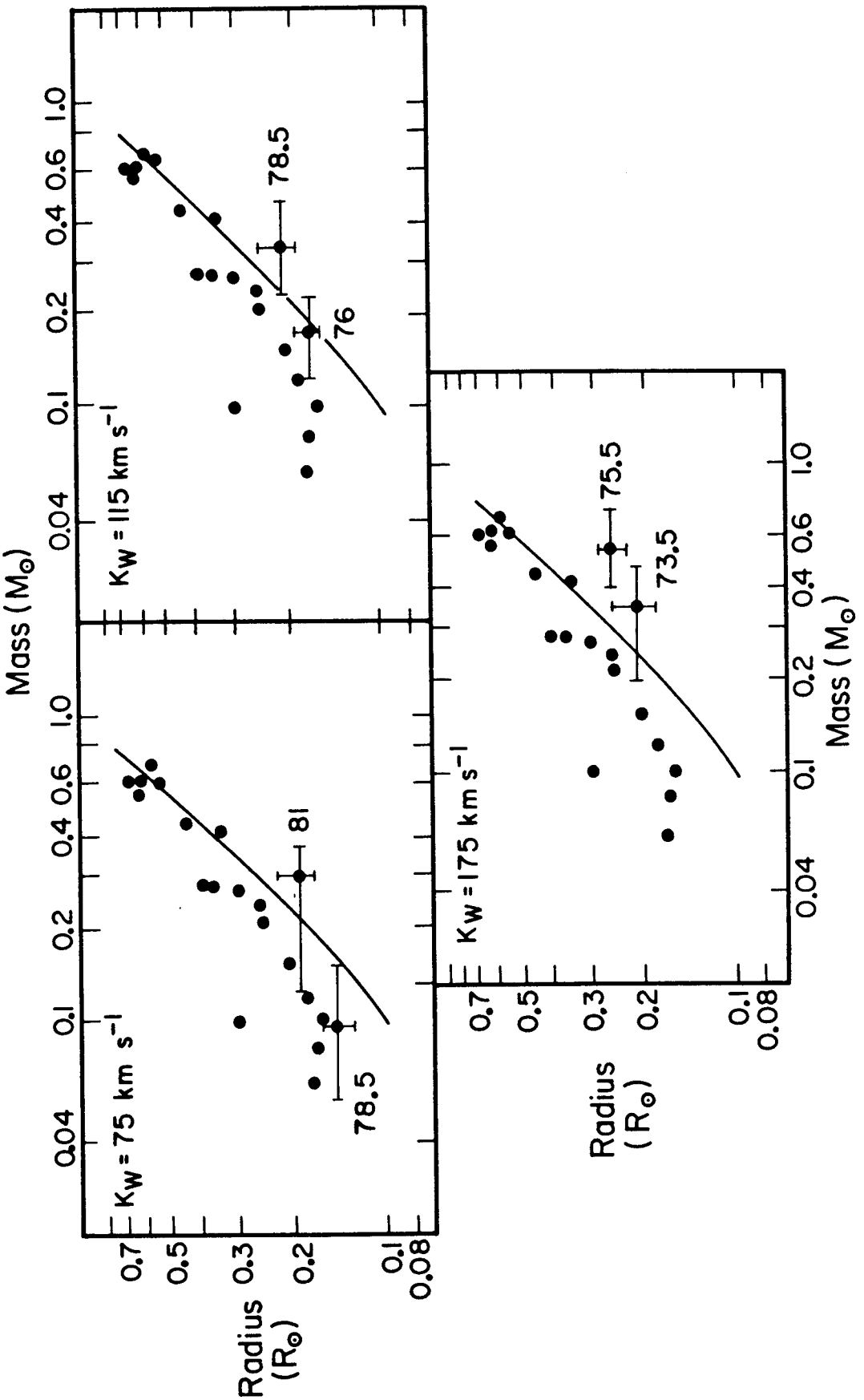
Mass ($M_\odot$)
Radius ($R_\odot$)
K_W = 75 km s^{-1}
K_W = 115 km s^{-1}
K_W = 175 km s^{-1}
78.5
81
78.5
76
75.5
73.5
0.04
0.1
0.2
0.4
0.6
1.0
0.08
0.3
0.5
0.7

Chapter 4.

A VISIBLE AND INFRARED STUDY OF THE ECLIPSING DWARF NOVA OY CARINAE: II THE INFRARED LIGHT CURVES.

SUMMARY.

This paper presents three simultaneous visible (V) and infrared (J,H,K) light curves of the eclipsing cataclysmic binary system OY Carinae, in quiescence. The infrared light curves show a secondary minimum, not seen in the visible, which arises from the ellipsoidal variations of the red dwarf and its eclipse by the accretion disc surrounding the white dwarf companion. The depths of the primary and secondary eclipses in the infrared and the observed colours of the system outside eclipse imply that between one-half and four-fifths of the uneclipsed infrared light comes from the red dwarf and that more than three-fifths of the infrared light of the disc is eclipsed in primary minimum. The latter result requires that the magnitudes of the red dwarf lie between K = 14.2 and K = 14.7. The distance to the system, deduced from these limits and an estimate of the surface brightness of the red dwarf, lies between 100 and 300 pc.

The infrared light of the disc comes largely from optically thin gas in either the outer disc or the chromosphere. The radial extent of this gas may be somewhat larger than that producing the visible continuum.

1. INTRODUCTION.

The transfer of matter between the components of binary stars is common, but Cataclysmic Variable Stars (hereafter, CVs) are the only systems in which emission from the transferred material provides most of the visible light. As such, they have been intensively studied over the past decade (for a recent review, see, e.g., Cordova and Mason 1982). They consist of a red dwarf that fills its Roche Lobe and transfers matter to a white dwarf companion. The large angular momentum of this matter causes it to form a disc around the white dwarf. In many systems, the copious emission of the disc has frustrated attempts to study the red dwarfs, even in the red and infrared, where they emit most of their light (see, e.g., Young and Schneider 1981; Berriman and Szkody 1983).

The study of the red dwarfs is important because they provide the best available means of finding the distances to the systems. The distances themselves are of importance in two problems: the study of the luminosity of the accretion disc (necessary in the development of realistic disc models) and the derivation of the space density of the systems (necessary in studies of their evolution).

An as yet little used probe of the red dwarfs is the infrared light curves of highly inclined CVs: if the star supplies much of the infrared light, these light curves will show not only an eclipse of the disc by the red dwarf, but

also a second, shallow minimum half a cycle later. This "secondary" minimum arises from the tidally induced ellipsoidal variations of the red dwarf, which are doubly sinusoidal in shape, and from the eclipse of the red dwarf by the disc. Such light curves are readily distinguishable from those of systems whose light comes mostly from the disc, which characteristically show a single deep eclipse.

Infrared light curves are also of interest in the study of the infrared continuum of the disc. Whereas the visible continuum is thought to come from hot optically thick gas comprising the bulk of the disc (Warner and Nather 1971), the infrared continuum will have a much larger contribution from any cool, optically thick gas and optically thin gas that is present. The cool opaque gas lies in the outer disc, and can be as cool as ~2500 -3000K (Frank and King 1981). The optically thin gas produces the Balmer emission lines, and lies either in the outer disc (Williams 1980) or in a chromosphere above the disc (Jameson, King and Sherrington 1980).

In this paper, we study simultaneously measured visible (V) and infrared J, H, K) light curves of the 15th magnitude dwarf nova OY Carinae, in quiescence. It is an important system because its visible light curves show the eclipse of the white dwarf, a characteristic shared by only two other dwarf novae: HT Cas (Patterson 1981) and Z Cha (Bailey 1979). In a previous paper (Berriman 1983; Paper I), a study of the visible eclipses showed that the inclination of the system

lies between 73.5° and 81°, and that the red dwarf lies either on or slightly below the Main Sequence mass-radius relation. Sherrington et al (1982) have also presented infrared light curves of OY Car, but without simultaneous visible measurements.

2. OBSERVATIONS.

The data were acquired at the Cassegrain focus of the 2.5m DuPont telescope at Las Campanas Observatory, Chile. Paper I (Berriman 1983) describes the observations in detail. Three successive cycles of OY Car in quiescence were measured in the infrared: one at J, one at H and one at K, with occasional out-of-eclipse measurements of the J-H and H-K colours. An infrared/visible dichroic beam splitter in the infrared photometer allowed the measurement of simultaneous visible (V) light curves through each cycle. The V magnitudes differ by several hundredths of a magnitude from those of the Johnson V filter, because the dichroic does not transmit light at the red edge of the V filter.

The visible and infrared magnitudes of OY Car were established by measurements, made between cycles, of the nearby star used as a spectrophotometric standard by Bailey and Ward (1981), and shown on their finding chart. The high internal reproducibility of these measurements, better than 2 per cent when corrected for atmospheric extinction with standard air mass coefficients, shows that the data did not suffer from differential refraction between the visible and the infrared, nor from mechanical instabilities in the photometer.

The magnitudes of the local standard star were found from observations of several standard stars. They are: $V = 14.72 \pm 0.02$, $K = 10.79 \pm 0.02$, $J-H = 0.77 \pm 0.03$ and $H-K = 0.18 \pm 0.02$, consistent with those of an early M giant (Frogel et al 1978).

Figures 1,2 and 3 show the light curves and colours of the system. The time resolution of the J and H measurements is 80s out of eclipse and 160s in eclipse, and that of the K measurements, 160s throughout. The faintness of the source is primarily responsible for the uncertainties in the infrared data. The V data originally consisted of 10s integrations, but as shown in the figures, have been averaged over four integrations. The uncertainties in the V measurements out of eclipse come from flickering, and in eclipse, from photon statistics.

3. DESCRIPTION OF THE LIGHT CURVES.

The standard model of the structure of a CV readily explains the features of the visible and infrared light curves. In this model (see, e.g., Warner and Nather 1971), the red dwarf fills its Roche Lobe and transfers matter to the white dwarf. This matter has a large angular momentum, and thus forms a disc around the white dwarf. A "hot spot" forms where the recently transferred matter strikes the outer disc. Because OY Car is highly inclined ($i = 73.5^{\circ}$ to 81°), this hot spot is seen only as it rotates into the line of sight of the Earth, giving rise to the shoulder seen in the visible light curves between phases 0.6 and 0.9. Between phases 0.1 and 0.6, the disc, presumed to be optically thick in the visible, obscures the hot spot. The shoulder is most prominent in cycles 11092 and 11093; in cycle 11091, it is fainter than in the succeeding cycles. Such cycle-to-cycle changes most probably reflect changes in the mass transfer rate. The primary eclipse (phases 0.0 to 0.1) is seen in the original high time resolution data to consist of an eclipse of the hot spot, the disc and the white dwarf; these data are presented in Paper I (Berriman 1983).

Two features of the visible light curve show directly that the disc and hot spot supply most of the visible light of the system: the fact that the eclipse of the hot components is deep (>3 mag) and the fact that there is not a secondary minimum near phase 0.5, which would arise from the ellipsoidal

variations of the red dwarf and its eclipse by the disc.

The infrared light curves differ from the visible ones: they have a secondary minimum at phase 0.5, best seen at H (cycle 11092), and a primary minimum that is shallower than in the visible. They do not show a significant contribution from the hot spot (i.e. there is no asymmetry between phases 0.6 and 0.9). The light curves of Sherrington et al (1982) show the same characteristics. The presence of the secondary minimum shows that the red dwarf, which emits most of its light between 1μm and 2μm, supplies much of the infrared light of the system. Corroborating this conclusion is the fact that, in each cycle, the observed visible to infrared colours are similar to those of cool dwarfs. For example, V-K is typically ~2 out of eclipse, and at mid-eclipse in cycle 11093 (when most of the disc is eclipsed), it is ~3.5, the colours of cool dwarfs range from 2.0 (K0) to 6.8 (M6) (Frogel et al 1978; Young and Schneider 1981). The red dwarf cannot, however, produce all the infrared light because the disc is seen to be eclipsed by the red dwarf at phase 0.0.

The observed infrared colours are the result of the superposition of the light of the red dwarf on that of the disc. The observed value of H-K of ~0.4 is redder than that of M dwarfs (Frogel et al 1978), which implies that the much of the infrared light of the disc comes from cool, opaque gas or optically thin gas; the hot opaque gas producing the visible continuum of the disc does not supply much of its infrared light.

The absence of the hot spot is consistent with the hypothesis that the hot spots in quiescent CVs have temperatures in the range T ~ 10,000K to 50,000K (Warner and Nather 1971; Wu and Panek 1982) and are optically thick in the visible and infrared continuum (Warner 1976). It thus radiates predominantly in the blue and visible. For example, a hot spot having a Rayleigh-Jeans spectrum between 0.5μm and 2μm and whose flux at V is ~1.2mJy (corresponding to V = 16.3, required to produce the observed visible amplitude of the shoulder, 0.5 mag) would produce a flux of 0.14mJy at 1.6μm, less than 5 per cent of the observed fluxes at these wavelengths.

Another feature of the visible light curves not seen in the infrared is the pronounced flickering. It is thought to originate in rapid variations in the density and velocity of the infalling material, which produce rapid fluctuations in the temperature of the hot spot. The absence of infrared flickering is consistent with this hypothesis, because the temperature fluctuations of 30-40 per cent about a mean temperature of 50,000K (Szkody 1976) that are required to reproduce the observed flickering give rise to flickering whose amplitude increases into the blue.

4. THE RED DWARF.

(a) Contribution of the red dwarf to the infrared light.

To determine the brightness of the red dwarf, the infrared light curves must be decomposed into the relative contributions of the red dwarf and the disc. The available data allow this to be done in two ways, described below: from the depths of the primary and secondary minima, and from the observed visual to infrared colours.

i) The infrared light curves.

Model of the light curves.

The secondary minimum comes from the ellipsoidal variations of the red dwarf and its eclipse by the disc; the depth of this minimum thus measures the contribution of the red dwarf to the infrared light. The depth of the primary minimum is determined by the proportion of the light coming from the disc and by the fraction of the disc that is eclipsed.

To determine how much of the light comes from the red dwarf and how much of the disc the red dwarf obscures, the observed eclipse depths have been compared with those of a simple model of the light curves, along the lines of that used by Berriman et al (1983) to study the tidally distorted red dwarf in U Geminorum. Briefly, the model considers the system to consist of two sources of light, the tidally distorted red

dwarf and the accretion disc. The latter is regarded as having a constant brightness in time, because the observations show that the system does not flicker significantly in the infrared.

Consider first the amplitude of the tidal distortions of the red dwarf and its eclipse by the disc. The photosphere of the red dwarf is represented by the equipotential of its Roche surface, as given in a cylindrical coordinate system whose origin is at the centre of mass of the red dwarf. The ellipsoidal light curve is computed by integrating the flux emitted over the area of the photosphere visible in the line of sight of the observer, at a large number of phases throughout the orbit. The calculations take account of the gravity darkening of the red dwarf and of its irradiation by the hot components of the system, but not of limb darkening. The amplitude of the ellipsoidal variations, for the plausible mass ratios and inclinations deduced for OY Car in Paper I ($q = 0.11 - 0.54$; $i = 73.5^{\circ} - 81^{\circ}$), lies between 0.23 and 0.30 magnitudes; the calculations of the synthetic light curves use an amplitude of 0.27 mag.

This technique to study the ellipsoidal variations has also been used to find the amplitude of the eclipse of the red dwarf by the disc. The geometry of the eclipse is similar to that of Figure 4 of Berriman et al (1983), but the inclination of OY Car is higher (73.5° to 81°) and the orbital separation is smaller ($0.6R_{\odot}$-$0.9R_{\odot}$). The eclipse is produced by the obscuration of a small area of the red dwarf by the disc,

which is strongly foreshortened and appears elliptical projected onto the sky. The simulation of the eclipse is similar to that of the the ellipsoidal variations, except that the light from the obscured part of the red dwarf is excluded from the calculations of the integrated light. In OY Car, the radius of the disc producing the infrared light lies in the range 10(10)- 2 x (10)cm (derived in Section 4). For such a disc and the geometry of OY Car (mentioned immediately above), the eclipse of the red dwarf increases the amplitude of the secondary minimum beyond that of the ellipsoidal variations by 0.1 to 0.2 mag. The amplitude of the eclipse changes only weakly with disc size because the disc is strongly foreshortened at high inclinations.

In the simulated light curves used for comparison with the observations, the light of the disc has been superposed on the tidal distortions and the eclipse of the red dwarf. Figure 4(b) shows the variation of the depth of the secondary minimum with the proportion of light provided by the disc at phases 0.25 and 0.75 (the brightest points of the light curves). This variation is shown for a red dwarf that is tidally distorted (Curve 1) and for one that is both tidally distorted and eclipsed by the disc (Curve 2). Because the disc is not eclipsed at secondary minimum, the depth naturally decreases as the disc supplies progressively more of the light.

Figure 4(a) shows the corresponding variation of the amplitude of the primary minimum, when a given fraction of the disc is eclipsed. If the disc is uneclipsed (corresponding to the lowest curve in Figure 4a), the tidal distortions of the red dwarf will be the only source of variability, and, as in the case of the secondary minimum, the amplitude decreases as the proportion of the light coming from the disc increases. When the disc supplies a known fraction of the uneclipsed light, the amplitude increases with the fraction of the disc eclipsed because more light is being obscured.

The eclipse depths computed by the above method exclude the heating of the red dwarf by the hot components of the system. The principal effect of such heating would be to make the secondary minimum shallower than produced by the ellipsoidal variations alone, because the hot components heat the inner hemisphere of the red dwarf (see, e.g., Figure 4c of Berriman et al 1983 for an illustration of this phenomenon). This type of light curve is incompatible with those observed by ourselves and by Sherrington et al (1982), which have a secondary minimum at least ~0.2 mag deep.

Comparison with observations.

The depths of the eclipses have been found directly from an examination of the light curves. At each wavelength, the depths of the primary and secondary minima are in the range 0.6-1.0 mag and 0.2-0.4 mag, respectively (within the 3σ

uncertainties of the measurements). These large ranges reflect the fact that because OY Car is faint, the statistical accuracy and time resolution of the data are relatively low.

To reproduce the observed secondary minimum, Figure 4b shows directly that at phases 0.25 and 0.75 the red dwarf supplies at least half the light at J, H and K. According to Figure 4a, when the red supplies this fraction of the light, it eclipses more than three-fifths of the disc to account for the observed primary eclipse depths. This is well shown in Figure 5, where the model light curves for a system in which the disc and red dwarf contribute equally to the light has been superposed on the light curves at H (cycle 11092).

Given that more than 60 per cent of the disc is eclipsed, the K magnitude of the red dwarf lies between 14.2 and 14.7. This analysis differs from that of Sherrington et al (1982), who deduced that the red dwarf has K = 14.4 by supposing that the disc is totally eclipsed in primary minimum.

(ii) Observed colours of the system.

Because the observed colours result from the superposition of the light of the red dwarf on that of the disc, they must be decomposed into the relative contributions of each component in order to estimate the infrared magnitudes of the red dwarf. This decomposition is difficult because the disc is complex, consisting of optically thick and optically thin components, both of which are likely to be

multi-temperatured. Suppose that the light of the disc comes from an arbitrary combination of the the hottest opaque gas thought to be present, and the coolest transparent gas. The disc then has its bluest colours, and consequently the contribution made by the red dwarf to the observed colours is the maximum possible. In contrast, the light curves give the minimum contribution: the combination of the two analyses thus provides strong restrictions on the magnitudes of the red dwarf in OY Car.

Berriman and Szkody (1983) have investigated how the maximum contribution may be found, under the assumption that the optically thick gas is cooler than 50,000K and the optically thin gas is hotter than 5,000K. These bounds have been deduced in theoretical calculations of the energy balance of the disc, for mass transfer rates of ~10(-10) $M_\odot$ yr-1, thought to be present in quiescent dwarf novae (see, e.g., Williams 1980; Mayo et al 1981).

The actual analysis is best carried out with the aid of a "flux ratio" diagram, which is similar to the conventional colour-colour diagram, except that the axes are the ratios of the flux densities at the wavelengths under consideration. Figure 6 shows such a diagram, based on the ratios $F_\nu(V)/F_\nu(H)$ and $F_\nu(K)/F_\nu(H)$, on which are plotted the ratios of the two kinds of emission from the disc, at their limiting temperatures, and the observed ratios of OY Car out of eclipse. The ratio $F_\nu(V)/F_\nu(H) = 1.0 \pm 0.1$, which corresponds to $V = 15.5 \pm 0.1$, has been found from the observations in

cycle 11092 made between phases 0.1 and 0.6 (when the hot spot is obscured). The ratio $F_\nu(K)/F_\nu(H)$ is less precisely known because the data are fewer. The mean colour, based on measurements of all three cycles, is H-K = 0.45 ± 0.05 ($F_\nu(K)/F_\nu(H)$ = 0.95), but the observed colours lie between 0.3 ($F_\nu(K)/F_\nu(H)$ = 0.8) and 0.6 ($F_\nu(K)/F_\nu(H)$ = 1.1); the mean and its uncertainty and the observed range are shown on the Figure. The V-H colour is typical of quiescent dwarf novae, but the H-K colour is atypically red, because the hot opaque gas, which lies in a small, highly inclined disc, does not supply as much of the infrared light as it does in other systems (discussed in the next Section).

The usefulness of the diagram lies in the fact that, because the axes of the diagram are linear, the flux ratios of a composite object lie on a straight line connecting the flux ratios of the individual components (Rabin 1980, 1982; Wade 1982). The flux ratios of the disc thus lie along the line AB in Figure 6. By the same principle, the flux ratios of OY Car lie along the straight line joining the flux ratios of the red dwarf and the accretion disc. Furthermore, the distance from the observed ratio to the boundary line AB gives the maximum fractional contribution of a red dwarf of a given type to the total light at H, itself represented by the distance from the red dwarf to the boundary line.

The only constraint to the spectral type of the red dwarf is provided by the observed colour of V-K > 3.5 (at the base of primary eclipse in cycle 11093, which implies that it must be an M star. Given that such a star is present, the diagram shows directly that for the mean value of $F_\nu(K)/F_\nu(H)$, the red dwarf supplies no more than one-half the infrared light, whatever class of M dwarf it is. This is the most likely value of the maximum contribution of the red dwarf. Since this value is the same as the minimum contribution, as determined from the light curves, it is likely that the red dwarf actually provides half the light at 1.6μm. This conclusion cannot, however, be regarded as definitive because the observed range of the ratio $F_\nu(K)/F_\nu(H)$ is sufficiently large that the red dwarf may supply up to four-fifths of the infrared light: such a contribution would come from a late M star in a system having H-K = 0.3 ($F_\nu(K)/F_\nu(H)$ = 0.8). If the red dwarf does supply half the light, then both its tidal distortions and its eclipse produce the secondary minimum, as Figure 4b shows that the tidal distortions alone do not account for the observed depth of this minimum.

(b) The distance to OY Car.

The spectral type of the red dwarf cannot be found from the present data (as discussed above), but it is likely that it is a Main Sequence star, because the colours are consistent with this view (as discussed above) and because it was shown in Paper I that the star lies either on or slightly below the

Main Sequence mass-radius relation.

This being so, the distance to the system can be found from Bailey's (1981) empirical result that the surface brightness at K of cool field dwarfs and giants depend only weakly on their effective temperature, as measured by their V-K colour.

The surface brightness of the red dwarf depends upon its temperature, that is, upon its luminosity and radius, or equivalently, its observed brightness, distance and radius. Since the radius, R_R, (see Paper I) and apparent brightness, K, of the red dwarf are known, the distance, d, to the system follows directly from Bailey's definition of surface brightness:

$$\log d = \frac{K}{5} + 1 - \frac{S_K}{5} + \log\left(\frac{R_R}{R_\odot}\right),$$

where S_K is the surface brightness.

The uncertainty in the distance is given by:

$$\sigma^2_{\log d} = \frac{\sigma_K^2}{25} + \frac{\sigma^2_{S_K}}{25} + \left(\frac{\log_{10} e}{R_R}\right)^2 \sigma^2_{R_R}$$

where σ_K, σ_{S_K}, and σ_{R_R} are the uncertainties in the K magnitude, surface brightness and radius of the red dwarf respectively. The red dwarf in OY Car is redder than V-K = 3.5 (see above), which, according to Bailey's calibration, corresponds to a surface brightness at K of $S_K = 4.6 \pm 1.0$. The large uncertainty comes from the

dispersion in the calibration (see his Figure 1). In Paper I, the radius of the red dwarf was found to lie between $0.14 \pm 0.02\ R_\odot$ and $0.25 \pm 0.03\ R_\odot$; for K= 14.2, the distance to the system correspondingly lies between 120 to 200 pc; and for K= 14.7, between 160 and 260 pc. The uncertainty in each distance is $\sigma_{\log d} = 0.25$. We thus consider that OY Car lies between 100 and 300pc for the rest of this paper. This range of distances comes about largely through uncertainties in the radius of the red dwarf, rather than through uncertainties in the K magnitude of the red dwarf.

Sherrington et al (1982) find that the distance is between 100 and 140pc. Their range of distances is much narrower than ours because they assumed that the disc was totally eclipsed during their measurements, and that the red dwarf is a lower Main Sequence star of radius $0.15R_\odot$, which Paper I has shown is not necessarily the case.

5. THE INFRARED CONTINUUM OF THE DISC.

(a) Radius of the accretion disc in the infrared.

In addition to the distance of the system and the colours of the disc, a third quantity needed to study the nature of the infrared light of the disc is the size of the region producing it. It can be found from the observed width of the primary minimum in the infrared, following the method of Sulkanen, Brasure and Patterson (1981). They showed that in a system of inclination i, the radius, R_d, of the disc giving rise to an eclipse whose fractional half-width, $\Delta\phi_{1/2}$, is

$$R_d + R_c = 2\pi a \Delta\phi_{1/2} \sin i,$$

where a is the orbital separation and R_c is the half chord on the red dwarf passing through the centre of the disc. In terms of the radius of the red dwarf, it is given by

$$\frac{R_c}{a} = \sqrt{\left(\frac{R_R}{a}\right)^2 - \cos^2 i}$$

The radius of the disc is then:

$$R_d = 2\pi a \Delta\phi_{1/2} \sin i - \sqrt{\left(\frac{R_r}{a}\right)^2 - \cos^2 i}\; a$$

The fractional half-width of the disc has been found from the light curves of Sherrington et al (1982), which give a more precise estimate of this quantity than do ours because their time resolution and statistical accuracy are higher. Its value at 1.2μm and 1.6μm, measured on different nights, is $\Delta\phi_{1/2} = 0.075 \pm 0.015$. Because the eclipse widths do not vary

from night to night and because the infrared light curves were similar between the two series of measurements, this value is most probably the same in the present light curves.

The geometry of OY Car and the radius of the red dwarf have been found in Paper I from the visible eclipses and the semi-amplitude of the radial velocity of the red dwarf. Briefly, three series of solutions were derived, corresponding to different values of the semi-amplitude, K_w. This is necessary because K_w is known only to a factor of ~2, being found from the emission lines, which reflect more accurately the complex motion of the disc in which they originate than of the white dwarf.

For each value of K_w, the inclination can be found to an accuracy of ~2°; at K_w = 75 km s-1, it lies between 78.5° and 81°; at 115 km s-1, between 76° and 78.5° and at 175 km s-1, between 73.5° and 75°; the corresponding values of R_R/a and a are given in Table 1 of Paper I. For each series of solutions, the radius of the disc, as given by the above formula, lies between
(1.0± 0.3) x 10(10) cm-(2.0± 0.5) x 10(10) cm. Both the large variation in radius over a range of inclination of ~2 and the large uncertainties of ~25 per cent arise because the orbital separation is very sensitive to inclination (as explained in Paper I); it ranges from ~0.6 to $0.9R_\odot$ in each of the three series of solutions.

The disc may be somewhat larger in the infrared than in the visible, where most of the light comes from a region of radius ~7 x 10(9) cm (Ritter 1980). The radius actually derived is the distance of the hot spot from the white dwarf, but the hot spot in most systems is sited in the outer regions of the disc that produce the visible continuum (Smak 1971).

(b) The nature of the infrared continuum.

That the observed H-K colour of OY Car is redder than those of cool dwarfs implies that the infrared continuum of the disc comes from either the optically thin gas producing the Balmer lines or opaque gas cooler than ~3000K. Here, we consider the possible contributions of each type of emission to the observed light.

(i) Power radiated by an optically thin plasma.

First suppose that all the infrared continuum of the disc comes from the optically thin plasma that produces the Balmer emission lines. If the emissivity of the plasma at an infrared frequency ν is $\varepsilon_\nu(T)$, and the system lies at d pc, the emission integral of the plasma, $\int N^2 dV$, required to supply the observed infrared fluxes is given by:

$$\int N^2 dV = 4\pi d^2 F_\nu \varepsilon_\nu(T)^{-1}$$

where F_ν is the observed flux density at frequency ν.

The properties of the plasma have been computed from the deduced flux of the disc at 2.2μm; essentially the same results are found from the flux densities at J and at H. The arguments of Section 4 showed that the disc supplies between one-fifth and one-half of the observed infrared light of the system out of eclipse. We shall assume that the disc actually supplies half the light because this is its most likely contribution and because the conclusions drawn are essentially

the same over the above range of contributions. The flux density of the disc is thus 0.15mJy at 2.2μm.

Row 1 of Table 1 presents the emission integrals corresponding to this flux density; the emission coefficients of Ferland (1980) have been used throughout. Shown in the Table are the properties of the plasma deduced for the upper and lower bounds to the distance of the system and for temperatures of 5,000K and 100,000K, thought to be the range of temperatures of the plasma in the accretion disc (Williams 1980; Jameson, King and Sherrington 1980). The emission integrals are higher at the lower temperatures because hot, optically thin gas radiates inefficiently. The integrals in Table 1 are all consistent with those deduced from observations of the Balmer lines. For example, the observed power in the Hδ line is 3.9 x 10(-21) W cm-2 (Bailey and Ward 1981), which comes from a plasma having an emission integral $\int N^2 dV$ =1 x 10(55) cm-3 at 100pc, and 1 x 10(56) cm-3 at 300 pc, typical of those present in other quiescent dwarf novae (Oke and Wade 1982). These integrals may be somewhat underestimated because the Balmer lines in CVs are thought to be optically thick (Oke and Wade, op cit).

(ii) Size of the plasma.

Because the Balmer decrements are flat (Oke and Wade, op cit), the plasma is thought to have densities of N~10(13)cm-3 or greater. The volumes of plasmas having such densities are given in Table 1, as are the radii of uniformly thick

accretion discs having these volumes, given by

$$R_d = \left(V / \pi z \right)^{1/2}$$

where z is the thickness of the disc, taken to be 10(9) cm, one tenth the radius of the disc (Mayo et al 1981). The radii presented in Table 1 are those corresponding to a plasma density of 10(13) cm-3. If the system lies at 300pc, the plasma must be denser than this, otherwise the disc is larger than permitted by the observations. Densities of ~5 x 10(13) cm-3 would reduce the radius of the disc sufficiently.

The location of the gas cannot be determined unequivocally: the disc radii corresponding to both the allowed temperatures and distances have a sufficiently wide range that they are equally well consistent with emission from a chromosphere above the disc or from the outer disc.

(iii) Contribution of hot opaque gas.

The power emitted by the plasma is in general no larger than that emitted by the plasmas in other CVs (Oke and Wade 1982), but it nevertheless provides a much larger fraction of the infrared light (see, e.g., Berriman and Szkody 1983; Berriman et al 1983). This is because the main body of the disc, which is hot and optically thick, is atypically small by a factor of ~4 compared with other systems (Sulkanen, Brasure and Patterson 1981) and is also highly inclined. It cannot supply much of the infrared light, even though opaque gas radiates much more efficiently than does optically thin gas.

To show this, consider a system at inclination i having a physically thin but optically thick disc at an effective temperature T_{eff}. It emits a power P_ν,

$$P_\nu = \pi R_d^2 \cos i \, B_\nu(T_{eff})$$

where R_d is its radius.

Empirical determinations of the temperature of the gas producing the visible continuum have not been made, but theoretical calculations show that the temperature is most likely in the range 10,000K to 50,000K (see, e.g., Williams 1980). At 2μm, the corresponding power radiated by a disc at 50,000K is 1.4 x 10(9) W Hz-1, which is 30 per cent of the observed infrared power. The actual fraction the opaque gas contributes is likely to be much less, because gas at ~50,000K most probably occupies only the inner disc (Williams 1980). This small contribution does not alter the essential properties of the optically thin plasma deduced above.

(iv) Cool, opaque gas.

Suppose now that most of the infrared light of the disc comes from cool opaque gas, which the observed colours show has a temperature close to ~3000K. Such emission can come from the top surface of the disc, and, because the system is highly inclined, from the outer wall of the disc.

If the emission comes largely from the surface of the disc, then to produce the observed fluxes, the disc must have a radius R_d, given by

$$R_d = \left(4 d^2 F_\nu \Big/ \pi \cos i \, B_\nu (T_{eff}) \right)^{1/2}$$

For gas at ~3000K, the radius of the disc lies between ~10(11)cm at 100pc and 5 x 10(11) cm at 300pc, much larger than the observed size of the disc.

Similarly, if the outer wall of the disc supplies all the infrared light, its thickness z is given by

$$P_\nu = 2\pi R_d z \, B_\nu (T_{eff}) = 4\pi d^2 F_\nu$$

that is,

$$z = 2 d^2 F_\nu \Big/ R_d \, B_\nu (T_{eff})$$

For a wall at T = 3,000K and for a disc radius of R_d = 10(10) cm (deduced in Section a above), the disc has a thickness z~10(12) cm. This value is unreasonably large, as such an outer wall would obscure the white dwarf and the rest of the accretion disc, which are seen in the visible light curves. Discs in dwarf novae are, in fact, thought to be roughly one-tenth the radius of the disc (Mayo et al 1981); in OY Car, the disc is thus ~10(9) cm thick.

Cool opaque gas does not therefore produce a significant fraction of the observed light. The best model of the infrared continuum of the disc is thus one in which transparent gas produces most of the light. This view of the infrared light of the disc differs from that of Sherrington et al (1982), who supposed that the disc is everywhere optically thick.

6. CONCLUSIONS.

1. The J, H, and K light curves of OY Car in quiescence show a secondary minimum at phase 0.5, produced by the ellipsoidal variations of the red dwarf and its eclipse by the disc. The depth of this minimum, ~0.2 at each wavelength, and the observed visible to infrared colours out of eclipse require that the red dwarf supplies between one-half and four-fifths of the uneclipsed light of the system at H, with one half being the most likely contribution.

2. In primary eclipse, the red dwarf eclipses more than three-fifths of the infrared light of the disc. The infrared brightness of the red dwarf, deduced from the observations in primary eclipse, is between 14.2 and 14.7, and the distance to the system is between 100 and 300pc.

3. The infrared continuum of the disc comes largely from the optically thin plasma that produces the Balmer emission lines.

Table 1: Properties of an optically thin plasma producing the observed infrared continuum of the accretion disc in OY Car.

Property	Distance = 100 pc		Distance = 300 pc	
	T = 5,000K	T = 100,000K	T = 5,000K	T = 100,000K
Emission Integral $\int N^2 dV$ (CM^{-3})	$(1.2 \pm 0.4) \times 10^{55}$	$(7.1 \pm 1.4) \times 10^{54}$	$(1.6 \pm 0.3) \times 10^{56}$	$(4.0 \pm 0.8) \times 10^{55}$
Volume of Plasma (CM^3)	$(1.8 \pm 0.4) \times 10^{29}$	$(4.4 \pm 0.9) \times 10^{29}$	$(1.6 \pm 0.3) \times 10^{21}$	$(4.0 \pm 0.8) \times 10^{30}$
Radius of Disc (CM)	$(8.0 \pm 0.8) \times 10^{9}$	$(4.0 \pm 0.4) \times 10^{9}$	$(6.0 \pm 0.6) \times 10^{10}$	$(3.0 \pm 0.3) \times 10^{10}$

REFERENCES.

Bailey, J. 1979, Mon Not Roy ast Soc, 187, 645.

———— 1981, Mon Not Roy ast Soc, 917, 31.

Bailey, J., and Ward, M. 1981, Mon Not Roy ast Soc, 194, 17p.

Berriman, G. 1983, In Preparation.

Berriman, G., and Szkody, P. 1983, Mon Not Roy ast Soc, submitted.

Berriman, G., Beattie, D.H., Gatley, I., Lee, T.J., Mochnacki, S.W., and Szkody, P. 1983, Mon Not Roy ast Soc, In Press.

Cordova, F.A., and Mason, K.O. 1982, To appear in " Accretion Driven X-ray Sources", eds, W.H.G. Lewin and E.J. van der Heuvel (Cambridge University Press, England).

Cordova, F.A., Mason, K.O., and Fenimore, E.E. 1981, Reported in Cordova and Mason, 1981.

Ferland, G.J. 1980, Pub Ast Soc Pac, 92, 596.

Frank, J.F., and King, A.R. 1981, Mon Not Roy ast Soc, 195, 505.

Frogel, J.A., Persson, S.E., Aaronson, M., and Matthews, K. 1978, Astrophys J, 220, 75.

Jameson, R.F., King, A.R, and Sherrington, M.R. 1980, Mon Not Roy ast Soc, 191, 559.

Mayo, S.K., Wickramasinghe, D.T., and Whelan, J.A.J. 1981, Mon Not Roy ast Soc, 193, 793.

Patterson, J. 1981, Astrophys J Suppl Ser, 45, 517.

Oke, J.B., and Wade, R.A. 1982, Astron J, 87, 670.

Rabin, D. 1982, preprint.

———— 1980, Ph.D. Thesis, Calif. Inst. of Tech.

Ritter, H. 1980, Astron Astrophys, 85, 362.

Sherrington, M.R., Jameson, R.F., Bailey, J., and Giles, A.B. 1982, Mon Not Roy ast Soc, 200, 861.

Smak, J. 1971, Acta Astron, 21, 15.

Sulkanen, M.E., Brasure, W.L., and Patterson, J. 1981, Astrophys J, 244, 579.

Szkody, P. 1976, Astrophys J, 207, 824.

Vogt, N., Schoembs, R., Krzeminski, W., and Pederson, H. 1981, Astron Astrophys, 94, L29.

Wade, R.A. 1982, Astron J, 87, 1558.

Warner, B. 1976, Proc IAU Symposium 73, eds. P.P. Eggleton et al. Reidel, Dordrecht.

Warner, B., and Nather, R.E. 1971, Mon Not Roy ast Soc, 152, 219.

Williams, R.E. 1980, Astrophys J, 235, 939.

Wu, C.C., and Panek, R.J. 1982, Astrophys J, 262, 244.

Young, P.J., and Schneider, D.P. 1981, Astrophys J, 247, 960.

FIGURE CAPTIONS.

Figure 1

Simultaneous light curves of OY Car at V and J, with occasional measurements of the J-H and H-K colours. Cycle numbers (in brackets) are derived from the Ephemeris of Vogt et al (1981); see Paper I. Error flags are shown for those data whose uncertainties exceed the typical 2σ uncertainties shown on the Figure.

Figure 2.

As Figure 1, but at V and J.

Figure 3

As Figure 1, but at V and K.

Figure 4

The variation of the amplitude of the primary and secondary minima of the simulated light curves with the proportion of light provided by the disc, $F(disc)/F(total)$. The brightness of the curves has been set arbitrarily to 0.0 mag at phases 0.25 and 0.75. The dashed horizontal lines are the ranges of the amplitudes of the primary and secondary minima of the light curves at J and H (as deduced in the

text).

(a) Variation of the depth of primary minimum with the fraction of the disc eclipsed, given at the end of each curve.

(b) Variation of the depth of secondary minimum, if it comes from the ellipsoidal variations of the red dwarf alone (Curve 1), and from the ellipsoidal variations and the eclipse of the red dwarf by the disc (Curve 2).

Figure 5

The light curve of OY Car at H (cycle 11092) is repeated. Superposed on it are the model light curves for a system in which the red dwarf and disc each supply one-half of the uneclipsed infrared light of the system. The secondary minimum includes both the tidal distortions of the red dwarf and the eclipse of the red dwarf by the disc. The primary minima shown are are those resulting when increasing fractions of the disc are eclipsed by the red dwarf. These fractions are given on the left hand side of the primary minimum, next to the dashes, which indicate the bases of the eclipses.

Figure 6.

A flux ratio diagram based on the ratios $F_\nu(V)/F_\nu(H)$ and $F_\nu(K)/F_\nu(H)$, (adapted from Berriman and Szkody 1983), showing the observed ratios of OY Car. The error flag indicates the 1σ uncertainties about the mean $F_\nu(K)/F_\nu(H)$ ratio, and the

extension of the flag shows the observed range of the ratio. To derive the maximum contribution of the red dwarf to the infrared light, the disc is considered to consist of an arbitrary combination of emission from optically thin gas at 5,000K and optically thick gas at 50,000K; its flux ratio may lie anywhere along the line AB.

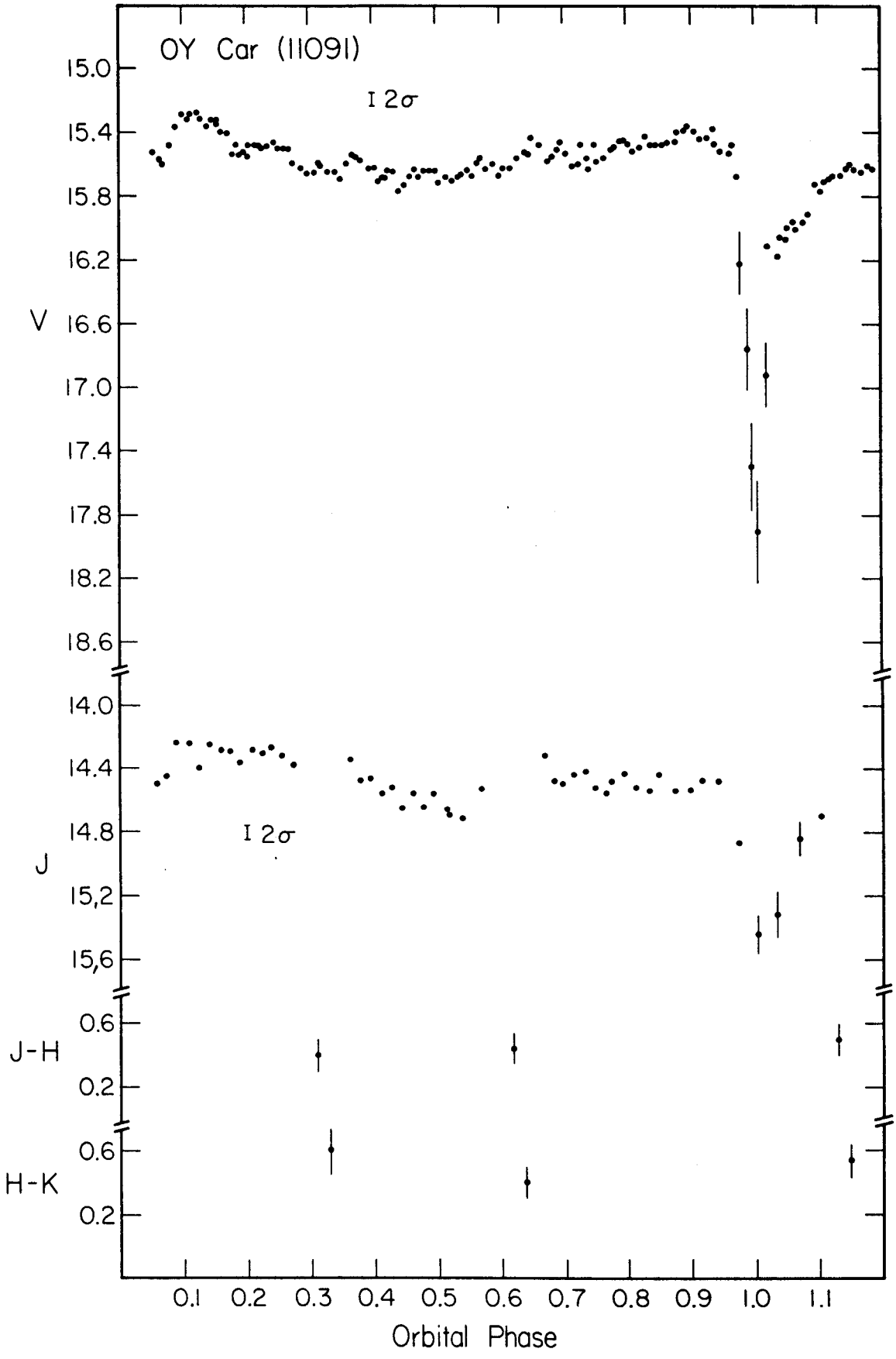
OY Car (11091)
I 2σ
V
15.0
15.4
15.8
16.2
16.6
17.0
17.4
17.8
18.2
18.6
I 2σ
J
14.0
14.4
14.8
15,2
15,6
J-H
0.6
0.2
H-K
0.6
0.2
0.1
0.2
0.3
0.4
0.5
0.6
0.7
0.8
0.9
1.0
1.1
Orbital Phase

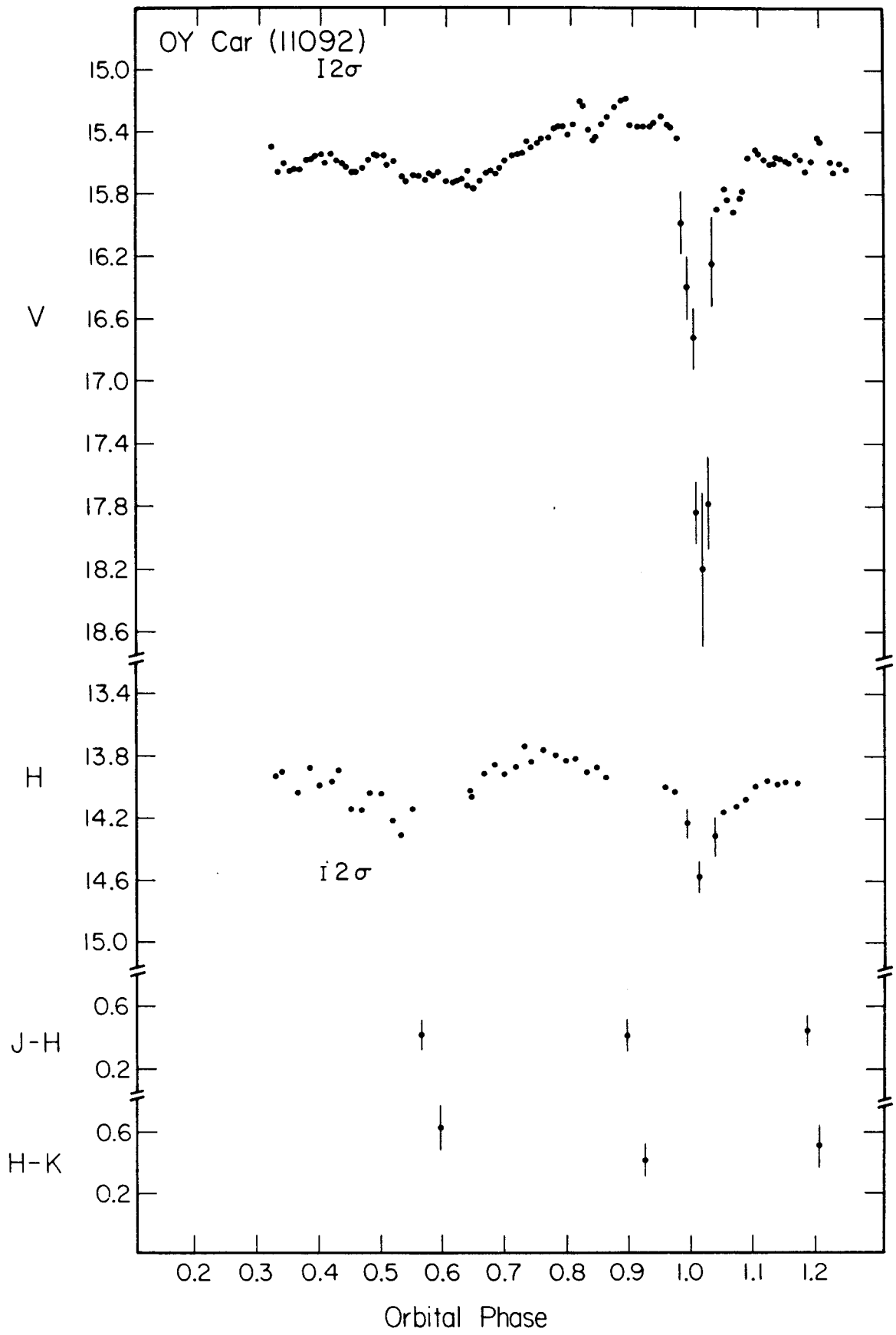
OY Car (11092)
12σ
15.0
15.4
15.8
16.2
V
16.6
17.0
17.4
17.8
18.2
18.6
13.4
13.8
H
14.2
12σ
14.6
15.0
0.6
J-H
0.2
0.6
H-K
0.2
0.2 0.3 0.4 0.5 0.6 0.7 0.8 0.9 1.0 1.1 1.2
Orbital Phase

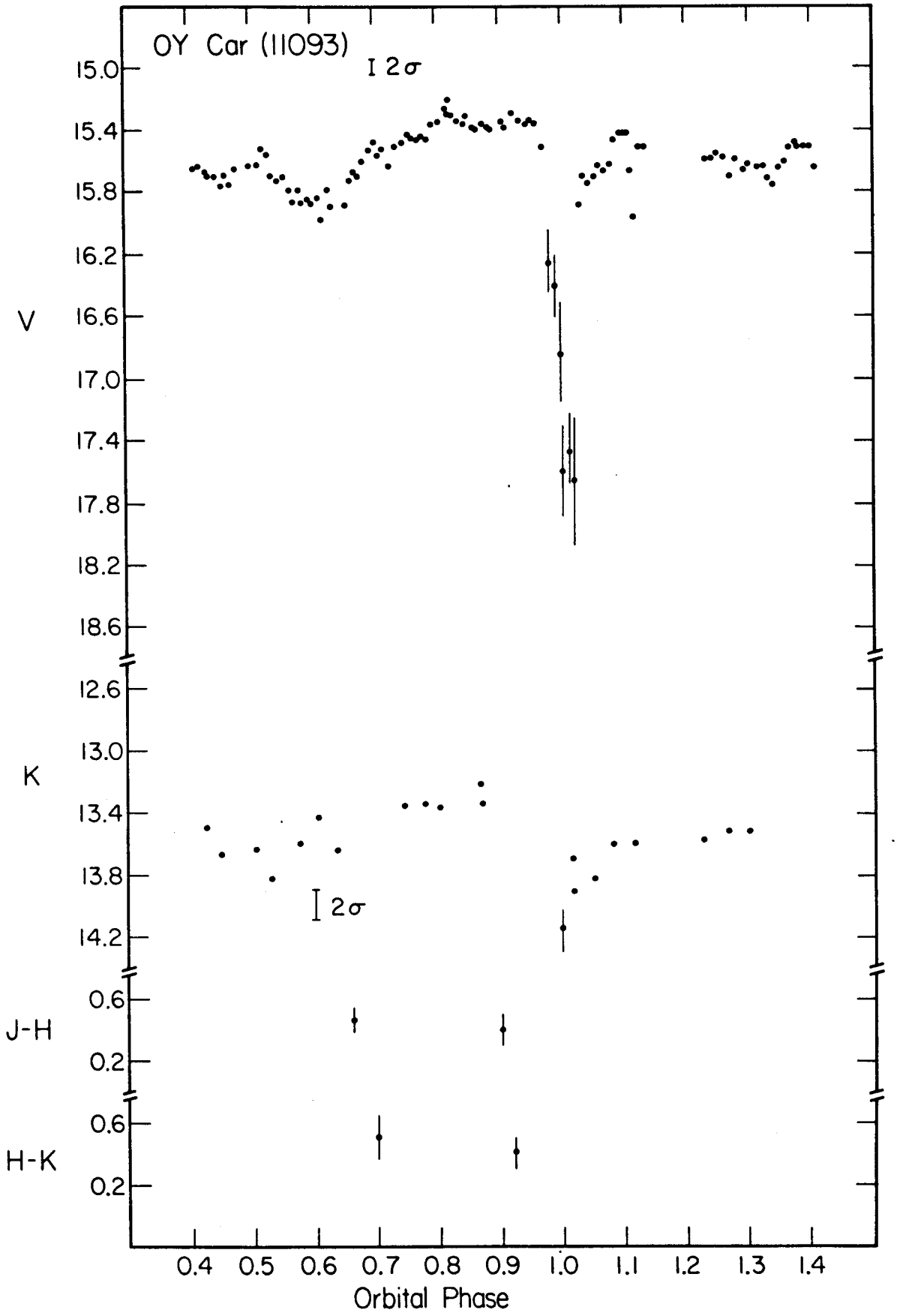
OY Car (11093)
I 2σ
V
15.0
15.4
15.8
16.2
16.6
17.0
17.4
17.8
18.2
18.6
K
12.6
13.0
13.4
13.8
14.2
2σ
J-H
0.6
0.2
H-K
0.6
0.2
0.4
0.5
0.6
0.7
0.8
0.9
1.0
1.1
1.2
1.3
1.4
Orbital Phase

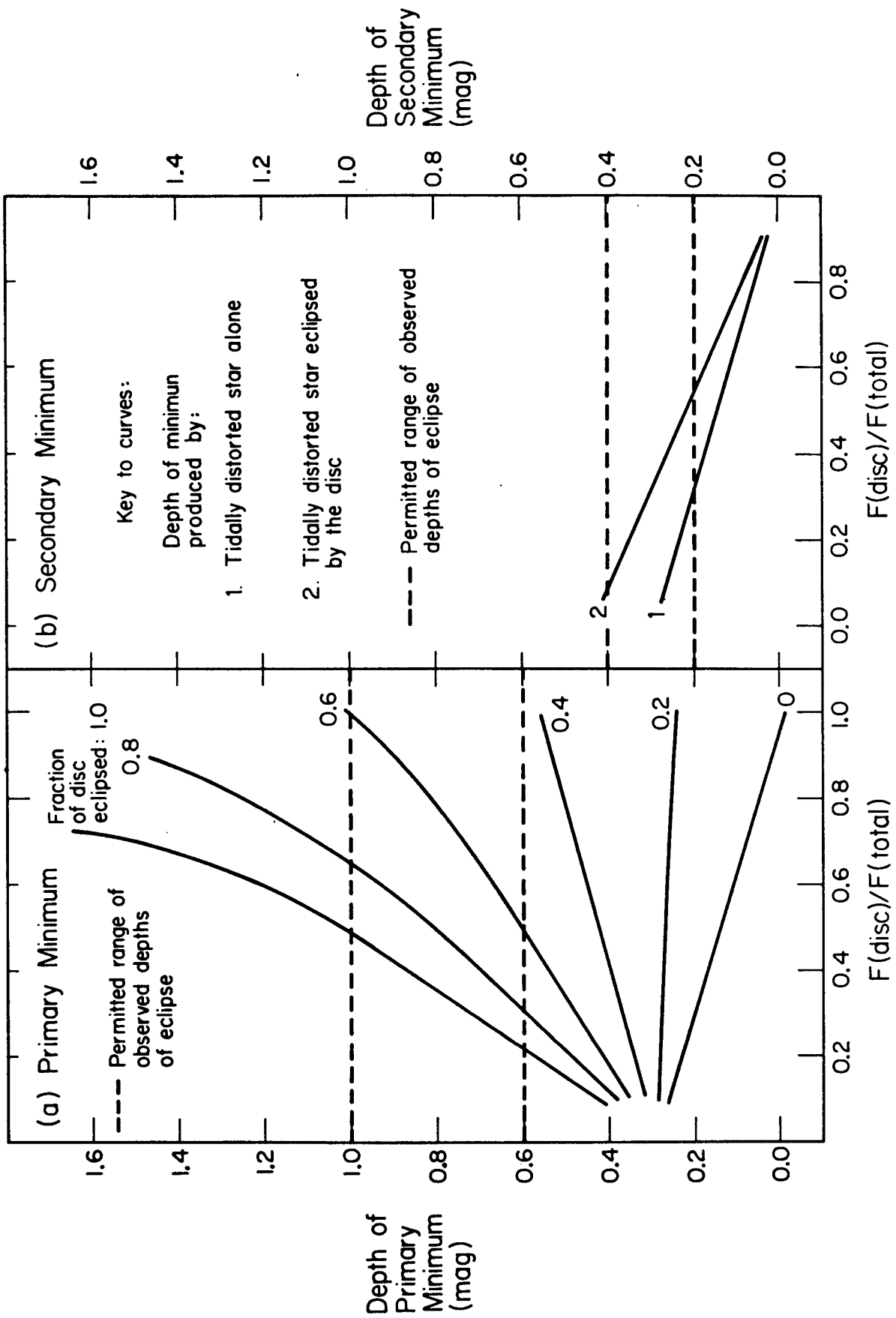
(a) Primary Minimum
(b) Secondary Minimum
Permitted range of observed depths of eclipse
Fraction of disc eclipsed: 1.0
0.8
0.6
0.4
0.2
0
Key to curves:
Depth of minimun produced by:
1. Tidally distorted star alone
2. Tidally distorted star eclipsed by the disc
Permitted range of observed depths of eclipse
Depth of Primary Minimum (mag)
Depth of Secondary Minimum (mag)
F(disc)/F(total)
F(disc)/F(total)
0.0
0.2
0.4
0.6
0.8
1.0
1.2
1.4
1.6
1
2

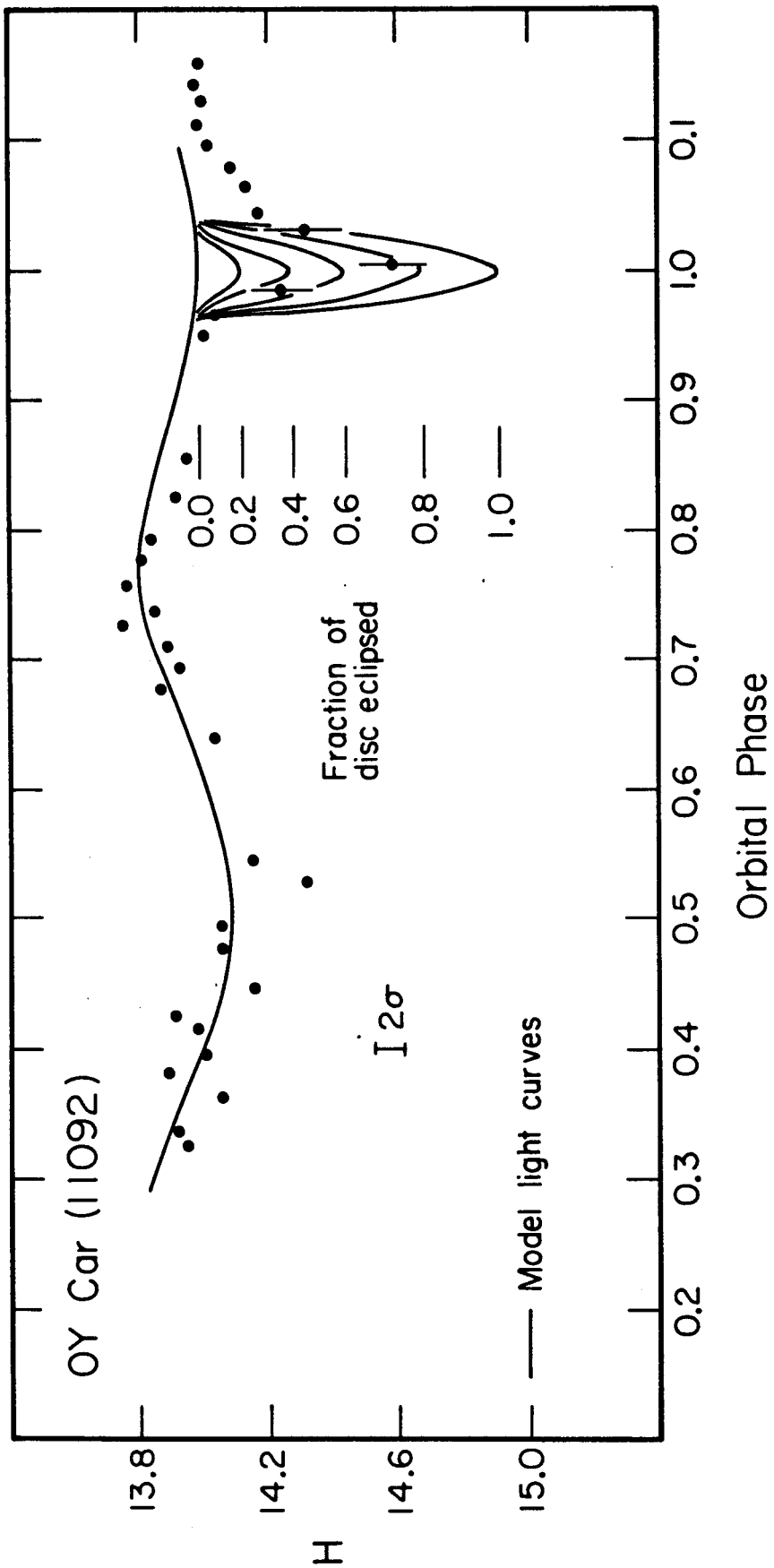
OY Car (11092)
Model light curves
2σ
Fraction of disc eclipsed
0.0
0.2
0.4
0.6
0.8
1.0
H
13.8
14.2
14.6
15.0
0.2
0.3
0.4
0.5
0.6
0.7
0.8
0.9
1.0
0.1
Orbital Phase

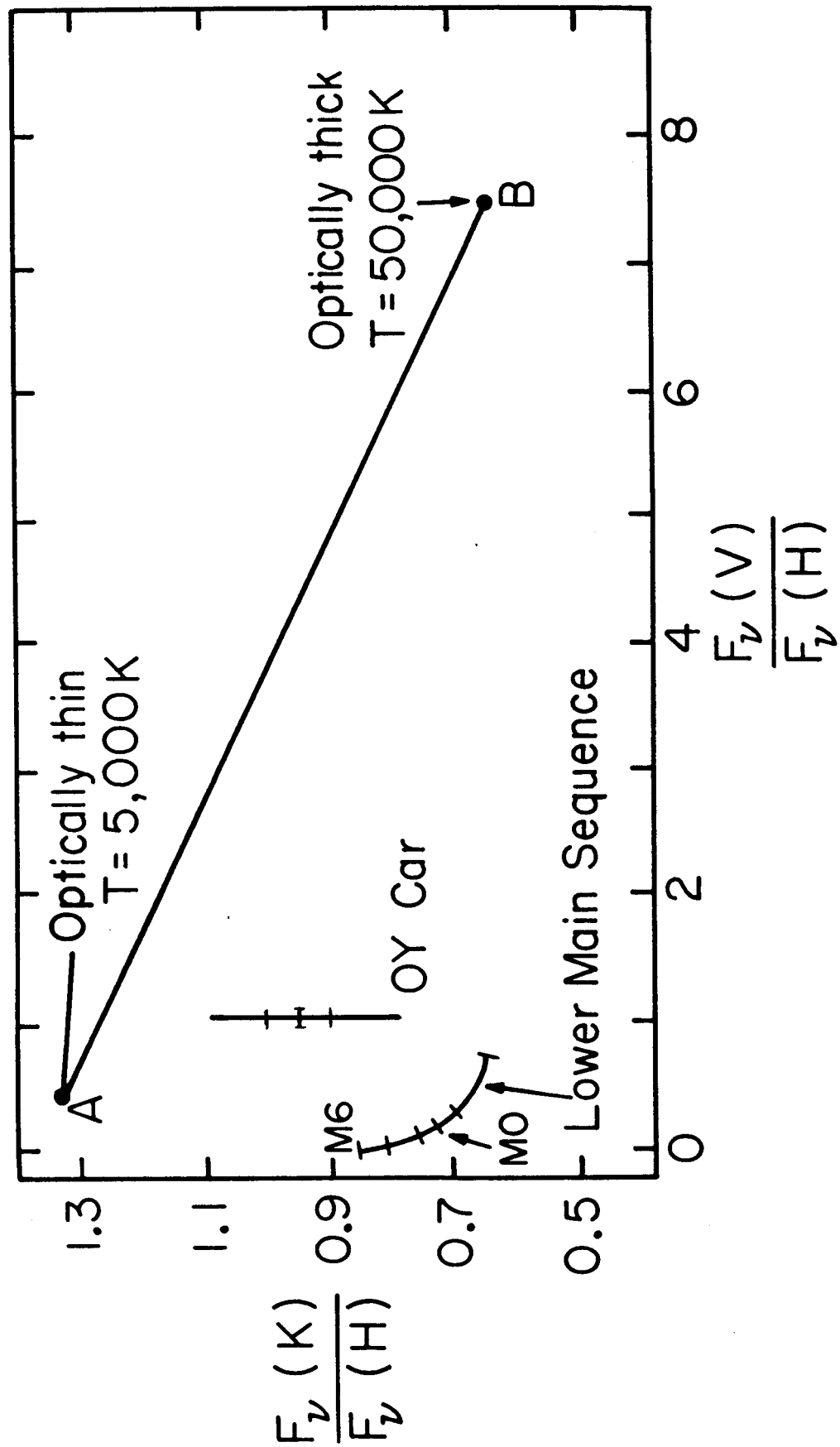
Optically thin
T = 5,000 K
Optically thick
T = 50,000 K
A
B
OY Car
M6
M0
Lower Main Sequence
1.3
1.1
0.9
0.7
0.5
0
2
4
6
8
$\frac{F_\nu (K)}{F_\nu (H)}$
$\frac{F_\nu (V)}{F_\nu (H)}$